5-2015

Molecular Mechanisms Underlying AlcoholInduced Cerebral Artery Smooth Muscle BK Channel Inhibition and Eventual Cerebral Vasoconstriction

Guruprasad Kuntamallappanavar
University of Tennessee Health Science Center

Molecular Mechanisms Underlying AlcoholInduced Cerebral Artery Smooth Muscle BK Channel Inhibition and Eventual Cerebral Vasoconstriction

Document Type
Dissertation

Degree Name
Doctor of Philosophy (PhD)

Program
Biomedical Sciences

Track
Molecular Therapeutics and Cell Signaling

Research Advisor
Alejandro M. Dopico, Ph.D.

Committee
William Earl Armstrong, Ph.D. Charles W. Leffler, Ph.D. Kafait U. Malik, Ph.D. Steven J. Tavalin, Ph.D.

DOI
10.21007/etd.cghs.2015.0169

Molecular Mechanisms Underlying Alcohol-Induced Cerebral Artery Smooth Muscle BK Channel Inhibition and Eventual Cerebral Vasoconstriction

A Dissertation
Presented for
The Graduate Studies Council
The University of Tennessee
Health Science Center

In Partial Fulfillment
Of the Requirements for the Degree
Doctor of Philosophy
From The University of Tennessee

By
Guruprasad Kuntamallappanavar
May 2015

DEDICATION

I dedicate this dissertation to
my father Chandrappa K.M., to my mother Channabasamma K.M.
and to my brothers Kotresh K.M. and Gururaj K.M.
for their unconditional love and support.

ACKNOWLEDGEMENTS

ABSTRACT

Introduction and Rationale: Ethanol (EtOH) at concentrations obtained in circulation during moderate to heavy episodic drinking, such as during binge drinking (30-60 mM) causes cerebral vasoconstriction in many species, including humans. Using rodents as a model to study ethanol-induced cerebral artery constriction, our laboratory demonstrated that ethanol-induced cerebral artery constriction is due to drug-induced reduction of STOCs (Spontaneous Transient Outward Currents) in cerebral artery smooth muscle. In this tissue, STOCs result from the activity of large conductance, calcium-and voltage-gated potassium (BK) channels. Indeed, ethanol (50 mM) decreases the steady-state activity (NP_o) of vascular myocyte BK channels leading to an increase in cerebral artery tone. In native tissues, functional BK channels are oligomers of four channel-forming slo1 subunits that are associated with small, accessory subunits (β1-4). β subunits do not form channels themselves but modify BK current phenotype, including its pharmacology. In particular, the vascular smooth muscle-abundant BK β1 subunit is required for ethanol to inhibit cerebral artery myocyte BK channels under physiological conditions of voltage and calcium. In contrast, the neuronally-predominant β4 subunit does not support this ethanol action. The molecular bases of ethanol-mediated inhibition of β1 subunit-containing BK channels and resulting cerebral vasoconstriction remain unknown.

Objective: Identify the BK β1 subunit regions and β1 subunit-dependent channel gating mechanisms underlying ethanol-induced inhibition of cerebral artery smooth muscle BK channel inhibition and eventual cerebral artery constriction.

Methods: Combination of recombinant DNA and other molecular biology in vitro approaches, patch-clamp electrophysiology, allosteric gating modeling, reversible permeabilization of arteries with cDNAs, and artery pressurization techniques.

Results: Ethanol sensitivity of slo1 current is dependent on the channel's activating ion, i.e., Ca^{2+}_i. Moreover, ethanol-induced modification of activity of slo1 (cbv1) and heteromeric cbv1+β1 BK channels is primarily due to modulation of calcium-driven gating: in particular, increase in Ca^{2+}_i affinity; decrease in allosteric interaction between 1) RCK and voltage sensing domains and 2) RCKs and pore gate domains. Ethanol facilitation of channel inhibition is favored by β1-and β2 but not β3 or β4 subunits. Consistent with the involvement of calcium-dependent mechanism, the former two drastically increase the channel's apparent calcium sensitivity whereas the latter fail to do so. Transmembrane domains of BK-β1 subunit are essential for ethanol-mediated inhibition of β1-containing BK channels. In particular, the second transmembrane domain of β1 subunit is necessary for both inhibition of β1-containing BK channels and cerebral artery constriction evoked by ethanol.

Conclusion: BK β1 subunit TM2 enables ethanol-induced inhibition of β1-containing BK channels and cerebral artery constriction, with drug action on channel activity being dependent on modification of calcium-gating parameters.

TABLE OF CONTENTS

LIST OF TABLES

LIST OF FIGURES

LIST OF ABBREVIATIONS

β2-IR	Beta2 subunit without N-terminus inactivation peptide
ATP	Adenosine 5'-triphosphate
BAC	Blood alcohol concentration
BK	Big (large) conductance, calcium- and voltage-gated potassium
Ca^{2+}_i	Calcium
$[Ca^{2+}]_i$	Intracellular calcium concentration
$CaCl_2$	Calcium chloride
Cl^-	Chloride
CTD	Cytosolic tail domain
Ctx	Charybdotoxin
DMEM	Dulbecco's modified eagle medium
EC	Extracellular side
EDHF	Endothelium derived hyperpolarizing factor
EDRF	Endothelium derived repolarizing factor
EGTA	Ethylene glycol-bis(2-aminoethylether)-N,N,N',N'-tetraacetic acid
EtOH	Ethanol
G	Macroscopic channel conductance
G/G_{max}	Ratio of conductance to maximum conductance
HA	Horrigan Aldrich
HEDTA	N-{2-[Bis(carboxymethyl)amino]ethyl}-N-(2-ydroxyethyl)glycine
HEPES	2-[4-(2-hydroxyethyl)piperazin-1-yl]ethanesulfonic acid
Ibtx	Iberotoxin
IC	Intracellular side
I/O	Inside-out
KCl	Potassium chloride
KCNMB1	Gene encoding for BK-β1 protein
K/O	Knock-out
KOH	Potassium hydroxide
K_v	Voltage-gated potassium channels
LCA	Lithocholate
Mg^{2+}	Magnesium
$[Mg^{2+}]$	Intracellular Mg^{2+} concentration
$MgCl_2$	Magnesium chloride
MOPS	3-propainesulfonic acid
MS-222	Tricaine methanesulfonate
MWC	Monad-Wayman-Changuex
N	Number of channel in the membrane patch
Na^{2+}	Sodium
$[Na^{2+}]$	Sodium ion concentration
NaCl	Sodium chloride
NP_o	Index of channel steady-state
NPS	Nitroprusside
OH^-	Hydroxyl ion

PBS	Phosphate buffer saline
PGD	Pore gate domain
P_o	Channel open probability
PSS	Physiological saline solution
RCK	Regulator of conductance for potassium
STOC	Spontaneous transient outward current
TBS	Tris-buffered solution
TBS-T	TBS with 0.1% tween
TES	Tetraetyhyl Silane
TM	Transmembrane
Ryr	Ryanodine receptor
$V_{0.5}$	Voltage required to achieve half-maximal conductance
VDCC	Voltage dependent calcium channels
V_{max}	Voltage required to maximal conductance

CHAPTER 1.   INTRODUCTION

1.1.   Cerebrovascular Diseases and Binge Drinking

1.1.1. Epidemiology of Cerebrovascular Diseases

Cerebrovascular disease is a leading cause of long-term disability in the United States (U.S.) and other western countries and ranks No.4 among all causes of death (www.cdc.gov). In particular, stroke ranks third among all causes of mortality. On average, every four minutes someone dies of stroke. In 2007, stroke accounted for 1 in 18 deaths in the U.S. Moreover, the total expenditure on stroke in the U.S. is estimated to be $43 billion per year (www.cdc.gov; Beaglehole., 1990; Mohler et al., 1999; Callahan., 2001) (Beaglehole 1990; Mohler *et al.* 1999; Callahan 2001).

1.1.2. Alcohol Consumption and Health

Alcohol is one the most commonly abused drugs. Excessive alcohol consumption is considered to be the 3rd life-style related cause of death in the U.S., leading to 88,000 deaths annually (www.cdc.gov; www.niaaa.nih.gov).

Alcohol drinking pattern can be arbitrarily classified into the three following categories:

1.1.2.1. Light Drinking

Drinking less than 2 drinks per day, usually leading to Blood Alcohol Concentration (BAC) of 0.002-0.005% (1-20 mM).

1.1.2.2. Moderate Drinking

Drinking less than 4 drinks per day, which usually leads to BAC of 0.15-0.25% (35-50 mM).

1.1.2.3. Heavy drinking

Drinking more than 4 drinks per day, usually leading to BAC of 0.25-0.50% (50->100 mM).

1.1.3. What Is a Standard Alcoholic Drink?

In the United States, a standard alcoholic "drink" refers to 14 grams (0.6 ounce or 1.2 table spoons) of pure alcohol (ethyl alcohol, ethanol, EtOH) (www.niaaa.nih.gov). This much amount of pure alcohol is usually found in

- 12 ounces of beer, which contains 5% of alcohol
- 5-ounces of wine, which typically contains 12% of alcohol
- 1.5 ounces of 80% distilled spirits or liquor (e.g., gin, rum, whiskey, vodka), which on average contain 40% alcohol.

1.1.4. Binge Drinking

National Institute of Alcohol Abuse and Alcoholism (NIAAA) defines binge drinking as moderate-to-heavy episodic drinking, in which a man consumes 5 or more drinks or an adult woman consumes 4 or more drinks in about 2 hours. (www.niaaa.gov).

Unfortunately, binge drinking remains a major health problem in the U.S, representing the major form of excessive alcohol abuse: approximately 92% of U.S. adults who drink excessively report binge drinking in the past 30 days; more than 38 million adults binge drink every year; on average 2 in 3 high schoolers who drink, do so by binge drinking. Overall, binge drinking causes more than 88,000 deaths in the U.S. every year (www.cdc.gov). Binge drinking has been shown to be associated with short term and long term major health problems, including cardiovascular and cerebrovascular diseases. (Wechsler *et al.* 2002; Barnett *et al.* 2003).

1.1.5. Binge Drinking as a Risk Factor for Cerebrovascular Diseases

Epidemiological studies show that moderate to heavy episodic drinking, such as binge drinking, significantly increases the risk for cerebrovascular spasm, brain hemorrhage and stroke (Klatsky *et al.* 1986; Moore and Pearson 1986; Marmot and Brunner 1991; Puddey *et al.* 1999; Gil-Nunez and Villanueva 2001). Binge drinking with blood alcohol concentration (BAC) of 0.15-0.50% (35-80 mM) is associated independently of any other factor with an increased risk for stroke and deaths from ischemic stroke (Haapaniemi *et al.* 1997; Zakhari 1997; Suter and Vetter 1999; Reynolds *et al.* 2003). Cerebrovascular disease associated with moderate-heavy episodic alcohol consumption is independent of beverage type and alcohol metabolism but linked to ethanol itself (Arkwright *et al.* 1982; Altura *et al.* 1983; Altura and Altura 1984; Zakhari 1997). Moderate to heavy drinking causes cerebral artery constriction, which has been related to cerebral vasospasm, ischemia, and stroke (Arkwright *et al.* 1982; Rimm *et al.* 1996; Wannamethee and Shaper 1996).

Direct ethanol exposure of different vasculatures may result in vasodilation or vasoconstriction depending on species, ethanol concentration, and type of vascular bed

(Altura *et al.* 1983; Altura and Altura 1984; Potter and Beevers 1984; Jackson *et al.* 1985; Puddey *et al.* 1985; Puddey *et al.* 1987). However, there is strong evidence that acute exposure to ethanol>18 mM produces constriction of cerebral arteries, including in humans. Constriction of cerebral arteries is due to ethanol itself, and replicated *in vivo* and *in vitro* models used to study ethanol-induced cerebral artery constriction in several species (Altura and Altura 1982; Altura *et al.* 1983; Altura and Altura 1984; Puddey *et al.* 1987; Marmot and Brunner 1991; Zhang *et al.* 1993; Gordon *et al.* 1995; Seppa *et al.* 1996; Wannamethee and Shaper 1996; Liu *et al.* 2004).

Rat and mouse arteries have proved successful *in vivo* and *in vitro* models to study ethanol-induced cerebral artery constriction and stroke (Altura and Altura 1982; Altura *et al.* 1983; Altura and Altura 1984; Zhang *et al.* 1993; Gordon *et al.* 1995; Liu *et al.* 2004; Bukiya *et al.* 2009; Bukiya *et al.* 2011). However, the mechanisms underlying ethanol-induced cerebrovascular constriction remained largely unknown for many years. Several studies have suggested that endogenously produced vasoactive compounds, such as endothelial factors (EDRF, EDHF) or neural factors from the vascular smooth muscle-surrounding parenchyma modulate ethanol-induced vasoconstriction (Jackson *et al.* 1985; Iwase *et al.* 1995). However, ethanol-induced constriction of cerebral arteries is evoked by ethanol acting primarily on the arterial smooth muscle itself (Altura and Altura 1982; Altura *et al.* 1983; Altura and Altura 1984; Zhang *et al.* 1993; Gordon *et al.* 1995; Yang *et al.* 2001; Liu *et al.* 2004). In a major breakthrough towards identifying the molecular targets mediating ethanol action on cerebral arteries, our group discovered that ethanol at concentrations obtained in circulation during moderate-to-heavy binge drinking (10-100 mM) constricted rat and mouse cerebral arteries *via* inhibition of BK channel activity in cerebral arterial smooth muscle (Liu *et al.* 2004; Bukiya *et al.* 2009; Bukiya *et al.* 2011).

1.2.   Physiology of BK Channels

1.2.1. Physiological Role of BK Channels in Arterial Smooth Muscle

Resistant size cerebral arteries are main determinants of controlling blood flow, whether systemically or locally. Under physiological conditions, resistant size arteries exist in a partially constricted state, from which they may dilate or further constrict depending on the perfusion needs and metabolic demands of tissues and organs. Intravascular pressure is considered one of the major stimuli for such arterial constriction. Arterial myocytes present some degree of contraction in response to intravascular pressure, which is known as myogenic tone as reported in cerebral arteries (Jaggar and Nelson 2000; Jaggar *et al.* 2000; Wellman *et al.* 2002; Wellman and Nelson 2003). Indeed, myocytes respond to increase in intravascular pressure by graded membrane depolarization, which leads to Ca^{2+} influx *via* depolarization-activated Voltage-dependent Ca^{2+} Channels (VDCC). The resulting increase in global cytosolic Ca^{2+}_i leads to smooth muscle contraction and thus cerebral artery constriction. On the other hand, BK channels participate in a negative-feedback loop that limits the depolarization-triggered by increase in Ca^{2+}_i, myogenic tone and vasoconstriction, as found in many species and vessels

3

including rabbit (Brayden and Nelson 1992), and rat cerebral (Erdos *et al.* 2002), and human pial arteries (Wellman *et al.* 2002; Wellman and Nelson 2003). This key role of BK channel is due to its unique position as transducer between cell metabolism and membrane potential: a rise in internal Ca^{2+} leads to BK channel activation, which generates positive outward currents that drive the myocyte membrane potential in a negative direction and, eventually, close voltage-dependent Ca^{2+} channels. Thus, BK channel activation counteracts contraction due to voltage-dependent Ca^{2+} influx, causing vascular smooth muscle relaxation and eventual vasodilation. Conversely, a decrease in BK activity blunts the negative feedback on voltage-dependent Ca^{2+} influx, leading to vasoconstriction (Brayden and Nelson 1992; Asano *et al.* 1993; Jaggar and Nelson 2000; Jaggar *et al.* 2000; Cheng and Lederer 2008; Subramani *et al.* 2009) (**Figure 1-1**).

1.2.2. Basic Structure of BK Channels

BK channels are members of the slo channel family, first identified in Drosophila melanogaster. The gene encoding for BK channel is called *Slo* or *Slo1* or *KCNMA1*. In mammalian tissues, BK channels formed from tetrameric association of channel-forming α subunits. There are three slo channel family members, namely slo1, slo2 and slo3. The protein products of all Slo channel family members share basic very distinct characteristic features (Xia *et al.* 2004; Salkoff *et al.* 2006), such as 1. High selectivity for K^+ ions 2. Large unitary conductance and 3. Activation by intracellular Ligands (For example, Slo1 by Ca^{2+}; Slo2 by Na^{2+}; Slo3 by OH^-).

Structurally, slo1 (alpha) subunits can be divided into three major domains: The voltage-sensing domain (VSD), including transmembrane segments S1-S4, which senses the voltage; a pore-gate domain (PGD), including S5-S6, that controls ion permeation and selectivity; and a C-terminal cytoplasmic domain (CTD) that includes two Regulators of potassium conductance (RCK) domains, which recognizes intracellular ligands such as Ca^{2+}, Mg^{2+}. In addition, unique to BK channel, there is an additional transmembrane domain, S0 that presents N-terminus to the extracellular side of the membrane (**Figure 1-2**). In most tissues, α subunits are associated with relatively small regulatory termed β subunits (β1- β4) (Latorre *et al.* 1989; Behrens *et al.* 2000; Brenner *et al.* 2000; Salkoff *et al.* 2006; Cheng and Lederer 2008; Horrigan 2012).

1.2.3. Beta Subunits of BK Channels

While basic characteristics of BK channels (such as voltage- and calcium-sensitivity, high conductance) are reproduced by functional tetramers composed from slo1 subunits (Liu *et al.* 2006; Lee and Cui 2010; Horrigan 2012), some biophysical and pharmacological properties are drastically modified by dynamic association of BK α subunit with regulatory β subunits. Beta subunits themselves do not form functional channels *per se*, rather they are thought to be associated with alpha subunits in a 1:1 ratio (**Figure 1-2**) (Wallner *et al.* 1995).
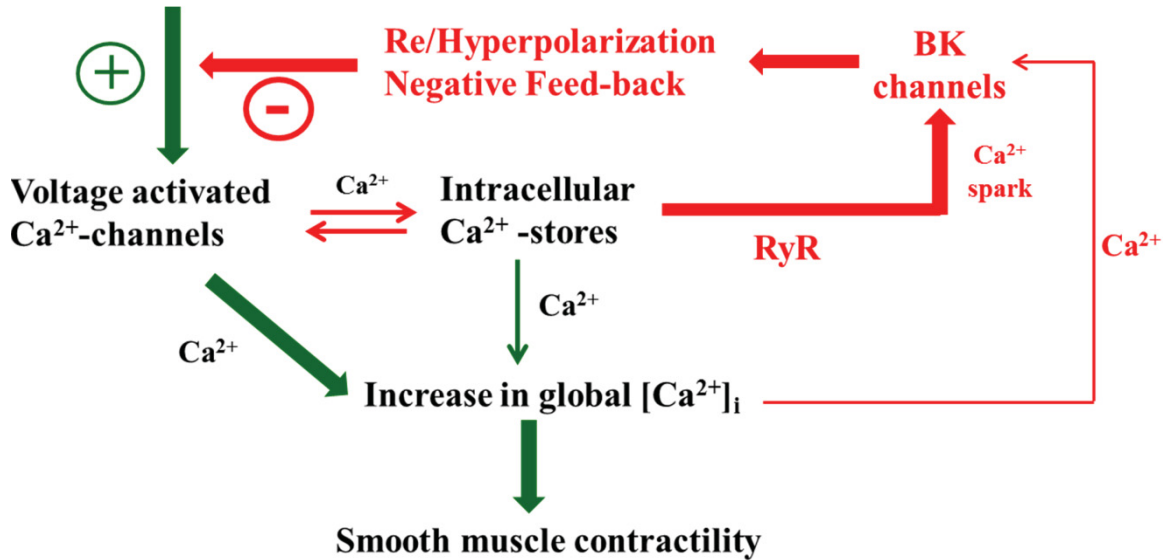
Figure 1-1.   Role of BK channels in regulation of vascular tone

Notes: A) Schematic diagram showing that in arterial smooth muscle cells, activation of BK channels provides negative feedback on voltage-dependent calcium influx, limiting the smooth muscle contractility. Membrane depolarization leads to activation of voltage-dependent Ca^{2+}_i channels (VDCC), thus increases the levels of global Ca^{2+}_i. That provides major contribution for smooth muscle contractility. Increased intracellular Ca^{2+}_i leads to Ca^{2+}_i-induced Ca^{2+}_i release from intracellular Ca^{2+}_i stores. This in turn activates nearby BK channels to provide negative feedback for smooth muscle contractility.

Source: Modified with permission from Cheng H. Lederer WJ (2008). Calcium sparks. *Physiol Rev* 88:1491-1545.
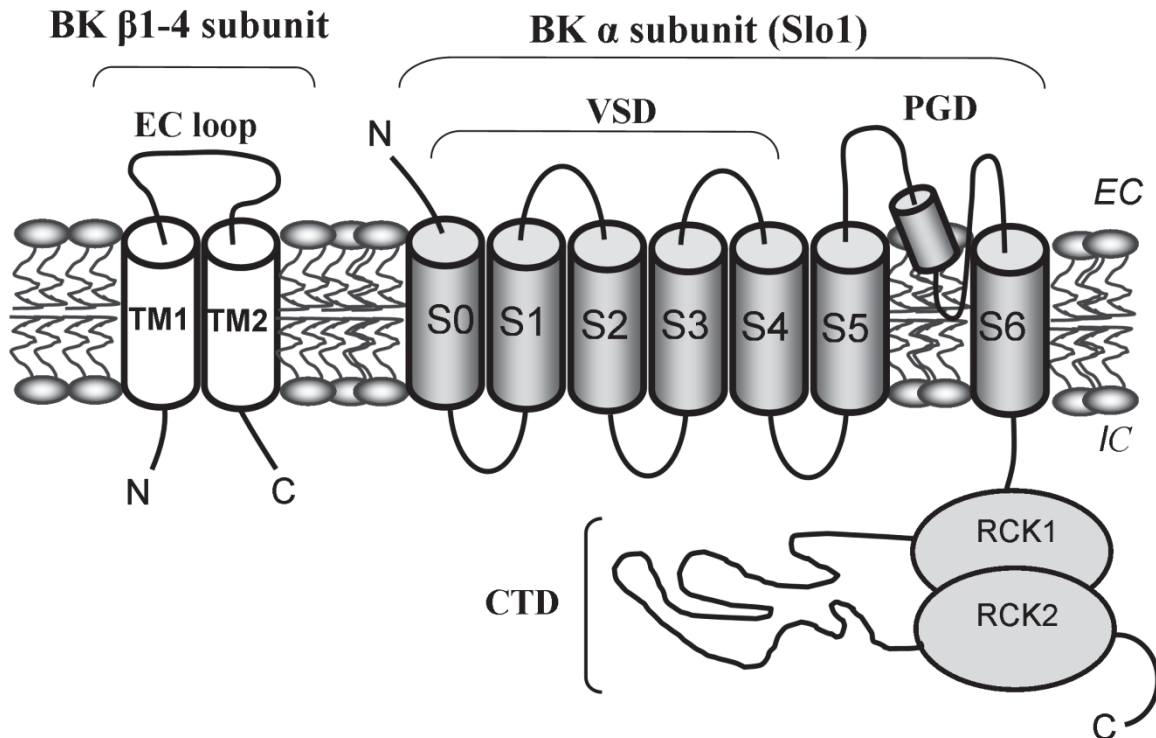
Figure 1-2.   Schematic structure of BK channels containing accessory subunit (β1-4)

Notes: Cartoon showing an α or slo1 (cbv1)-β1 heterodimer. The slo1 monomer shows N-terminus, transmembrane (TM) segments from S0-S6 and intracellular regulator of conductance for K^+ (RCK) domains. Among slo1 TM domains, S0-S4 domains forms voltage sensing domain (VSD), which senses changes in membrane potential; S5-S6 domains involved in forming pore of the channel, called pore-gate domain (PGD). The RCKs, contains recognition sites for intracellular ligands such as Ca^{2+}_i and Mg^{2+}_i. Four slo1 monomers associate to render functional channel forming BK channels. β subunits contain an N-terminal, two transmembrane domains (TM1 and TM2), extracellular (EC) loop, and a C-terminal. EC and IC correspond to the extracellular and intracellular edges of the membrane; RCK: Regulator of Conductance for K^+ domain.

Source: Reprinted with permission from Kuntamallappanavar G. Toro L. and Dopico A.M. (2014). Both transmembrane domains of BK beta1 subunits are essential to confer the normal phenotype of beta1-containing BK channels. *PLoS One* 9(10): e109306.

β subunits are characterized by differential distribution among the tissues (Behrens *et al.* 2000; Brenner *et al.* 2000). Of the four β subtypes, β1 is the predominant isoform in vascular smooth muscle (Tanaka *et al.* 1997; Brenner *et al.* 2000; Cox and Aldrich 2000). β1 subunit drastically increases the apparent Ca^{2+} sensitivity of the channel, and slows down activation and deactivation kinetics (Brenner *et al.* 2000; Cox and Aldrich 2000). β2 is expressed in adrenal gland and brain (Behrens *et al.* 2000) and characterized by the presence of an intracellular inactivating domain that empowers the ionic current with fast inactivation (Brenner *et al.* 2000). β3 is predominant in testis and skeletal muscle (Uebele *et al.* 2000). However, it does not alter calcium (Ca^{2+}_i) sensitivity, activation or deactivation kinetics (Brenner *et al.* 2000). β4 is abundantly expressed in brain. β4-containing BK channels are characterized by 1) resistance to the BK peptidic blockers iberotoxin (Ibtx) and charybdotoxin (Ctx) due to the presence of a large extracellular loop; and 2) slow activation and deactivation kinetics (Brenner *et al.* 2000).

From a structural point of view, beta subunits consists of two transmembrane domains (TMs) interconnected by a long extracellular (EC) loop and short cytoplasmic N- and C-termini (**Figure 1-2**) (Behrens *et al.* 2000; Brenner *et al.* 2000; Cox and Aldrich 2000).

1.2.4. Role of BK β1 Subunit in Regulation of Arterial Tone

BK β1 serves as a key molecule that enables activation of BK channels in response to micromolar Ca^{2+}_i concentration released from the sarcoplasmic reticulum. β1 is known to increase BK channel's apparent Ca^{2+}_i sensitivity (Meera *et al.* 1996; Tanaka *et al.* 1997; Brenner *et al.* 2000; Brenner *et al.* 2000; Cox and Aldrich 2000; Patterson *et al.* 2002). β1 knock-out mice suffer from a variety of abnormalities due to impaired vasorelaxation mechanisms. These abnormalities are linked to BK channel function in cardiovascular system leading to hypertension, stroke, brain hemorrhage and cardiac hypertrophy without major alterations involving BK in other tissues or organs (Brenner *et al.* 2000; Pluger *et al.* 2000). Interestingly, BK channels from β1 knock-out mice lack response to Ca^{2+}_i sparks, a vasodilating signal regenerated by the activity of ryanodine receptors. Furthermore, these studies have also demonstrated that cerebral arteries from β1 knock-out mice constrict more than *wt* with mean arterial blood pressure of β1 knock-out mice being significantly elevated in comparison to control (Brenner *et al.* 2000; Lohn *et al.* 2001; Patterson *et al.* 2002). Notably, genetic hypertensive rats show down regulation of BK β1, normal spark amplitude but reduced STOC amplitude, underscoring the importance of BK β1 in spark-STOC coupling in vascular smooth muscle (Amberg and Santana 2003).

1.3.   Alcohol and BK Channels

1.3.1. Ethanol Modulation of BK Channel Activity

It was first documented in mid 90's that acute ethanol exposure (10-100 mM) increases the BK steady-state activity; in turn contribute to alcohol-induced inhibition of vasopressin, oxytocin, and growth hormone release (Dopico *et al.* 1996; Jakab *et al.* 1997; Dopico *et al.* 1998; Dopico 2003). In addition, BK channel activation by ethanol has been also reported in several other preparations and further linked to pathophysiological processes that are affected by ethanol exposure, such as neurotransmitter release, nociception, action potential firing in *N.accumbens* neurons, motor coordination in *C.elegans*, endothelial proliferation and nitric oxide production (Brodie *et al.* 2007) However, ethanol-induced BK current activation is not a universal phenomenon, with BK channels in rat supraoptic neuron somata (Dopico *et al.* 1999) and in N. Accumbens dendrite being refractory to 100 mM ethanol (Martin *et al.* 2004). Moreover, ethanol drastically inhibits the BK channels in rat aorta (Walters *et al.* 2000), and cerebral arteries from rat and mouse, eventually leading to cerebral artery constriction (Liu *et al.* 2004; Bukiya *et al.* 2009; Bukiya *et al.* 2011).

1.3.2. Factors Modulating Ethanol Action of BK Channel Activity

Previous studies demonstrated that the final ethanol effect on BK channel activity is a result of the orchestration of several factors such as: 1. post-translational modification (phosphorylation) of pore-forming slo1 subunit (Liu *et al.* 2006); 2. co-expression of channel's auxiliary subunits (Martin *et al.* 2004; Bukiya *et al.* 2009; Wynne *et al.* 2009); 3. amount of cholesterol in the membrane where the ion channel resides (Crowley *et al.* 2003; Crowley *et al.* 2005; Bukiya *et al.* 2011; Yuan *et al.* 2011); 4. phospholipid species in the membrane surrounding channel (Crowley *et al.* 2005; Yuan *et al.* 2011). Collectively, results from reductionist systems such as reconstitution of recombinant slo1 protein in artificial bilayer revealed that ethanol action on BK channels requires two minimum set of targets i.e., slo1 subunit itself and one or two phospholipid species in the bilayer (Crowley *et al.* 2005; Brodie *et al.* 2007; Yuan *et al.* 2011). Whether final ethanol effect of ethanol on BK channel is potentiation or inhibition, modulation of BK channel activity in response to acute ethanol exposure is ultimately determined by modification of slo1 channel gating processes, without modification in channel expression or unitary conductance (Dopico *et al.* 1996; Dopico *et al.* 1998; Dopico 2003; Martin *et al.* 2004). Thus, ethanol effect on BK current is limited to gating modifier.

Slo1 channel gating is defined by four basic processes: 1. voltage-driven gating 2. Ca^{2+}-driven gating 3. Mg^{2+}-driven gating 4. intrinsic gating (Cox and Aldrich 2000). Thus, ethanol may alter one or more of these gating processes to modify the steady-state activity of the channel and eventually perturb cell physiology and organ function.

1.3.3. Role of BK β1 Subunit in Ethanol-Induced Cerebral Vasoconstriction

Several studies demonstrated that ethanol action on arterial smooth muscle leads to ethanol-induced cerebral vasoconstriction (Altura and Altura 1982; Altura *et al.* 1983; Altura and Altura 1984; Gordon *et al.* 1995; Yang *et al.* 2001; Liu *et al.* 2004). Our laboratory documented that the cerebral arterial constriction by ethanol concentrations obtained during binge drinking is due to ethanol-induced inhibition of smooth muscle BK channel, as it is vanished in the presence of the selective BK channel blocker iberiotoxin (Ibtx) with blockers of other voltage-dependent K^+ channels failing to modulate ethanol action (Liu *et al.* 2004). Remarkably, BK β1 subunit is required for ethanol-induced cerebral artery constriction (Bukiya *et al.* 2009): indeed, using the *KCNMB1* K/O mice model, we demonstrated that BK channel-mediated ethanol-induced vasoconstriction is not observed in the absence of BK channel β1 subunits (Bukiya *et al.* 2009). Furthermore, this finding was paralleled by patch-clamp recordings of native BK channels from freshly isolated cerebral artery myocytes showing that BK channels from *wt* myocytes are inhibited by ethanol whereas, BK channels in *KCNMB1* K/O myocytes were resistant to ethanol inhibition. Additionally, native BK channels from skeletal muscle fibers, where β1 is poorly, if at all, expressed, were also resistant to ethanol-induced inhibition (Bukiya *et al.* 2011).

1.4.   Significance of the Study

Episodic, moderate-to-heavy alcohol intake leads to cerebral artery constriction, vasospasm, and stroke, which are primarily determined by ethanol action on cerebral artery smooth muscle itself. In addition, it was demonstrated that the BK channel in cerebrovascular smooth muscle is the major cell effector of ethanol-induced cerebral artery constriction and its inhibition by ethanol action is favored by the expression of the smooth muscle-abundant regulatory β1 subunit (Liu *et al.* 2008; Bukiya *et al.* 2009). Alcohol-induced constriction (~10% decrease in diameter) is sufficient to decrease the cerebral blood flow by ~30% because diameter and blood flow are related by a 3rd power relationship.

Considering the high prevalence of binge drinking and cerebrovascular disease, the association between alcohol intake and cerebrovascular pathology and the high mortality and disability that result from cerebrovascular disease, it is crucial to identify the molecular targets and mechanisms that mediate ethanol-driven cerebrovascular disorders. Although, pharmacotherapy (e.g., accamprosate, naltrexone) or other forms of approaches are aimed at treating alcohol-driven disorders by breaking the circuit of addiction, however, none of these therapies are aimed to prevent or ameliorate the cerebrovascular disorders related to binge drinking and acute ethanol intoxication.

Specific aims in this proposal are designed to identify the specific region(s) in the β1 subunit that are responsible for ethanol-induced BK channel inhibition and resulting cerebrovascular constriction as well as the specific gating mechanisms that lead to ethanol-inhibition of β1-containing BK channel currents . Knowing which specific

region(s) of β1 subunit and the specific gating processes that are targeted by ethanol to disrupt BK channel function and thus evoke cerebrovascular constriction could help to develop pharmacological agents/tools that would counteract these ethanol actions by acting on specific BK region/gating processes. Should these counteracting agents be found free of side effects and suitable to human pharmacokinetics, they could be used in our pharmaco-therapeutic arsenal to oppose ethanol-driven cerebrovascular constriction and disease.

CHAPTER 2.   HYPOTHESIS

2.1.   Goal

The overall goal of this study is to identify the molecular targets that underlie ethanol-induced inhibition of β1-containing BK channels and the resulting cerebral artery constriction. I will reach this goal by addressing the following specific aims.

2.2.   Specific Aims (SA)

2.2.1. Specific Aim 1

Determine the role of activating ion and accessory beta subunits in ethanol modulation of BK channels.

2.2.1.1. Specific Aim 1 (Part-A)

Determine the role of activating ion in ethanol modulation of BK channels.

After documenting that ethanol modulation of BK channel activity is a function of the channel's activating ion, i.e. intracellular Ca^{2+}_i (Liu *et al.* 2008), I expressed BK channel pore-forming α subunits cloned from rat cerebral artery myocytes (termed cbv1; AY330293) in *Xenopus* oocyte expression system. This slo1 variant showed all properties of other BK channel-forming slo1 proteins, including its independent gating by Ca^{2+}_i and Mg^{2+}_i. Using the same expression system, I also expressed other slo family members i.e. slo2 and slo3, which are primarily gated by ions other than Ca^{2+}: i.e., Na^+ and OH^- respectively. Then, I used patch-clamp electrophysiology to determine the role of activating ion in ethanol modulation of the different members of the slo channel family. Part-A of SA1 is addressed in Chapter 4.

2.2.1.2. Specific Aim 1 (Part-B)

Determine the role of different BK β subunits in ethanol modulation of BK channels.

Previous studies have identified that BK β subunits modulate the apparent Ca^{2+}_i sensitivity of the channel (Brenner *et al.* 2000; Cox and Aldrich 2000), this modulation likely contributing to ethanol-induced inhibition of β1-containing BK channels. These channels are thought to constitute native channel, in cerebral artery smooth muscle, which mediate cerebral artery constriction by ethanol (Liu *et al.* 2004; Bukiya *et al.* 2009). Thus, I co-expressed cbv1 with different BK β subunits and used patch-clamp

11

electrophysiology to determine the role of different accessory β subunits in ethanol modulation of BK channel. Part-B of SA1 is addressed in Chapter 5.

2.2.2. Specific Aim 2

Identify the specific β1 subunit-dependent gating processes that are targeted by ethanol leading to modification of BK currents.

Several groups have documented that BK β1 subunits increase the BK channel's apparent Ca^{2+}_i sensitivity (Brenner *et al.* 2000; Cox and Aldrich 2000; Bao and Cox 2005; Orio and Latorre 2005). This β1 action, however, results from complex modulation of various specific aspects of BK channel gating, some being Ca^{2+}_i-dependent while others being Ca^{2+}_i-independent: 1) mild increase in the Ca^{2+} affinity to closed state(s) (K_d) of the channel; 2) decrease in the intrinsic energetic barrier of the channel to transition from closes to open states in absence of any ligand or transmembrane voltage (i.e., L_0=closed to open equilibrium constant) (Cox and Aldrich 2000; Bao and Cox 2005; Orio and Latorre 2005).3) stabilization of voltage sensor activation [$V_h(J)$], when the channel is closed. 4) Mild increases in allosteric interaction (factor C) between Ca^{2+}_i binding and channel opening and thus promotes channel opening (Cox and Aldrich 2000; Bao and Cox 2005). Based on this background information, I conducted normalized macroscopic conductance (G/G_{max})-voltage (V) curves obtained over a wide range of $[Ca^{2+}]_i$ from homomeric cbv1 *vs.* cbv1+β1 constructs under condition similar to those proposed to test SA1. The resulting plots were fitted to the 70-state Horrigan-Aldrich (HA) allosteric model (Horrigan and Aldrich 1999; Horrigan and Aldrich 2002; Orio and Latorre 2005; Sun *et al.* 2013; Gonzalez-Perez *et al.* 2014) to determine which specific aspects of channel gating were modified by ethanol (50 mM) and led to inhibition of β1-containing BK channel currents. SA2 is addressed in Chapter 5.

2.2.3. Specific Aim 3

Identify the specific β1 subunit region(s) that is responsible for ethanol-induced inhibition of β1-containing BK channels.

Previous studies have demonstrated that BK β1 subunit enables ethanol-induced BK channel inhibition at physiological ionic conditions whereas BK β4 subunit does not contribute to this ethanol action (Liu *et al.* 2008; Bukiya *et al.* 2009). Based on these findings, I co-expressed cbv1 with chimeric subunits made by swapping different regions between BK β1 and BK β4. Then, I used patch-clamp electrophysiology on the resulting heteromeric BK complexes in the same expression system and conditions previously used to study cerebral artery recombinant BK channel function. The strategy was to investigate ethanol action on BK channel complexes containing β1/β4 chimeras where the swapped region was progressively smaller. Therefore, I narrowed down the specific region(s) (C-end, TM1, EC loop, TM2, N-end) in the BK channel β1 subunit that was responsible for

ethanol-induced decrease in BK channel steady-state activity. SA3 is addressed in Chapter 6.

2.2.4. Specific Aim 4

Address the involvement of the β1 subunit region(s) that mediates ethanol-induced BK channel inhibition in alcohol-induced cerebral artery constriction

After identifying the specific region in the BK β1 subunit that is responsible for ethanol-induced BK channel inhibition, I used a combination of reversible permeabilization and isolated artery pressurization to determine the contribution of such specific subunit domain to ethanol-induced cerebral artery constriction. Thus, I applied 50 mM ethanol to middle cerebral arteries isolated from *KCNMB1* knock-out mouse, these arteries being previously transfected with *wt* β1 or different chimeric β1/β4 proteins. Arteries from *KCNMB1* knock-out transfected with *wt* β1 and arteries from *wt* (C57BL/6) mouse served as positive controls for ethanol action while arteries from *KCNMB1* knock-out mice and *KCNMB1* knock-out mice arteries transfected with empty vector served as negative controls. SA4 is addressed in Chapter 6.

CHAPTER 3.   MATERIALS AND METHODS

3.1.   Vertebrate Animals

3.1.1. Ethical Aspect of Research

The animal care and use of animals, and performed research were conducted in accordance with policies from the Institutional Animal Care and Use Committee (IACUC) at the University of Tennessee Health Science Center (UTHSC) and provision of animal welfare act (USDA). UTHSC is an Institution accredited by the Association for Assessment and Accreditation of Laboratory Animal Care (AAALAC). Our AAALAC-accredited facility is staffed with three full-time veterinarians, two of them being board-certified in laboratory animal care. The veterinary care of all vertebrate animals on campus was handled by the Department of Comparative Medicine (DCM). DCM meets all applicable federal and state laws on animal care, and fully complies with the Publich Health Service (PHS) policy on Humane Care and Use of Laboratory Animals. In order to minimize the transmission of infectious diseases, animals were housed by health status and species.

3.1.2. Information of Veterinary Care of Animals

Xenopus leavis frogs were maintained in aquaria containing artificial pond water and fed with calf's liver and a nutritionally balanced frog brittle to satiation twice a week. The health of frogs under these conditions was very good. The health status of the frogs, prior surgery was performed following standard evaluations, such as swimming behavior, appetite and amount of shedding.

Mice (*wt* CL57/B or *KCNMB1* knock-out) were housed on a 12 hour light/dark cycle, with water and pellet food *ad libitum*. Their health status prior experimentation was performed following standard evaluations, such as appearance, behavior, activity, appetite, excreta, and weight.

3.1.3. Procedures to Minimize Discomfort, Distress, Pain and Injury

Frogs were anesthetized with hypothermia (ice water) prior to surgery. Immediately after surgery and suturing, frogs are immersed in pond water containing MS-222 (200-300 mg/l, according to frog size) as anesthetic for 5 minutes, and the animal body temperature is brought gradually back to room temperature to avoid shock. Then, animals were switched back to pond water. Frogs recovered quickly from surgery with no complications.

Several hours before decapitation, mice are housed in the lab where the procedure was performed. They were handled several times by the operator before being killed. These simple measures minimized the stress experienced by the animal before the actual experiment.

3.1.4. Method of Euthanasia

When the removal of ovarian material was complete, anesthetized animals with MS-222 were euthanized by decapitation. The method is consistent with the recommendations of the Panel of Euthanasia of the American Veterinary Medical Association (AVMA).

Mice were euthanized by decapitation using sharp scissors. The method is also consistent with the recommendations of the Panel of Euthanasia of the AVMA.

3.2. Cloning of cDNA and Transcription

3.2.1. cDNA Coding for BK Channels

Cerebral artery smooth muscle cell slo1 isoform, cbv1 (AY330293) and associated β1 (FJ154955) cDNA were cloned from rat cerebral arteries. Briefly, first, basilar and middle cerebral arteries were dissected out from rat brain on ice. Smooth muscle cells from these arteries were isolated and identified under inverted microscope using Hoffman optics. Individually isolated myocytes were aspirated in to Eppendorf tubes containing approximately 50 μL PicoPure extraction buffer (Arcturus). Total RNA from approximately 100 myocytes was obtained using PicoPure kit (Arcturus). Then, reverse transcription of first strand cDNA was carried out using superscriptII reverse transcriptase with oligo(dT) primer (Invitrogen) (Jaggar *et al.* 2005). Cbv1 cDNA inserted into the pBScMXT vector was linearized with SalI and transcribed in vitro using T3 polymerase (mMessage-mMachine; Ambion, Austin, TX). Cbv1 cDNA inserted into pBScMXT is cleaved by BamHI (Invitrogen) and XhoI (Promega), and directly reinserted into pOX for expression in *X. laevis* oocytes. pOX vector-containing cbv1 was linearized with NotI (Promega) and then transcribed in vitro using T3 polymerase.

Slo2.1, slo 2.2, and slo3 cDNAs were generous gifts from Len Kaczmarek (Yale University School of Medicine, New Haven, CT) and Larry Salkoff (Washington University School of Medicine, St. Louis, MO). These constructs were recloned into pOX vector for oocyte expression. The cDNA-containing vectors were linearized with NotI and were transcribed using T3 polymerase and the mMessage mMachine kit (Ambion, Austin, TX) (Liu *et al.* 2013).

15

3.2.2. cDNA Coding for BK Channel Accessory Beta Subunits

BK $\beta 1$ cDNA cloned into the EcoR I and Sal I sites of the pCI-neo vector was linearized with Not I and transcribed using T7. Then, BK $\beta 1$ cDNA was re-cloned into pOX vector for oocyte expression. pOX- $\beta 1$ was then linearized and transcribed in vitro using either T7 polymerase (mMessagemMachine; Ambion, Austin, TX) (Bukiya *et al.* 2009; Bukiya *et al.* 2013).

Wt $\beta 2$ cDNA in pXMX vector was a generous gift from Christopher Lingle (Washington University School of Medicine, St. Louis, MO) linearized with MluI and transcribed with T7. $\beta 2$ subunit with the inactivation bowl removed ($\beta 2$-IR), $\beta 3$, $\beta 4$, and $\beta 1/\beta 4$ chimeric cDNAs ($\beta_1 TMs_4$, $\beta_4 TMs_1$, $\beta_4 TM1_1$ and $\beta_4 TM2_1$) were generous gifts from Ligia Toro (University of California, LA). $\beta 2$-IR in pXMX vector was linearized with NotI and transcribed with T7. $\beta 3$ cDNA inserted into the pOX and was linearized with SalI and transcribed with T7. $\beta 4$ cDNA was subcloned into pOX vector and linearized by NotI and transcribed using T3. $\beta 1/\beta 4$ chimeric cDNAs were inserted into pOX vectors. Linearization of pOX vectors containing chimeric $\beta 1/\beta 4$ was carried out with NotI and linear cDNAs were transcribed using T3. $\beta 1/\beta 4$ chimeras by swapping different domains of $\beta 1$ and $\beta 4$ in such a way that swapped region became progressively smaller.

Different $\beta 1/\beta 4$ chimeras we used were: 1. $\beta_1 TMs_4$, which contained h$\beta 4$ TMs on h$\beta 1$ "background" (i.e., h$\beta 1$ EC loop and IC ends); 2. $\beta_4 TMs_1$, which contained h$\beta 1$ TMs on h$\beta 4$ "background" (i.e., h$\beta 4$ EC loop and IC ends); 3. $\beta_4 TM1_1$, which contained h$\beta 1$ TM1 on h$\beta 4$ "background" (i.e., h$\beta 4$ TM2, EC loop and IC ends); 3. $\beta_4 TM2_1$, which contained h$\beta 1$ TM2 on h$\beta 4$ "background" (i.e., h$\beta 4$ TM1, EC loop and IC ends); 4. $\beta_4 L_1$, which contained EC loop from h$\beta 1$ on h$\beta 4$ "background" (i.e., h$\beta 4$ TMs and IC ends; 5. $\beta_1 L_4$, which contained EC loop from h$\beta 4$ on h$\beta 1$ "background" (i.e., h$\beta 1$ TMs and IC ends).

All cDNA sequences were confirmed by automatic sequencing at the UTHSC Molecular Research Center.

3.3   Oocyte Isolation from *Xenopus Leavis* and RNA Injection

3.3.1. Model Justification: *Xenopus Leavis* Oocytes

We choose *Xenopus laevis* oocytes to heterologously express BK channel because: 1) these cells express negligible amount of endogenous BK channels; 2) they contain endogenous ion channels (primarily mechano-gated cation and Cl^-_{Ca} channels (Miledi and Parker 1984; Meissner *et al.* 1989) that can be easily differentiated from BK channels based on conduction and gating; 3) by varying amount of cRNA and interval between cRNA injection and patch-clamping, we can control amount of channel expression; 4) using oocytes, we already characterized ethanol effect on cbv1 and cbv1+$\beta 1$ channels (Bukiya *et al.* 2009); 5) we functionally expressed and characterized

the heteromeric channels containing chimeric βs that are necessary to address SA3 (Bukiya *et al.* 2009); 6) we collected lithocholate (LCA) data on cbv1 and cbv1+βs (Bukiya *et al.* 2007; Bukiya *et al.* 2008; Bukiya *et al.* 2009). LCA and Ibtx are pharmacological tools that we will use to confirm the functional presence of β1-, β4-, and β1/ β4 chimera-containing BK channels; 8) Dr.Dopico and his personnel have >20 yr. experience with the oocyte model.

3.3.2. Oocyte Isolation from *Xenopus Leavis* Oocytes

Female *Xenopus laevis* frogs were purchased from *Xenopus* Express (Brooksville, FL). They were maintained in artificial pond water on a 12-hour light/dark cycle. In this environment, frogs do not show the behavior of seasonal breeding, thus oocytes were usually available throughout the year. Stages V and VI oocytes were predominantly collected because oocytes at these particular stages transcribe mRNA into protein/channels with higher efficiency. Surgical procedure was as follows: First, frogs were anesthetized by placing them on ice after exposure to ethyl 3-aminobenzoate methanesulfonate salt (MS-222) (250 mg/l, pH 7.4). A small surgical incision (of ~less than 1 cm) was made in the abdomen and the oocytes were extracted. Extracted oocytes were kept in a Ca^{2+}-free ND-96 solution (mM): 82.5 NaCl, 2 KCl, 1 $MgCl_2$, 5 HEPES, pH 7.4, which contains 2 mg/ml collagenase (type IV; Sigma-Aldrich), at room temperature on a horizontal shaker (70 oscillations per minute) for 15-20 minutes to remove the follicular layer. After defolliculation, the individually isolated oocytes were transferred to Ca^{2+}-containing ND-96 solution (mM): 82.5 NaCl, 2 KCl, 1.8 $CaCl_2$, 5 HEPES, pH 7.4, supplemented with 2.5 mM sodium pyruvate and 10,000 I.U. of penicillin and 10 mg of streptomycin in 500 ml (Dopico *et al.* 1996; Bukiya *et al.* 2009).

3.3.3. cRNA Injection

cRNA was dissolved in diethyl polycarbonate-treated water at 10 (cbv1/slo2.1and slo2.1/slo3) or 30 (βs or engineered βs) ng/μl; 1 μl aliquots are stored at -80°C. Cbv1; slo2.1/slo2.2; and slo3 cRNAs alone were injected approximately about 10ng/μl. On the other hand, co-injection of cbv1 (10ng/μl) with β1, β2, β2-IR, β3, β4, or engineered β (30ng/μl) cRNAs was conducted to achieve molar ratios of ≥6:1 (β:α) to ensure that all cbv1 subunits are saturated with βs (Dopico 2003; Liu *et al.* 2008; Bukiya *et al.* 2009). cRNA of ~23 nl/cell was injected into the oocyte cytoplasm using a drummond nanoinjector (Drummond Scientific Co., Broomall, PA). The interval between cRNA injection and patch-clamp electrophysiology recording was approximately 36 to 48 hours. During this time period, the injected oocytes were incubated at 14-16°C.

3.4.   Patch-Clamp Electrophysiology

3.4.1. Data Acquisition

Before electrophysiology recordings, oocytes were placed into a petri dish containing a hypertonic solution (mM): 200 K^+ aspartate, 20 KCl, 1 $MgCl_2$, 10 EGTA, 10 HEPES, pH 7.4, for 15-20 minutes. With this hypertonic treatment, the oocytes shrink, allowing the removal of the vitelline membrane with forceps and thus, exposing the oocyte membrane for subsequent patch-clamp recording. Then, the oocytes were placed into Ca^{2+}-containing ND-96 solution for 10–15 minutes before recording ionic currents. Ionic currents were recorded from excised, inside-out (I/O) macro patches. The following paragraphs show the compositions of bath and electrode solutions for recording different constructs.

Homomeric cbv1 and β subunit-containing BK channels: the bath and electrode solutions had the same composition (mM): 135 K-gluconate, 5 EGTA, 2.28 $MgCl_2$, 15 HEPES, 1.6 HEDTA, pH 7.35 (Liu *et al.* 2008; Bukiya *et al.* 2009).

For the experiments in which cbv1 channels were probed with ethanol at different $[Mg^{2+}]$, both bath and electrode solutions contained (mM): 140 K-methanesulfonate, 20 HEPES, 2 KCl, 5 EGTA; pH 7.2. The desired $[Mg^{2+}_i]$ was obtained by adding $MgCl_2$ (Shi *et al.* 2002).

Rslo2.1:rslo2.2 channel recording: bath and electrode solutions contained (mM): 130 K-gluconate, 5 EGTA, 10 HEPES, 29 glucose, and variant amounts of Na-gluconate: 10, 70, and 140 mM; pH 7.3 (Santi *et al.* 2006).

Mslo3 channel recording: Intracellular solution contained (mM): 140 K-methanesulfonate, 20 KOH, 10 HEPES (H^+), titrated with methanesulfonic acid or KOH to pH=6.0, 7.0, 8.0, or 9.0, which correspond to $[OH^-]$= 0.01, 0.1, 1, and 10 μM, respectively. Extracellular solution contained (mM): 140 K-methanesulfonate, 20 KOH, 10 HEPES (H^+) and 2 $MgCl_2$, titrated with methanesulfonic acid to pH=7.0 ($[OH^-]$= 0.1 μM) (Xia *et al.* 2004).

In all patch-clamp electrophysiology studies that require tight buffering of Ca^{2+} in solution, the free Ca^{2+} in solution was adjusted to the desired value by adding $CaCl_2$. When the desired free Ca^{2+} did not exceed 1 μM, HEDTA was omitted from the solution. The final concentration of the $MgCl_2$ was set to 1 mM. In all experiments, nominal free $[Ca^{2+}]$ is calculated using MaxChelator (WEBMAXC, Stanford University, Stanford, CA) and experimentally validated using Ca^{2+}-selective electrodes (Corning Incorporated Science Products Division, Corning, NY) (Dopico 2003). The use of gluconate- as main anion substituting for Cl^- allows minimizing the contamination of recordings by the activity of endogenous Cl^- channels.

We chose a wide range of Ca^{2+} concentration i.e 0-100 µM at the intracellular side of the excised membrane patch because this range covers the Ca^{2+} concentration estimated for the vicinity of BK channel both at resting condition and during cerebral artery myocyte contraction (Perez *et al.* 2001).

Immediately before experiments, patch-clamp electrodes were pulled from glass capillaries (Drummond Scientific Co.). Then, the tip of the electrode was fire-polished on a microforge (World Precision Instruments, Sarasota, FL) to achieve resistance of 2–6 MΩ for macroscopic current recording and 8-10 MΩ for single channel recording.

We chose I/O macro-patch recordings because: 1) I/O patches allow us to probe ethanol with tightly buffered $[Ca^{2+}]$ at the cytosolic side of the channel, controlling BK activity and its Ca^{2+}-dependent modulation by ethanol; 2) it is easier to freshly dilute ethanol in bath solution and apply it to the inner leaflet than perfusing a patch-pipette (as O/O or whole-cell recording would require to modify internal Ca^{2+}). Consistent with ethanol fast crossing of the cell membranes, BK response is identical whether ethanol is applied to the inner or outer leaflet (Dopico *et al.* 1996; Dopico *et al.* 1998; Dopico *et al.* 1999; Dopico 2003); 3) macroscopic currents are routinely used to conduct pharmacological studies on BK channel by us and others (Brenner *et al.* 2000; Cox and Aldrich 2000; Bukiya *et al.* 2009).

We chose an ethanol concentration of 50 mM because it is reached in blood circulation after episodic moderate-heavy drinking, and linked to cerebrovascular pathology in humans (Moore and Pearson 1986; Marmot and Brunner 1991; Zakhari 1997; Suter and Vetter 1999; Gil-Nunez and Villanueva 2001; Reynolds *et al.* 2003). Additionally, our previous studies demonstrating a direct ethanol action on native channels were conducted at this [EtOH] (Liu *et al.* 2004; Bukiya *et al.* 2009; Bukiya *et al.* 2011), allowing comparison and proper interpretation of the new data obtained with recombinant channel protein. We choose equimolar concentration of urea as a control to isosmotically replace ethanol.

After excision from the cell, the membrane patch was consecutively exposed to a stream of bath solution containing control (50 mM urea) then 50 mM ethanol, then control (with urea) as washout. Solutions were applied onto the patch cytosolic side *via* a micropipette tip with an internal diameter of 100 mm using a pressurized, automated DAD12 system (ALA Scientific Instruments, Farmingdale, NY). For all the studies, no nucleotides or other "regenerating" systems are added to the solutions because recombinant BK activity was found not to run-down under these conditions (Dopico *et al.* 1996; Dopico 2003; Liu *et al.* 2006; Liu *et al.* 2008). All the experiments were performed at room temperature (20°–22°C).

Single channel or macroscopic currents were recorded using an EPC8 amplifier (HEKA, Lambrecht, Germany), low-pass filtered at 1 kHz with an 8-pole Bessel filter (Frequency Devices 902LPF), and digitized at 5 kHz using a Digidata 1320A A/D converter and pCLAMP 8.0 (Molecular Devices). Macroscopic currents were evoked from a holding potential of -80 mV by 100 milliseconds long, 10 mV depolarizing steps

ranging from -150 to +150-200 mV. The current amplitude was averaged within 50–100 milliseconds after the beginning of the depolarizing step.

3.4.2. Estimating the Number of BK Channels in the Excised Patch

First, single channel recordings were obtained at very far negative voltages (from -120 mV to -20 mV) at nominal zero Ca^{2+}_i concentration, estimated ~5nM (Meera *et al.* 1996; Cox and Aldrich 2000; Bao and Cox 2005; Orio and Latorre 2005). Then the patch was switched to the solution containing 100 µM Ca^{2+}_i (for cbv1) and 10 µM Ca^{2+} (for cbv1+β1) and thus we recorded macroscopic currents recordings at moderate to high positive voltages (~30 mV to 200 mV). The number of channels (N) in the given excised patch was determined by the **Equation 3-1**:

$$N = I/(iP_o) \qquad \text{(Eq. 3-1)}$$

Where, *I* represents macroscopic current at a given voltage, and *i* and P_o represent single channel current and open channel probability at the same voltage, respectively.

3.4.3. Data Analysis

Patch-clamp data were analyzed with pCLAMP 9.2 (Molecular Devices). From, macroscopic current recording, G/G_{max}-V curves were fitted by Boltzmann function of the type of **Equation 3-2**.

$$G(V) = G_{max}/[1 + exp^{(\frac{V_{0.5}-V}{k})}] \qquad \text{(Eq. 3-2)}$$

Boltzmann fitting routines were run using the Levenberg-Marquardt algorithm to perform nonlinear least square fits. An index of channel activity was obtained from G/G_{max}-V plots in the form of $V_{0.5}$ (Bukiya *et al.* 2009), which is the membrane voltage needed to evoke half-maximal macroscopic current. Smaller $V_{0.5}$ values indicate increased activity of the channel.

Time constant activation (τ_{act}) and deactivation (τ_{deact}) in milliseconds were obtained by single exponential fits of current activation phase and deactivation time course respectively.

For single channel recordings, the product of number of channels in the patch (N) and channel open probability (P_o) was used as an index of channel steady-state activity. Using a built-in function in Clampfit 9.2 (Molecular Devices), NP_o was obtained from 30 second of gap-free recording under each experimental condition. Data were expressed as mean±SEM (n=number of oocytes/patches), plotted and fitted using Origin 8.5 (Originlab) and InStat3 (GraphPad).

3.5. Reversible Permeabilization

3.5.1. Solution Composition

The solution compositions used for reversible permeabilization are as follows. Solution 1 (in mM): 10 EGTA, 120 KCl, 5 ATP, 2 $MgCl_2$, 20 TES (pH 6.8 at 4°C); solution 2 (in mM): 120 KCl, 5 ATP, 2 $MgCl_2$, 20 TES (pH 6.8 at 4°C); solution 3 (in mM): 120 KCl, 5 ATP, 10 $MgCl_2$, 20 TES (pH 6.8 at 4°C); solution 4 (in mM): 140 NaCl, 5 KCl, 10 $MgCl_2$, 5.6 glucose, 2 MOPS (pH 7.1 at 22°C) (Lesh *et al.* 1995; Welsh *et al.* 2002).

3.5.2. Principle of Reversible Permeabilization

The reversible permeabilization technique is based on the principle that when the arteries are placed in solutions 1, 2, and 3 (Lesh *et al.* 1995; Welsh *et al.* 2002), ATP-binds to cell surface receptors and removes membrane-associated divalent cations. Thus, by increasing the membrane permeability of smooth muscle cells, selected vectors are delivered inside the myocyte for expression. Later, by removal of extracellular ATP and addition of high $[Mg^{2+}]$ in solution 4 reverses the increased membrane permeability followed by graded restoration of physiological concentrations of extracellular Ca^{2+}. Arteries are then placed in DMEM/F-12 culture medium supplemented with penicillin/streptomycin (1%) for 3-4 days to allow expression of our desired genes. Previous studies demonstrated that reverse permeabilization does not alter the ultrastructural features and contractile properties of smooth muscle cells (Lesh *et al.* 1995).

3.5.3. Procedure

Freshly isolated and de-endothelized mice middle cerebral arteries from *KCNMB1* K/O mouse were placed into the following four reversible permeabilization solutions sequentially: solution 1 at 4°C for 20 minutes, solution 2 containing expression vector (20 µg/ml) at 4°C for 90 minutes, solution 3 containing expression vector (20 µg/ml) for 30 minutes at 4°C, and solution 4 containing expression vector (20 µg/ml) for 30 minutes at room temperature. Ca^{2+} concentration in solution 4 was then incrementally increased to (in mM): 0.01, 0.1 and 1.8 at 15-minute intervals. Arteries were then placed in DMEM/F-12 culture medium containing penicillin/streptomycin (1%). Then the cultured dishes were incubated in a 74% N_2/21% O_2/5% CO_2 incubator at 37°C for 3-4 days to allow the expression of gene of interest. After 3-4 days, expression of desired genes in the intact artery was confirmed by Western blotting.

3.6.   Western Blotting

3.6.1. Procedure

Cerebral arteries were homogenized using RIPA buffer plus protease inhibitor (Thermo Fisher Scientific, Waltham, MA) and whole cell lysate was obtained. Protein samples were heated at 100^0C for 5 minutes. Protein samples (30 µg/lane) were then separated on a 4-15% SDS-polyacrylamide gel (Bio-rad, Hercules, CA). To monitor the progress on the gel prestained molecular weight markers were used (Lambda Biotech, SaintLouis, MO). Gel was run in SDS-Tris-Glycine containing MOPS-SDS running buffer at 200 V for 30 minutes. Following this step, proteins were transferred onto PVDF (polyvinylidene difluoride) membranes using transfer buffer (containing Tris-Glycine-Methanol) at 60 V for 90 minutes. The membranes were then blocked with 5% non-fat dry milk made in tris-buffered saline (TBS) containing 0.1% Tween 20 (TBS-T) for 2 hours at room temperature. Then, membranes were incubated with appropriate primary antibodies overnight at 4°C in Tris-buffered saline with 0.1% Tween 20 (TBS-T) and 5% nonfat dry milk. A $\beta4$ antibody (1:200 dilution, Alamone) was used to recognize the N-terminus of $\beta4$ subunit in β_4TM1_1 and β_4TM2_1 chimeras; a rabbit polyclonal aniti BK-$\beta1$ produced against EC loop of BK-$\beta1$ subunit (1:500 dilution, Abcam, Cambridge, MA); and mouse monoclonal anti-actin antibody recognizes the epitope located at N-terminus of the actin (1:500 dilution, Milipore, Billerica, MA). Following overnight incubation with primary antibody, membranes were washed six times with TBS-T for 5 minutes each. Membranes were then incubated with appropriate horseradish peroxidase-conjugated secondary antibodies (1:10,000 dilution, Milipore) for 1-2 hours at room temperature. After secondary antibody incubation, membranes were washed with six times with TBS-T for 5 minutes each. Proteins were then visualized using SuperSignal West Pico Chemiluminescent Substrate kit (Thermo Fisher Scientific, Waltham, MA).

3.6.2. Densitometric Analysis

Quantity One software v4.6.9 (Bio-Rad, Hercules, CA) was used to calculate the band density. Briefly, rectangular boxes of the same size were placed around bands in each lane, and then the background-subtracted band density was calculated. Average band density was obtained from the same blot acquired at different exposure times. Then, averaged band density for a particular protein sample was normalized to the actin band density of the corresponding sample.

3.7.   Artery Pressurization and Diameter Measurement

3.7.1. Model Justification

We choose the *KCNMB1* K/O mouse model because: 1) this mouse model has been proven successful in biomedical research to study cell and organism physiology in absence of BK channel β1 subunit expression (Xu *et al.* 1993; Brenner *et al.* 2000; Brenner *et al.* 2000; Pluger *et al.* 2000; Amberg and Santana 2003), including ethanol research studies in our laboratory for several years (Bukiya *et al.* 2009; Bukiya *et al.* 2011); 2) we have our own colony of *KCNMB1* K/O mice, ensuring availability of animals; 3) we are proficient in determination of cerebral artery diameter and BK function using this model (Bukiya *et al.* 2009; Bukiya *et al.* 2011).

Middle cerebral arteries were chosen because: 1) health relevance: middle cerebral artery is the artery most often occluded in stroke (www.strokecenter.org); 2) we conducted ethanol studies using this artery in control (C57BL/6) and *KCNMB1* K/O mice (Bukiya *et al.* 2009; Bukiya *et al.* 2011).

Adult male 8-12 week-old *KCNMB1*-K/O and C57BL/6 control mice were decapitated using sharp scissors. From mouse brain, middle cerebral arteries were isolated and cut into 2 mm long segments on ice under microscope (Nikon SMZ645; Nikon) Sufficient care was taken not to choose arteries with branches or tear in the artery's wall. Endothelium was removed by passing an air bubble into the vessel lumen for 90 seconds. Endothelium-denuded artery was cannulated at each end to the temperature-controlled perfusion chamber (Living Systems Instrumentation, Burlington, VT) containing PSS. Artery cannulated-chamber was mounted on the microscope (Nikon TS100). A Dynamax RP-1 peristaltic pump (Rainin Instruments, Inc., Oakland, CA) was used to perfuse the Physiological Saline Solution (PSS) (mM): 119 NaCl, 4.7 KCl, 1.2 KH_2PO_4, 1.6 $CaCl_2$, 1.2 $MgSO_4$, 0.023 EDTA, 11 glucose, and 24 $NaHCO_3$. PSS was equilibrated at pH 7.4 with a 21/5/74% mix of $O_2/CO_2/N_2$ and maintained at 35–37°C. Intravascular pressure was applied using water filled reservoir and pressure was monitored using a pressure transducer (Living Systems Instrumentation, Burlington, VT). A CCD camera (Sanyo VCB-3512T; Sanyo Electric Co., Moriguchi, Japan) was attached to an inverted microscope (Nikon Eclipse TS100; Nikon) to monitor changes in artery diameter. The external wall diameter of the artery was measured at 1 kHz in real time using the automatic edge-detection function of IonWizard software (IonOptics, Milton, MA).

3.7.2. Procedure

At the onset of the experiment, arteries were incubated at an intravascular pressure of 10 mmHg for 10 minutes. After the arteries attained the stable diameter under this condition, intravascular pressure was increased to ~60 mm Hg. This pressure was maintained throughout the experiment. The increased intravascular pressure resulted in

arterial dilation. The artery was then allowed to sense the elevated intravascular pressure and develop pressure-induced arterial constriction over a period of time (equivalent to myogenic tone). Once myogenic tone remained steady for a period of 15-30 minutes, pharmacological agents were perfused. Drugs were dissolved from stock solutions into PSS to achieve their final concentration and applied *via* perfusion chamber containing artery. After drug perfusion, the effect the particular drug was evaluated at the time when it evoked a steady diameter value, whether reduction (constriction) or enhancement (dilation).

After pressurization, first, artery contractility was tested with 60 mM K^+, which shifts the myocyte membrane potential from -40 to -20 mV and produces maximal contraction (Liu *et al*., 2004). After washout, bath application of 50 mM ethanol for 10 minutes in PSS was performed. After ethanol washout, 45 µM Lithocholate (LCA) was perfused. The maximal change in diameter reached within 10 minutes from the start of drug application was considered as the dependent variable. At the end of the experiment, passive diameter of the vessel was determined in the Ca^{2+}-free PSS (no $CaCl_2$ added, plus 10 mM EGTA to chelate trace amounts Ca^{2+}) (Bukiya *et al.* 2007; Bukiya *et al.* 2011). Arteries that failed to constrict for KCl and/or dilate in response Ca^{2+}-free PSS were discarded from analysis. The absence of a functional endothelium was determined with an application of the endothelium-dependent vasodilator acetylcholine (10 µM) *vs.* the endothelium-independent vasodilator sodium nitroprusside (NPS) (Liu *et al.* 2004; Bukiya *et al.* 2007).

3.7.3. Analysis

Ion Wizard software was used to measure artery diameter traces. Diameter measurement was obtained when artery attained stable diameter before and after application of each drug. Myogenic tone (in %) was determined using the **Equation 3-3**:

$$\% \ Change \ in \ Diameter = \left[1 - \left(\frac{Active \ diameter}{Passive \ diameter} \right) \right] X 100 \qquad (\textbf{Eq. 3-3})$$

3.8. Chemicals

100% pure ethanol was purchased from American Bioanalytical (Natick, MA). Lithocholate (LCA; 5β-cholanic acid-3α-ol) was purchased from Steraloids (Newport, RI). All other chemicals were purchased from Sigma Aldrich. Just before the experiment, LCA was initially dissolved in DMSO to obtain stock solution of 333 mM. Stock solution was sonicated for 30 minutes. Then, to obtain final concentration, stock solution was further diluted with PSS solution. As a control for LCA experiments, DMSO-containing PSS solution was perfused. Concentration of DMSO in "control" experiment matched the corresponding amount of DMSO in LCA-containing solution.

3.9. Statistical Analysis

Data were plotted and fitted using OriginLab 8.5. Statistical analysis was performed using GraphPad InStat software. In order to compare paired or unpaired data from two populations, Student's t-test with two-tail p value was used. On the other hand, ordinary one-way ANOVA followed by multiple Bonferonni test was used for all multiple data comparisons. $p < 0.05$, was considered statistical significance. Values were expressed as mean±SEM., and n=number of patches/arteries. Each patch was obtained from a different oocyte, and each pressurized artery measurement was obtained from a middle cerebral artery segment dissected out from a different animal.

CHAPTER 4.   THE CHANNEL'S ACTIVATING ION DETERMINES ETHANOL MODULATION OF BK CHANNELS

4.1.   Overview

Ethanol levels reached in circulation during moderate to heavy alcohol intoxication (30-60 mM) as during binge drinking modify BK channel steady-state activity (NP_o) and thus, BK channel-dependent physiology and behavior. In general, ethanol increases NP_o of neuronal BK channels while decreasing NP_o of vascular smooth muscle BK channels. There are various factors that play a role in ethanol's final effect on BK NP_o, including, channel subunit composition, post-translational modification of BK subunits, and the channel lipid microenvironment (Brodie *et al.* 2007). However, data from reductionist systems, such artificial bilayers of simple lipid composition where BK channel-forming (slo1) subunits can be functionally evaluated, reveal that ethanol modulation of BK NP_o solely requires slo1 subunits and the channel's physiological activator, that is Ca^{2+}_i (Crowley *et al.* 2003; Crowley *et al.* 2005; Liu *et al.* 2008). Moreover, ethanol action on slo1 NP_o is a function of activating $[Ca^{2+}]_i$ (Liu *et al.* 2008; Bukiya *et al.* 2009).

Slo2.1 (Slick), Slo2.2 (Slack), and Slo3 gene products render ion channel proteins that display a phenotype common to slo1: high conductance for K^+ and dual regulation of gating by transmembrane voltage and intracellular ion-recognition, with slo2 and slo3 being activated by Na^+_i and OH^-_i, respectively (Salkoff *et al.* 2006). Whether the control of ethanol action on BK channels by activating ion is unique to slo1 or, rather, extends to the other members of the slo family remains unknown. To address this question, I expressed BK channel pore-forming α subunits cloned from rat cerebral artery myocytes (cbv1) in *Xenopus laevis* oocytes. The cbv1 channel variant showed all properties of other slo1 channels, such as hslo1 (Brenner *et al.* 2000; Cox and Aldrich 2000), mslo1 (Liu *et al.* 2008; Liu *et al.* 2013) including independent gating by Ca^{2+}_i and Mg^{2+}_i. Using the same expression system and the inside-out configuration of the patch-clamp technique, which allows tight control of activation ion concentrations by perfusing with the cytosolic side of the channel (where the ion-sensors are located). I also expressed slo2 and slo3 and thus, I probed cbv1, slo2 and slo3 channels with 50 mM ethanol over a wide range of channel activating ion concentration. Then, I constructed conductance (G) or NP_o-voltage (V) plots from macroscopic current amplitude or P_o, depending on the level of channel expression. This study tests the following hypotheses:

- Slo1 channel sensitivity to ethanol is selectively dependent on its activating ion Ca^{2+}_i.
- Ethanol differentially modulates the different members of the slo channel family i.e. slo1, slo2 and slo3

4.2. Results

4.2.1. Ethanol Modulation of Slo1 Channel's Activity Is Selectively Dependent on Its Activating Ion i.e., Ca^{2+}_i

In this study, macroscopic current recordings were obtained from excised inside-out patches over a wide of range activating Ca^{2+}_i concentration (0-100 µM) in presence and absence of 50 mM ethanol. Iso-osmotically ethanol-substituting urea in bath solution was used as control. Voltage protocols were identical to those previously described, (see methods section **3.4.1**). From G-V plots, we obtained the voltage required to achieve half of the maximal conductance/NP_o ($V_{0.5}$). Data demonstrate that ethanol activates cbv1 channel activity at low $[Ca^{2+}]$ i.e., 0.3-10 µM, which is evident as a shift to the left in G/G_{max}-V plots and significant decreases in $V_{0.5}$ values in the $V_{0.5}$-$[Ca^{2+}]$ plot (**Figure 4-1A** and **B, Figure 4-2A** and **B**). First, ethanol did not modulate cbv1 channel activity at zero Ca^{2+}_i (**Figure 4-1D** and **Figure 4-2B**). Second, as $[Ca^{2+}]$ increases, ethanol-induced channels activation turns to mild inhibition, which is evident as small right-shift in the G/G_{max}-V plot and increase in $V_{0.5}$. Ethanol-induced activation-to-inhibition cross-over occurs at ~20 µM (**Figure 4-1A** and **C, Figure 4-2A** and **B**). Thus, ethanol action on cbv1 channels not only is dependent on Ca^{2+}_i presence but is a function of $[Ca^{2+}]_i$, which extends previous findings with mslo1 channels in the same expression system (Liu *et al.* 2008).

4.2.2. Mg^{2+}-/Voltage-Gated Cbv1 Channels Are Ethanol Insensitive

Next we decided to test the possibility that whether ethanol modulates cbv1 channels-gated independently of its physiological activating ion i.e., Ca^{2+}_i. Previous studies have clearly established that BK channels are gated by Mg^{2+}_i and voltage, independently of Ca^{2+}_i (Shi *et al.* 2002). Thus, next we explored ethanol action on Mg^{2+}/V-gated cbv1 channels in similar experimental conditions to those of cbv1 channel.

Before probing the channels with ethanol, functional expression and characteristic phenotype (such as voltage and magnesium sensitivity) of Mg^{2+}/V-gated cbv1 channels was verified. In this particular set of experiments, it should be underscored that the electrode solution did not have any added calcium (see **section 3.4.1**). As their characteristic feature, Mg^{2+}/V-gated cbv1 channels, in presence of increasing concentration of Mg^{2+} on intracellular side of the channel, the activity of channels was increased monotonically. This increase in activity was evident as a decrease in $V_{0.5}$ value as Mg^{2+} concentration was increased from 1 mM thru 100 mM. These results are in agreement with previously reported studies (see control data of **Figure 4-3A, B, C** and **D)** (Shi *et al.* 2002). Then, we explored ethanol action on Mg^{2+}/V-gated cbv1 channels. Here, we obtained macroscopic current recordings over a wide range of activating magnesium concentration (0-100 mM) in presence and absence of 50 mM ethanol (**Figure 4-3A**).
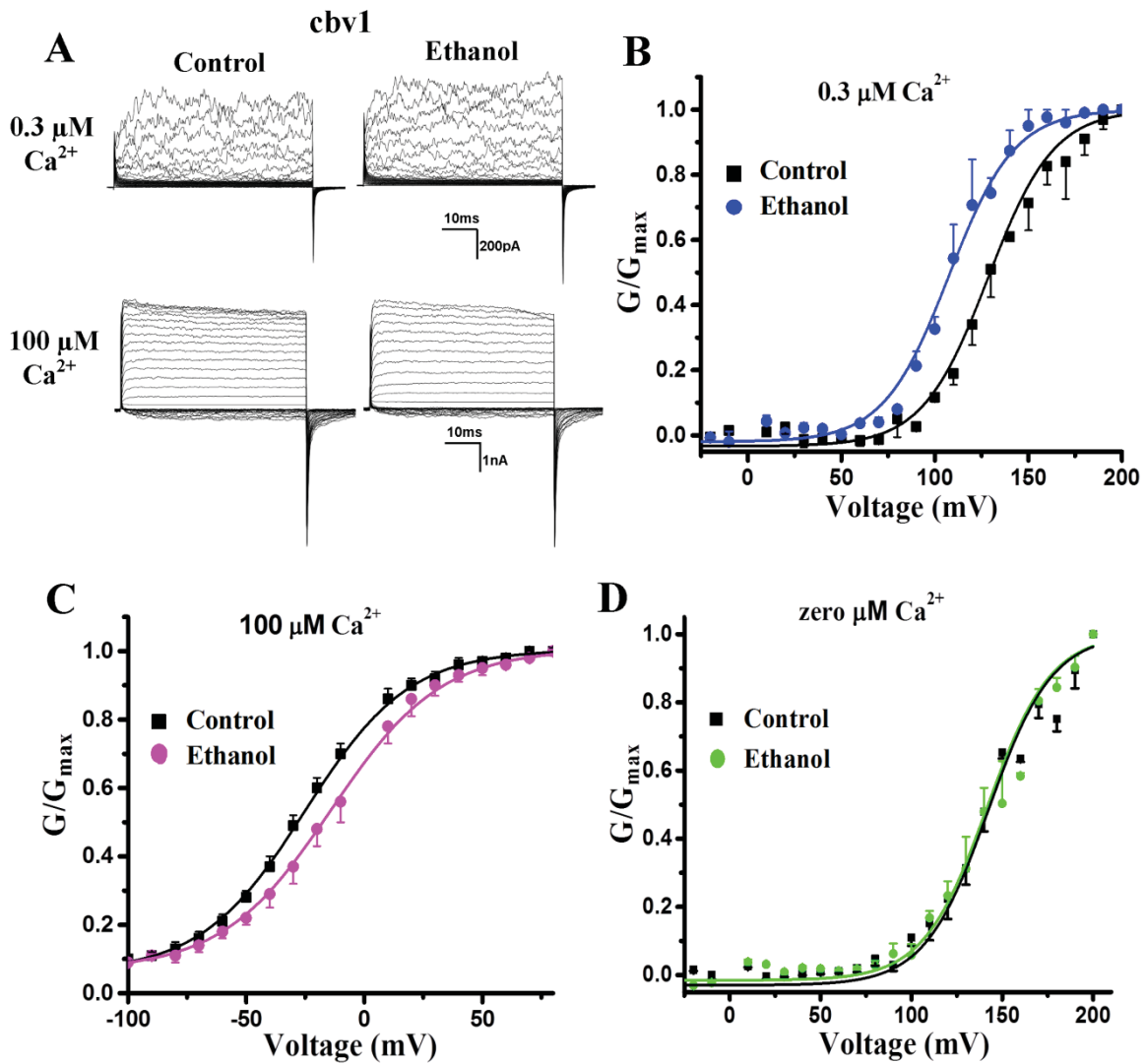
Figure 4-1. **Ethanol effect on BK channel activity is Ca^{2+}_i-dependent**

Notes: Ethanol (50 mM) activates homomeric cbv1 channels at submicromolar (0.3 µM) Ca^{2+}_i while causing mild inhibition at higher Ca^{2+}_i (100 µM). A) Macroscopic current recordings evoked from I/O patches at 0.3 and 100 µM Ca^{2+}_i in absence or presence of 50 mM ethanol following cbv1 expression in *Xenopus* oocytes. B) At 0.3 µM Ca^{2+}_i, ethanol shifts the G/G_{max}-V plot to the left indicating channel activation. C) At 100 µM Ca^{2+}_i ethanol shifts the G/G_{max}-V plot to the right indicating inhibition of channel activity. D) At nominal zero µM Ca^{2+}_i ethanol did not shift the G/G_{max}-V plot indicating ethanol fails to modulate cbv1 channel activity at nominal zero Ca^{2+}_i.
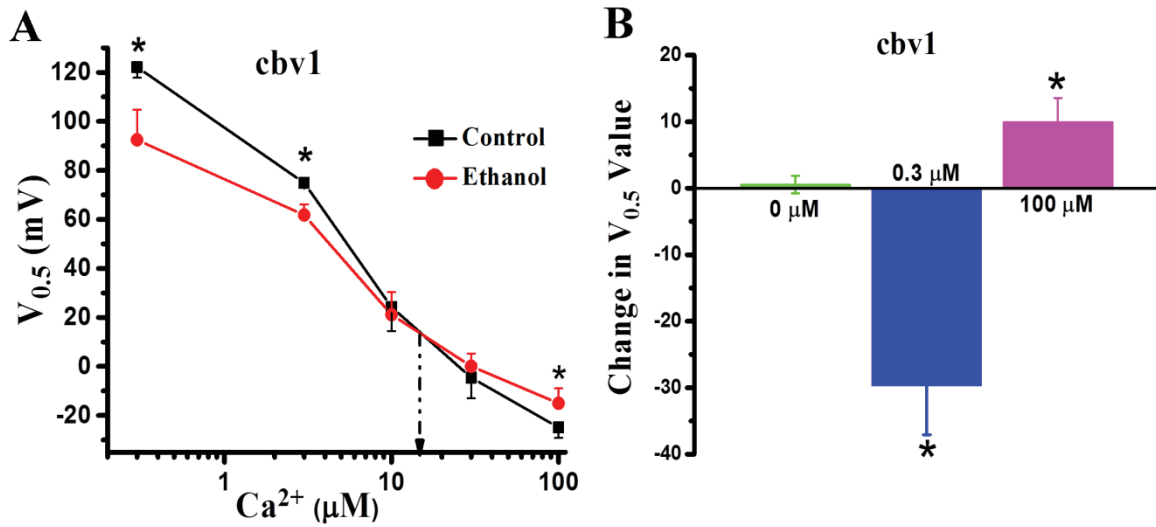
Figure 4-2. **Ethanol action on BK channel activity is function of Ca^{2+}_i**

Notes: Ethanol activates homomeric cbv1 channels at submicromolar Ca^{2+}_i while causing mild inhibition at higher Ca^{2+}_i. A) $V_{0.5}$ *vs.* $[Ca^{2+}_i]$ plot showing that the activation-to-inhibition crossover for ethanol effect on cbv1 channels occurs at ≈ 20 µM Ca^{2+}_i B) Bar graph showing ethanol-induced change in $V_{0.5}$ values from control obtained at 0.3 µM and 100 µM Ca^{2+}_i. Each data point represents the average of no less than 3 patches, each excised from a different cell. *Different from control ($p<0.05$).
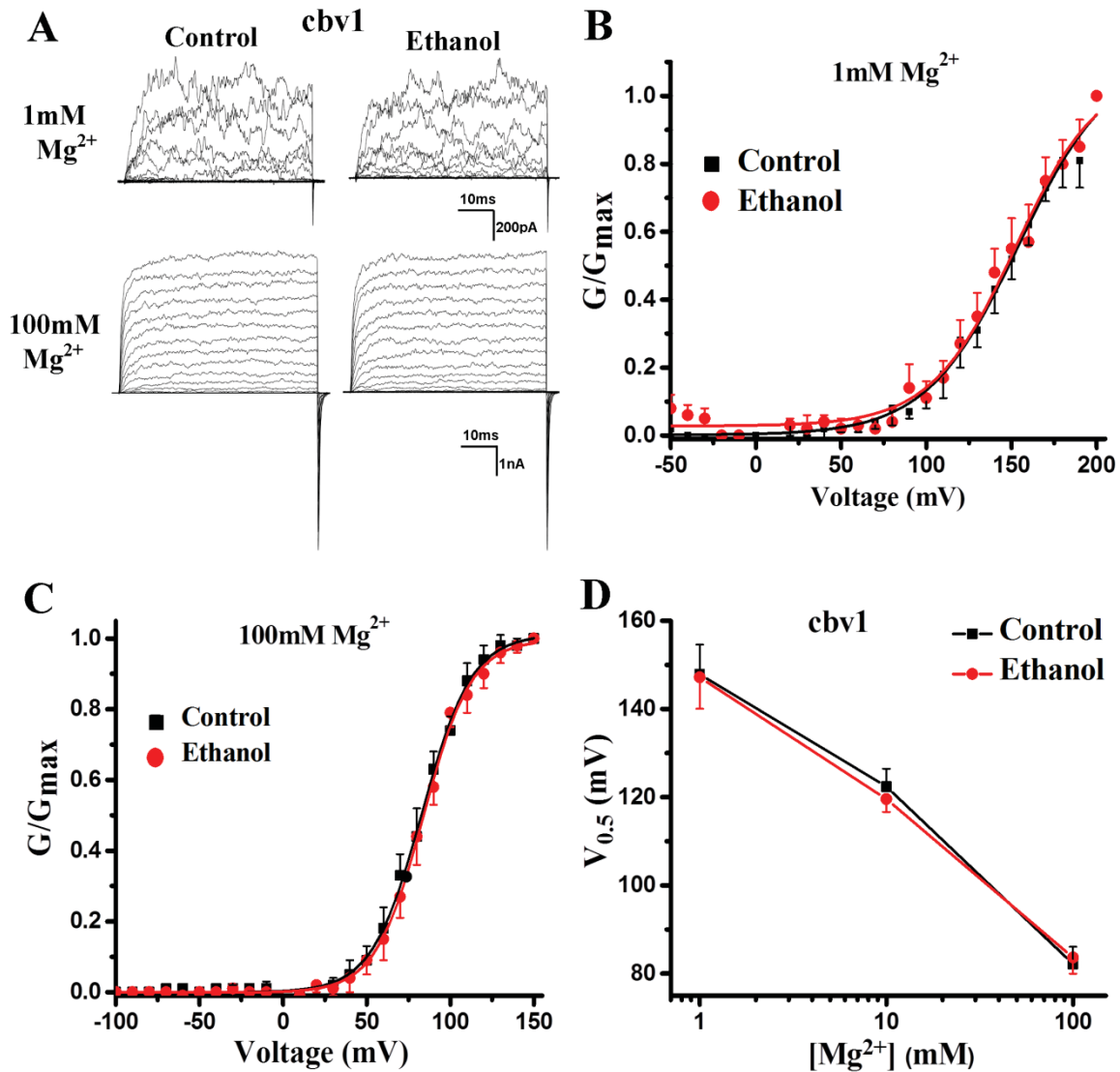
Figure 4-3.   Mg²⁺/voltage-gated cbv1 channels are ethanol-insensitive

Notes: In absence of Ca^{2+}_i, ethanol (50 mM) does not modulate cbv1 channel activity whether evoked at 1, 10 or 100 mM Mg^{2+}_i. A) Macroscopic current recordings from I/O patches recorded at 1 and 100 mM Mg^{2+}_i in absence or presence of 50 mM ethanol following cbv1 expression in *Xenopus* oocytes. B, C) In absence of Ca^{2+}_i, ethanol does not shift the G/G_{max}-V plots whether obtained at physiological (1 mM) or supra-physiological (100 mM) Mg^{2+}_i. D) $V_{0.5}$ *vs*. $[Mg^{2+}_i]$ plot showing the absence of ethanol effect on cbv1 channels over the wide range of $[Mg^{2+}]_i$ chosen.

Our data show that ethanol failed to modulate the BK channel activity over a wide range of activating $[Mg^{2+}]$, which is evident from the lack of significant differences in G/G_{max}-V and $V_{0.5}$-$[Mg^{2+}]$ plots between control and ethanol-containing solution (**Figure 4-3B, C** and **D**). Collectively, these findings suggest that when cbv1 channels are gated by Mg^{2+}/Voltage, their ethanol-sensitivity is lost.

4.2.3. Slo2 Channels Are Ethanol Insensitive over a Wide Range of Their Activating Ion Concentration

We next aimed to address whether ethanol distinctly modulates slo1 channels or, rather, it can also regulate slo2 and slo3 channel activity

First, we evaluated the ethanol action on slo2 channels, which are phylogenetically related to slo1 channels (Santi *et al.*, 2006). Slo2 channels are predominantly expressed in neurons and the heart, thus participate in adaptation of neuronal firing rate and slow afterhyperpolarizations that follow repetitive firing (Bhattacharjee and Kaczmarek 2005; Salkoff *et al.* 2006) and protection of excitable cells against hypoxia (Dryer 1994). Like slo1 channels, mammalian slo2 channels, exhibit high conductance for K^+ ions. However, they are sensitive to Na^+_i and Cl^-_i while being insensitive to physiologic levels of Ca^{2+}_i. (Bhattacharjee and Kaczmarek 2005; Salkoff *et al.* 2006).

From a structural point of view, slo2 channels are made of an intracellular N-terminus, TM6 transmembrane core (S1-S6) and intracellular cytosolic tail domain that contains the RCKs. The latter are involved in sensing of Na^{2+} and Cl^-ions. However, these channels are largely Ca^{2+}-insensitive. Noteworthy, in contrast to slo1 channels, slo2 channels do not possess S0 TM domain and S0-S1 cytosolic loop (Liu *et al.* 2013) (**Figure 4-4A**).

In this study, we used a combination of rslo2.1 and rslo2.2 cRNAs at a 1:1 molar ratio, which results in heteromeric rslo2.1:rslo2.2, Na^+-gated K^+ channels (Salkoff *et al.* 2006; Chen *et al.* 2009; Zhang *et al.* 2010). In the presence of intracellular activating Na^+_i (i.e., 70 mM Na^+ gluconate in the bath solution), we routinely obtained single channel recordings with an averaged unitary current amplitude of 6.1 ± 0.5 pA at +50 mV, as previously observed from slo2 channels permeating K^+ (Santi *et al.* 2006). As typically expected from these channels, rslo2.1:rslo2.2 channel activity was monotonically increased within a wide concentration of Na^+_i (10-140 mM) (**Figure 4-4B** and **C**) while being unresponsive to physiological levels of intracellular Ca^{2+}. Further, unlike slo1 channels, slo2 channels are proven to be very less voltage sensitive, (Santi *et al.* 2006)therefore, we obtained single channel recordings for studies involving slo2 channels.

Next, we investigated whether modification of activating Na^+_i levels could render rslo2.1:rslo2.2 channels sensitive to ethanol. At all Na^+_i levels tested (10–140 mM), the channel remained consistently resistant to 50 mM ethanol (**Figure 4-4B and C**).
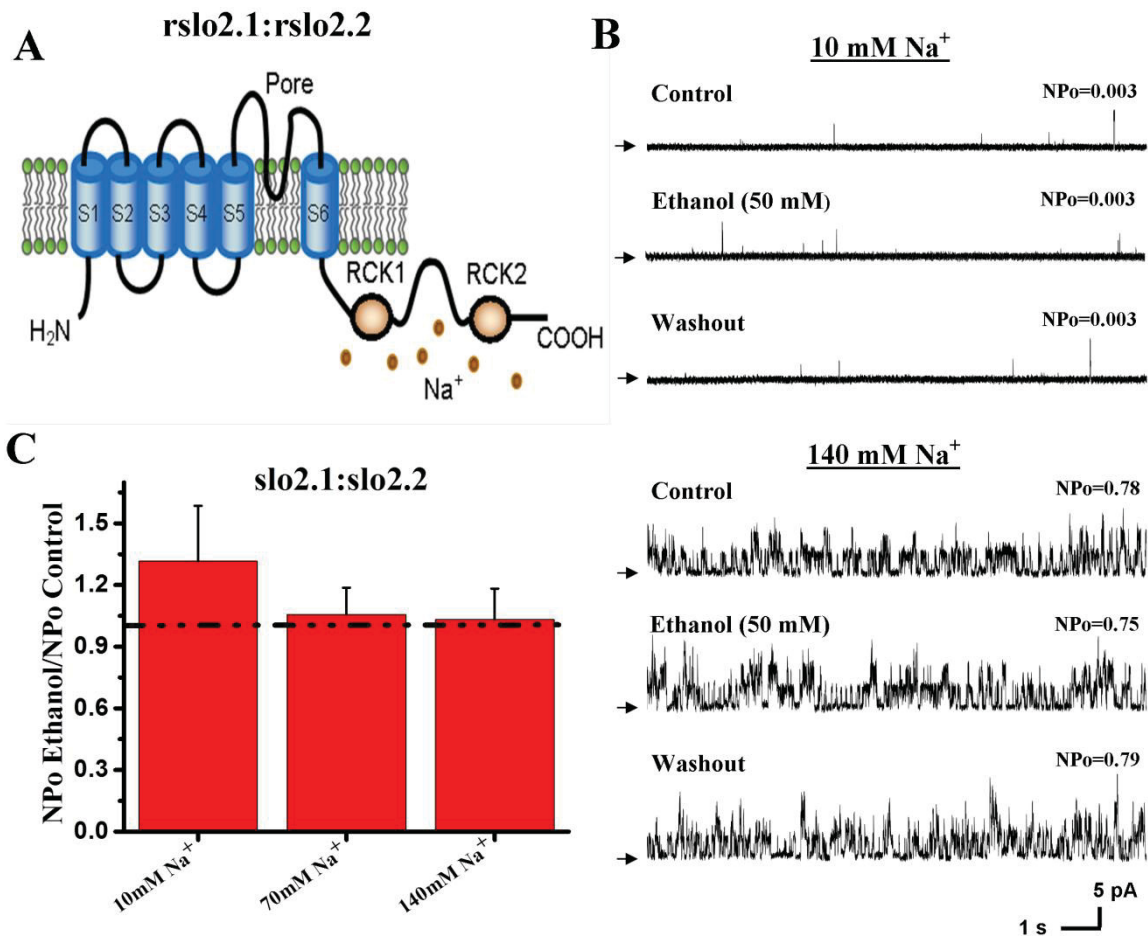
Figure 4-4.   Slo2.1:slo2.2 channels are insensitive to ethanol at a wide range of activating Na^+_i

Notes: A) Cartoon depicting a rslo2 monomer inserted in the membrane, showing slo2 TM segments and functional domains. B) Single channel recordings of slo2.1:slo2.2 channels recorded from I/O patches at 10 (top panel) or 140 mM (bottom panel) Na^+_i; V_m=+90 mV. Records were obtained before (top trace on each panel), during (middle trace), and immediately after (bottom trace) patch exposure to 50 mM EtOH. Arrows indicate the baseline (all channels closed). C) Averaged NP_o ratios in presence and absence of ethanol from slo2.1:slo2.2 at 10 (n=3), 70 (n=4) and 140 mM Na^+_i (n=4). In contrast to Ca^{2+}_i and slo1, the presence of Na^+_i cannot render slo2 channels ethanol-sensitive. A dotted line underscores lack of ethanol action.

Source: Modified with permission from Liu, J., Bukiya, A.N., Kuntamallappanavar, G., Singh, A.K. and Dopico, A.M. (2013). Disntict sensitivity of Slo1 channel proteins to ethanol. *Mol. Pharmacol* 83(1): 235-244.

This resistance of slo2 channels to ethanol is being in sharp contrast with the ethanol response from slo1 channels. Noteworthy, slo2 refractoriness to 50 mM ethanol is found over much wider range (considering both actual concentration and modification in channel activity) of Na^{2+} than Ca^{2+}_i that determines different slo1 responses to ethanol as follows: activation, refractoriness, and inhibition (Liu *et al.* 2008; Bukiya *et al.* 2009). Therefore, rslo2.1:rslo2.2 channels remain insensitive to intoxicating concentrations of ethanol even across a wide range of activating ion concentration and eventual changes in channel activity.

4.2.4. Slo3 Channels Are Ethanol Insensitive over a Wide Range of Their Activating Ion Concentration

We next addressed whether slo3 channels responded to ethanol like slo1 or, rather, remain resistant as found for slo2 (see previous section).

The H^+ sensitive (OH^--activated) slo3 channels are predominantly found only in mammalian testis, which contrasts with the wide distribution of slo1 and slo2 channels (Salkoff *et al.* 2006). Structurally, slo3 channels contain an N-terminus, seven transmembrane domains (S0-S6) and intracellular CTD-containing RCKs, which distinctly sense OH^- ions (**Figure 4-5A**). It should be underscored that, in contrast to slo1 channels, RCKs of slo3 channels do not sense physiological levels of Ca^{2+} (Salkoff *et al.* 2006).

Before investigating the ethanol action on slo3 channels, their functional expression in oocytes was confirmed. In the presence of intracellular activating alkaline medium (bath solution pH = 8.0, $[OH^-]$=1 μM), we were able to obtain single-channel events with unitary current amplitudes of 2.4 ± 0.3 pA at +80 mV, as previously reported for slo3 channels (Schreiber *et al.* 1998; Qian *et al.* 2002; Xia *et al.* 2004). Further, slo3 channel activity was consistently increased as OH^-_i concentration was increased from 0.01 μM thru 10 μM (which is equivalent to pH=6.0 thru pH=9.0) (**Figure 4-5B** and **C**). These results are in similar to previously published reports (Xia *et al.* 2004). Further, expression levels of slo3 channels were relatively low compared to slo1 channels. It is evident by brief channel openings in **Figure 4-5B**. Thus, macroscopic currents resulting from slo3 channels were of low magnitude and did not fit Boltzmann very well.

Then, 50 mM ethanol was applied to the cytosolic side of membrane patches to determine the ethanol-sensitivity of slo3 channels. Since the ethanol action on slo1 channel activity was a function of $[Ca^{2+}]_i$, we conducted this study at a wide range of activating levels of OH^-_i. Our results, however, demonstrate that at all OH^-_i levels tested (0.01–10 μM), the slo3 channel remained consistently unresponsive to 50 mM ethanol while being sensitive to OH^-_i levels (**Figure 4-5B** and **C**), a result that contrasts with that of slo1 channels while paralleling findings from slo2.
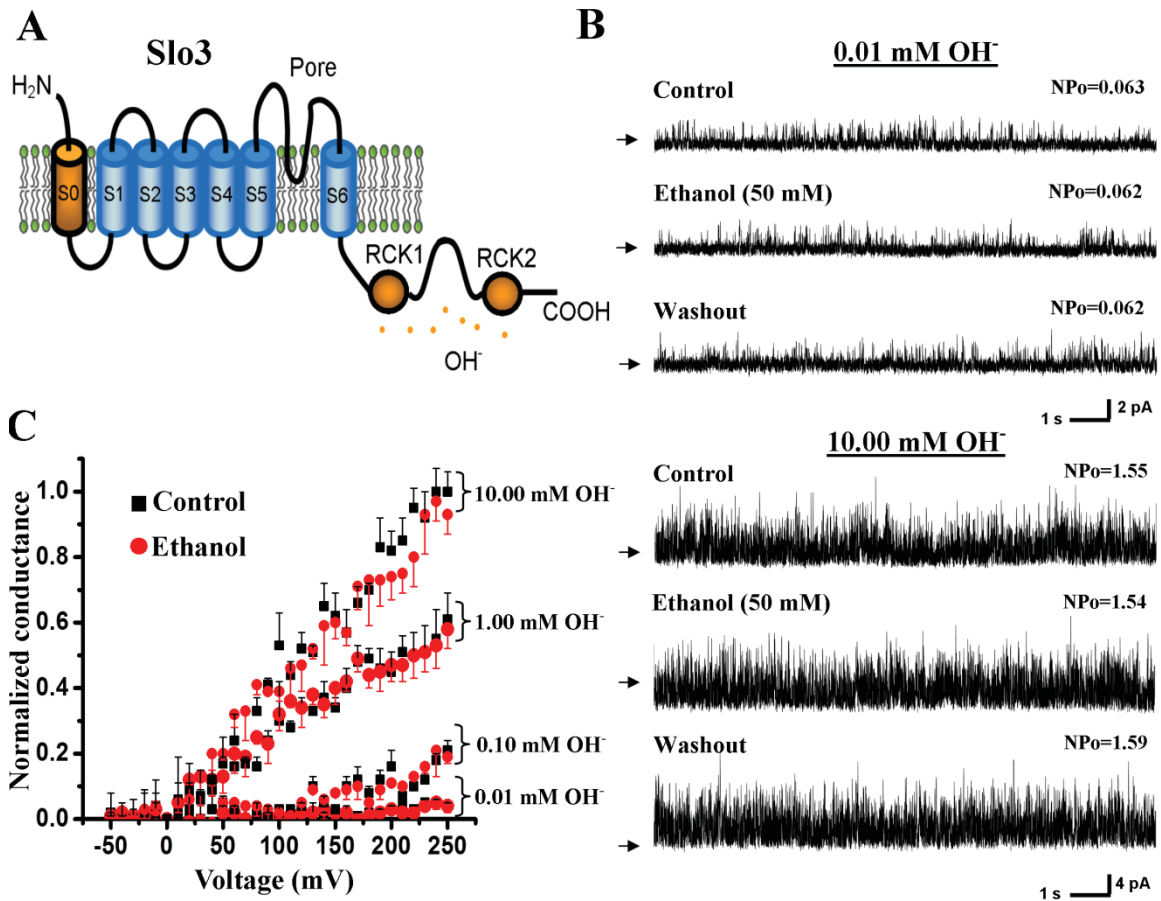
Figure 4-5. Slo3 channels are ethanol-insensitive at a wide range of activating OH⁻

Notes: A) Cartoon depicting a slo3 monomer inserted in the membrane, showing slo3 TM segments and functional domains. B) Single-channel recordings of slo3 channels from I/O patches at 0.01 (top panel) and 10 µM OH⁻ (bottom panel); V_m=+60 mV. Records were obtained before (top trace on each panel), during (middle trace), and immediately after (bottom trace) patch exposure to 50 mM EtOH. Arrows indicate the baseline (all channels closed). C) slo3 averaged macroscopic conductances (G) at 0.01, 0.1, 1 and 10 µM OH⁻$_i$ (normalized to G_{max} obtained at 10 µM OH⁻) in presence and absence of ethanol. Each data point represents the average of no less than 3 patches; each patch was excised from a different cell.

Source: Modified with permission from Liu, J., Bukiya, A.N., Kuntamallappanavar, G., Singh, A.K. and Dopico, A.M. (2013). Disntict sensitivity of Slo1 channel proteins to ethanol. *Mol. Pharmacol* 83(1): 235-244.

4.3.   Discussion

In this study, we tried to address the questions, 1) whether ethanol action on slo1 channels was selectively dependent on its activating ion i.e., Ca^{2+}_i and 2) ethanol sensitivity is unique to slo1 (cbv1) channels or it also extends to other members of slo family such as slo2, and slo3 channels. Our investigation was carried out in same expression system, under similar patch-clamp recording conditions and across wide range of activating ion concentrations. Throughout the study we used the ethanol concentration (50 mM) reached in blood during moderate-to-heavy intoxication. Data demonstrate that 1) Slo1 channel sensitivity to ethanol channel is dependent on Ca^{2+} but not in Mg^{2+} presence, even when the latter is present at levels that do activate slo1channels; 2) activating ion i.e., Ca^{2+} is required for and modulates ethanol regulation of slo1 channel activity, while being unable to embold slo2 or slo3 channels with ethanol sensitivity and 3) our findings strongly suggest that distinct sensitivity of slo1 channels coupled to channel Ca^{2+} sensing structures.

The ethanol modulation of BK channel (in our case, cbv1) activity by 50 mM ethanol shown in this study is similar to previously published reports with mslo1 channels expressed in *X. laevis* oocytes (Liu *et al.* 2003; Brodie *et al.* 2007; Liu *et al.* 2008; Bukiya *et al.* 2009); with hslo1 channels cloned from human brain and expressed in HEK cells (Feinberg-Zadek *et al.* 2008) or slo1 channels reconstituted into bilayers of one or two phospholipid species (Crowley *et al.* 2003; Crowley *et al.* 2005; Yuan *et al.* 2011). Collectively, it should be underscored that slo1 channel-forming subunit surrounded by a bare phospholipid bilayer is sufficient to render the BK channels sensitive to ethanol (Crowley *et al.* 2003; Crowley *et al.* 2005; Yuan *et al.* 2011).

From a structural point of view, the differential ethanol response of slo1 *vs.* slo2.1/slo2.2 and slo3 channels is quite remarkable. Similar to all other members of the superfamily of voltage-gated, outward rectifying K^+ channels, slo1 and slo2 proteins contain a transmembrane core of TM6. Additionally, each slo1 or slo2 channel-forming protein contains an ion-sensing CTD with its two RCKs (Jiang *et al.* 2002; Yusifov *et al.* 2008; Lee and Cui 2010; Yuan *et al.* 2011). In addition, RCK2 domain of rslo2.2 channel contains identification of a Na^+-coordination site ("sensor") (Zhang *et al.* 2010) and RCK domains in Slo1 CTD contains several Ca^{2+}-coordination sites ("sensors"). Therefore, ethanol refractoriness of slo2.1/slo2.2 channels indicates that a CTD-containing RCK domains that empowers the TM6 core of Kv structure with ion-sensing properties does not necessarily embold the resulting channel with sensitivity to intoxicating levels of ethanol (**Table 4-1**).

Like their slo1 counterparts, slo3 channels contain an N-terminus to S0-S1 cytosolic loop, the TM6 core and the RCK domains. In addition, RCK domains of slo3 channels contain a OH^--coordination site ("sensor") in their CTD (Xia *et al.* 2004). Thus, the refractoriness of slo3 channels to ethanol indicates that the N terminus to the S0–S1 cytosolic loop with an ion sensing portion of RCK domains of CTD that senses the OH^- are not sufficient to empower the TM6 KV core with sensitivity to intoxicating ethanol concentrations.

Table 4-1. **Summary of key structural features of different slo channel family members, their activating ligands and sensitivity to 50 mM ethanol**

Construct/ Channel	S0 Domain	RCKs	Activating Ion	Sensitivity to 50 mM Ethanol
Cbv1	Present	Present	Ca^{2+}_i	Yes
Cbv1	Present	Present	Mg^{2+}_i	No
Slo2	Absent	Present	Na^{2+}	No
Slo3	Present	Present	OH^-	No

Source: Modified with permission from Liu, J., Bukiya, A.N., Kuntamallappanavar, G., Singh, A.K. and Dopico, A.M. (2013). Disntict sensitivity of Slo1 channel proteins to ethanol. *Mol. Pharmacol* 83(1): 235-244.

Collectively, our results from mslo1, rslo2.1/2.2 and mslo3 channels led us to conclude that the slo family canonical design, which includes a TM6 voltage-dependent K^+ (K_V) core and CTDs that empower the channel with ion-sensing, does not necessarily render the channel protein sensitive to intoxicating concentrations of ethanol. Rather, we speculated that the presence of a Ca^{2+}- sensing machinery and thus Ca^{2+}-driven gating seem to be essential for ethanol modulation of slo1 channel activity (Liu *et al.*, 2008). Thus, 50 mM ethanol seems to differentially sense the coupling between different ions (Ca^{2+} versus Na^+, OH^-) and closed to open transition of conserved K^+ pore domain.

Previous studies demonstrated that slo1 channels are activated by two fairly independent gating "pathways": Ca^{2+} and Mg^{2+}/V-dependent pathways (Shi *et al.* 2002), which have been linked to the involvement of at least two different structural domains in determining channel activity. A low-affinity divalent cation-binding site is responsible for Mg^{2+}-dependent pathway, located near amino terminus of RCK1 domains. Whereas, high-affinity Ca^{2+} binding site and Ca^{2+}_i bowl regions are necessary for Ca^{2+}-dependent pathway activation, which is located at carboxy terminus of RCKs. It is thought that S6-RCK "linker" that connects S6 to RCKs serves as a passive spring during Ca^{2+}_i-or Mg^{2+}_i-dependent activation (Niu *et al.* 2004). It is evident from previous and current studies that ethanol fails to alter: 1) voltage-driven (Dopico *et al.* 1998; Dopico *et al.* 1999; Liu *et al.* 2008). 2) Mg^{2+}-driven gating (present study) and 3) cannot modify the slo1 channel activity in the absence of Ca^{2+} (present study and Liu *et al.*, 2013). From structural point of view, these results suggest that ethanol 1) does not alter major aspects of gating involving voltage sensors 2) does not affect the gating involving low-affinity divalent cation-binding site 3) these data seem to suggest that ethanol does not modify the behavior of peptidic "springs" that are connecting RCK domains to S6 gate as previously claimed (Niu *et al.* 2004; Treistman and Martin 2009). Rather, ethanol 4) modulates gating involving either the calcium bowl or RCK1 high-affinity site to modulate channel activity and thus current. Further, previous studies demonstrated that mutations of residues (Glu912 and Asp923) in Ca^{2+} bowl did not modulate the ethanol-induced activation or inhibition of slo1 channel (Liu *et al.* 2008). However, mutations (Asp362 and Asp367) in high affinity RCK1 site (Xia *et al.* 2002), abolished ethanol-mediated inhibition of the slo1 channel yet did not alter drug-induced channel potentiation. Interestingly, combining both the mutations 5D5N and D362A/D367A not only abolished the ethanol-induced inhibition but also abolished activation due to ethanol (Liu *et al.* 2008). Collectively, these results indicate that as far as Ca^{2+}_i able to reach one of its two high affinity recognition sites in the slo1 CTD, ethanol is able to modulate slo1 channel activity.

CHAPTER 5.   ETHANOL DISTINCTLY MODULATES BETA1 AND BETA2-CONTAINING BK CHANNELS

5.1.   Overview

Voltage- and Ca^{2+}_i-gated, large conductance K^+ (BK) channels control several physiological processes, participate in the pathophysiology of disease and are considered useful therapeutic targets (Brenner *et al.* 2000; Jaggar and Nelson 2000; Jaggar *et al.* 2000; Pluger *et al.* 2000; Erdos *et al.* 2002; Wellman *et al.* 2002; Dopico *et al.* 2012). Functional BK channels result from tetrameric association of α subunits. The basic BK channel phenotype, voltage-, Ca^{2+}-, and Mg^{2+}-driven gating is replicated when slo1 homotetramers are expressed in a variety of mammalian and non-mammalian systems (Brenner *et al.* 2000; Cox and Aldrich 2000; Bukiya *et al.* 2009). However, several key biophysical and pharmacological properties are drastically modulated by the presence of accessory β subunits (β1-β4). Most importantly, some β subunits are known to modulate the apparent Ca^{2+}_i sensitivity of the channel (Behrens *et al.* 2000; Brenner *et al.* 2000; Cox and Aldrich 2000; Bao and Cox 2005; Orio and Latorre 2005; Sun *et al.* 2013).

Acute exposure to ethanol concentrations obtained in human blood during alcohol intoxication (10-100 mM) modulates BK (slo1) channel steady-state activity (NP_o) (Brodie *et al.* 2007). This ethanol's action on homomeric BK channel is dependent on the presence of the channel's activating ion i.e., Ca^{2+}_i, ethanol final effect on slo1 channel (potentiation, refractoriness or inhibition) being a function of Ca^{2+}_i concentration (see **chapter 4**) (Liu *et al.* 2008; Liu *et al.* 2013). Several studies reported that β1 and β4 subunits modulate ethanol action on BK constituted by slo1+beta heteromers (Martin *et al.* 2004; Liu *et al.* 2008; Bukiya *et al.* 2009). Results are conflicting and difficult to interpret because these studies used different slo1 proteins and experimental conditions, including levels of Ca^{2+}_i. Both slo1 channels isoforms (Dopico 2003; Liu *et al.* 2003; Liu *et al.* 2006) and Ca^{2+}_i levels (Liu *et al.* 2008) are known to influence ethanol action on BK channels. To systematically probe the role of different beta subunits in ethanol action on BK channels and understand the underlying common and different gating mechanisms involved targeted by the drug, we expressed cbv1 (slo1) alone or with β1, β2, β2-IR, β3 or β4, and conducted G/G_{max}-V plots in absence and presence of 50 mM ethanol across a wide range of Ca^{2+}_i (0-100 µM). Further, the resulting plots were fitted with 70-state HA model. My study tested the following hypotheses.

- Ethanol differentially modulates BK current from channel complexes containing different beta subunits.
- Ethanol action on different β-containing BK channels depends on extent to which these accessory subunits modulate apparent change in Ca^{2+}_i-sensitivity.
- Ethanol modulates specific aspects of channel gating, which facilitates inhibition of current from β1-containing BK channel complexes

5.2.   Results

5.2.1.   Auxillary Beta Subunits Functionally Co-Express with Channel Forming Cbv1 Subunits

Before probing ethanol on BK channels of different subunit composition, we determined the functional co-expression of the different beta subunits (β1, *wt* β2, β2-IR, β3 and β4) with the channel-forming cbv1 subunit. Thus, using the oocyte expression system, macroscopic currents were evoked from a holding potential of -80 mV by 100 ms-long, 10 mV depolarizing steps from -150 mV to +150-200 mV. Macroscopic recordings were obtained from inside-out patches over a wide range of Ca^{2+}_i concentrations (nominal zero-100 µM) (**Figure 5-1A**). To identify the ion current phenotype from the different BK channel complexes, we obtained G/G_{max}-V plots, $V_{0.5}$-$[Ca^{2+}]$ plots, time constant for ion current activation (τ_{act}) and time constant for ion current deactivation (τ_{deact}) from each macroscopic current recording. τ_{act} and τ_{deact} were measured at the voltage at which the channel reached maximal conductance (V_{max}).

As previously reported for other slo1 channels (Brenner *et al.* 2000; Cox and Aldrich 2000; Bao and Cox 2005; Orio and Latorre 2005), the presence of β1subunits increased cbv1 channel activity as Ca^{2+}_i was raised above micro molar levels, which is evident by increased shift in $V_{0.5}$ values in $V_{0.5}$-Ca^{2+} plots (**Figure 5-1B**). These results are in agreement with previously published reports (Brenner *et al.* 2000; Cox and Aldrich 2000; Bao and Cox 2005; Orio and Latorre 2005; Contreras *et al.* 2012). It should be underscored that µM Ca^{2+}_i levels, while not only necessary, are optimal for β1 subunit to modulate slo1 channels so such modulation translates into observable increase in NP_o and/or macroscopic conductance. More specifically, β1 subunit-induced channel modulation results in an increased apparent Ca^{2+} sensitivity of the channel and thus enhanced steady-state activity/current (Brenner *et al.* 2000; Cox and Aldrich 2000; Nimigean and Magleby 2000; Bao and Cox 2005; Orio and Latorre 2005; Contreras *et al.* 2012). In addition, β1 subunit increased τ_{act} and τ_{deact} from their cbv1 values: at 10 µM Ca^{2+}_i. τ_{act} and τ_{deact} changed from 1.40±0.10 and 1.13±0.13 ms to 5.16±0.93 and 6.76±0.67 ms, for cbv1 and cbv1+β1, respectively (p<0.05 for both constants) (**Figure 5-1C**). This slowing down of macroscopic current activation and deactivation kinetics by BK β1 subunits is also in accordance with data from slo1 other than cbv1 (Brenner *et al.* 2000; Cox and Aldrich 2000; Bao and Cox 2005; Contreras *et al.* 2012).

From a structural point of view, *wt* β2 subunits possess an additional inactivation bowl/peptide in their N-terminus when compared to β1 subunits (Wallner *et al.* 1995; Wallner *et al.* 1999; Xia *et al.* 1999; Uebele *et al.* 2000; Xia *et al.* 2003). Indeed, co-expression of *wt* β2 with cbv1 channels consistently resulted in remarkably rapid inactivation of ionic current (**Figure 5-1A,** bottom left panel). This finding is consistent with findings from other laboratories that co-expressed *wt* β2 with slo1 other than cbv1 (Wallner *et al.* 1999; Xia *et al.* 1999; Uebele *et al.* 2000; Xia *et al.* 2003), and confirms previous data from our laboratory obtained with cbv1+*wt* β2 channel expressed in *X. laevis* oocytes (Bukiya *et al.* 2009).
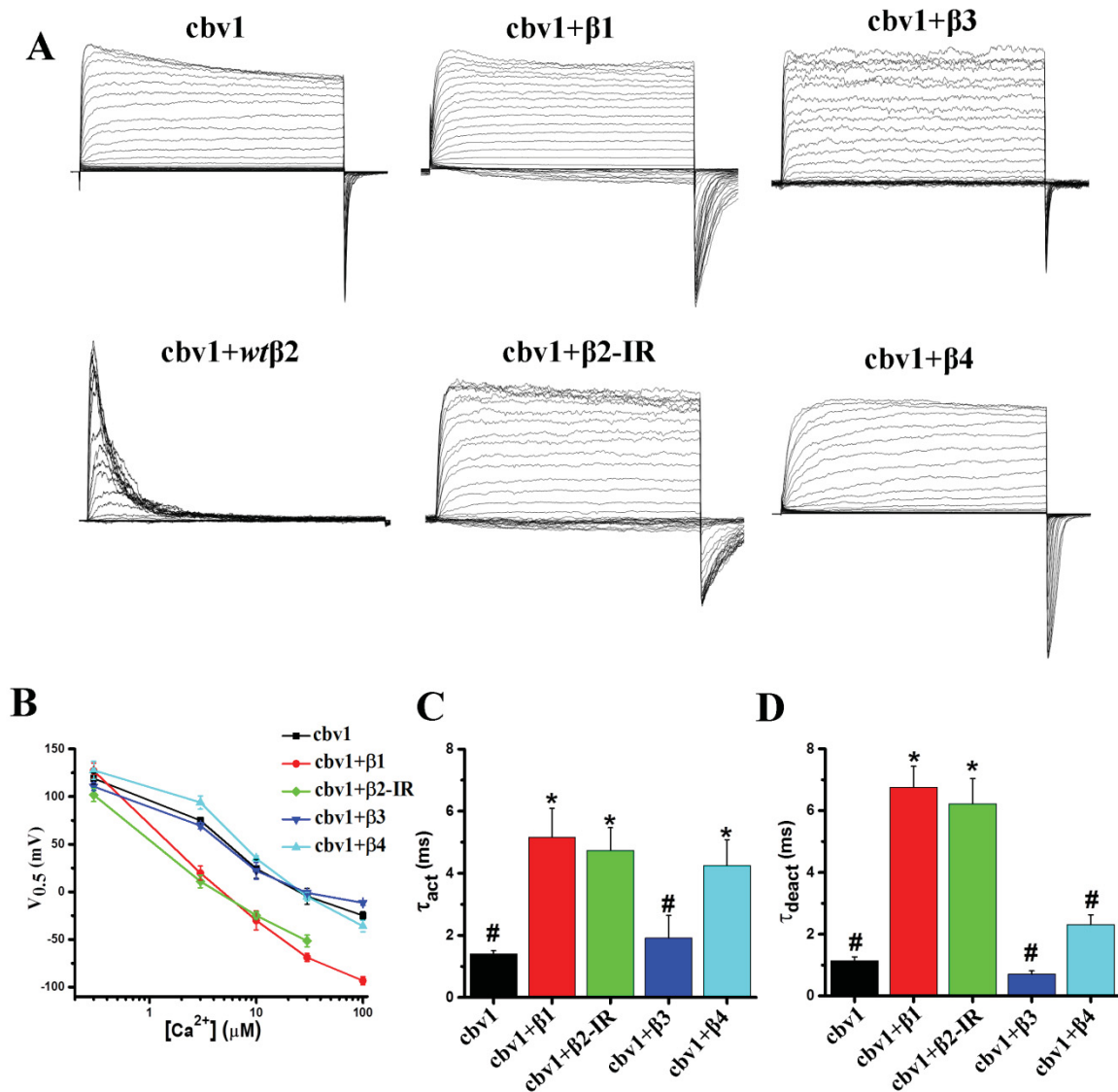
Figure 5-1.   Macroscopic currents after cbv1+β1–4 subunit expression in *Xenopus laevis* oocytes show characteristic features of BK currents

Notes: A) Representative current records from I/O macropatches expressing different BK channel subunit combinations (cbv1±β1, *wt* β2, β2-IR, β3, or β4). Currents were evoked by 100 ms-long (except for cbv1+*wt* β2; 600 ms-long), 10 mV depolarizing steps from −150 to +150 mV, with a holding potential set to -80 mV. cbv1+*wt* β2 channels are characterized by fast inactivation. B) $V_{0.5}$ *vs*. [Ca^{2+}_i] plot underscoring that the presence of different β subunits differentially modulate the apparent Ca^{2+}_i sensitivity of the channel complex. C) and D) Bar graphs show averaged activation (C) and deactivation (D) time constants (τ_{act}, τ_{deact}, respectively) obtained at V_{max} at Ca^{2+}_i=10 μM. Each data point represents the average of no less than 3 patches, each excised from a different cell. *Different from cbv1 (p<0.05); #Different from cbv1+β1.

40

As found with β1 subunit, co-expression of β2-IR subunit with cbv1 produced an increase in the channel's apparent Ca^{2+}_i sensitivity (**Figure 5-1B**). Further, when compared to homomeric cbv1 channels, the presence of β2-IR subunit induced remarkable slowdown of activation and deactivation kinetics, as previously shown by other researchers with slo1 channels other than cbv1 (Brenner *et al.* 2000; Orio and Latorre 2005; Sun *et al.* 2013). Indeed, at 10 μM Ca^{2+}_i, τ_{act} and τ_{deact} changed from 1.40±0.10 and 1.13±0.13 ms to 4.73±0.74 and 6.22±0.82 ms, for cbv1 and cbv1+β2-IR, respectively (P<0.05 for both constants) (**Figure 5-1C** and **D**).

In contrast to all other β subunits, functional co-expression of β3 subunits are characterized by their lack of modulation of apparent change in Ca^{2+}_i sensitivity, activation and deactivation kinetics. At 10 μM, τ_{act} and τ_{deact} values changed from 1.40±0.10 and 1.13±0.13 ms to 1.91±0.73 and 0.76±0.11 ms, for cbv1 and cbv1+β3, respectively (**Figure 5-1C** and **D**). These data are in agreement with previously published reports from other laboratories (Behrens *et al.* 2000; Brenner *et al.* 2000; Uebele *et al.* 2000).

In contrary to β1 and β2-IR, expression of β4 increased cbv1 $V_{0.5}$ at 0.3-10 μM Ca^{2+}_i while mildly decreasing $V_{0.5}$ at 30-100 μM Ca^{2+}_i (**Figure 5-1B**). These results indicate modulation of Ca^{2+}_i sensitivity by β4 subunit requires more than 20 μM Ca^{2+}_i. In addition, at 10 μM Ca^{2+}_i, β4 remarkably increased τ_{act}: 1.40+0.1 ms in cbv1 *vs.* 4.25±0.83 ms in cbv1+hβ4 (P<0.05) while mildly increasing τ_{deact} when compared to cbv1 channels (**Figure 5-1C** and **D**). Collectively, the β4-introduced changes in $V_{0.5}$, τ_{act} and τ_{deact} over cbv1 values are consistent with those previously reported with β4 and slo1 channels other than cbv1 (Behrens *et al.* 2000; Brenner *et al.* 2000; Orio *et al.* 2002).

5.2.2. β1 Subunit Facilitates Ethanol-Induced Inhibition of β1-Containing BK Channels

Ethanol action on slo1/cbv1 channels is a function of Ca^{2+}_i (Liu *et al.* 2008; Bukiya *et al.* 2009) (see **chapter 4**). Several laboratories, including ours, demonstrated that β1 subunit increases apparent Ca^{2+}_i sensitivity of the BK channel (Brenner *et al.* 2000; Cox and Aldrich 2000; Bao and Cox 2005; Orio and Latorre 2005; Bukiya *et al.* 2009; Kuntamallappanavar *et al.* 2014). Thus, we set to address the role of β1 subunit on ethanol modulation of BK channel activity, with a focus on Ca^{2+}-driven gating processes.

After characterizing functional expression of cbv1+β1 channels, 50 mM ethanol was applied onto the cytosolic side of these channels. All experimental conditions, data acquisition and analysis were similar to those used in our studies with cbv1 channels. Results showed that ethanol activated cbv1+β1 channels at low $[Ca^{2+}_i]$ i.e., 0.3 μM, which is evident as is a shift to the left in the G/G_{max}-V plots and thus significantly decreased $V_{0.5}$ values in the $V_{0.5}$-$[Ca^{2+}]$ plot (**Figure 5-2A** and **B**). As $[Ca^{2+}_i]$ increased, this activation turned to significant inhibition, which is evident as a significant right-shift in the G/G_{max}-V plot (**Figure 5-2C**) and thus increased $V_{0.5}$ values in the $V_{0.5}$-$[Ca^{2+}_i]$ plot (**Figure 5-3A** and **B**).
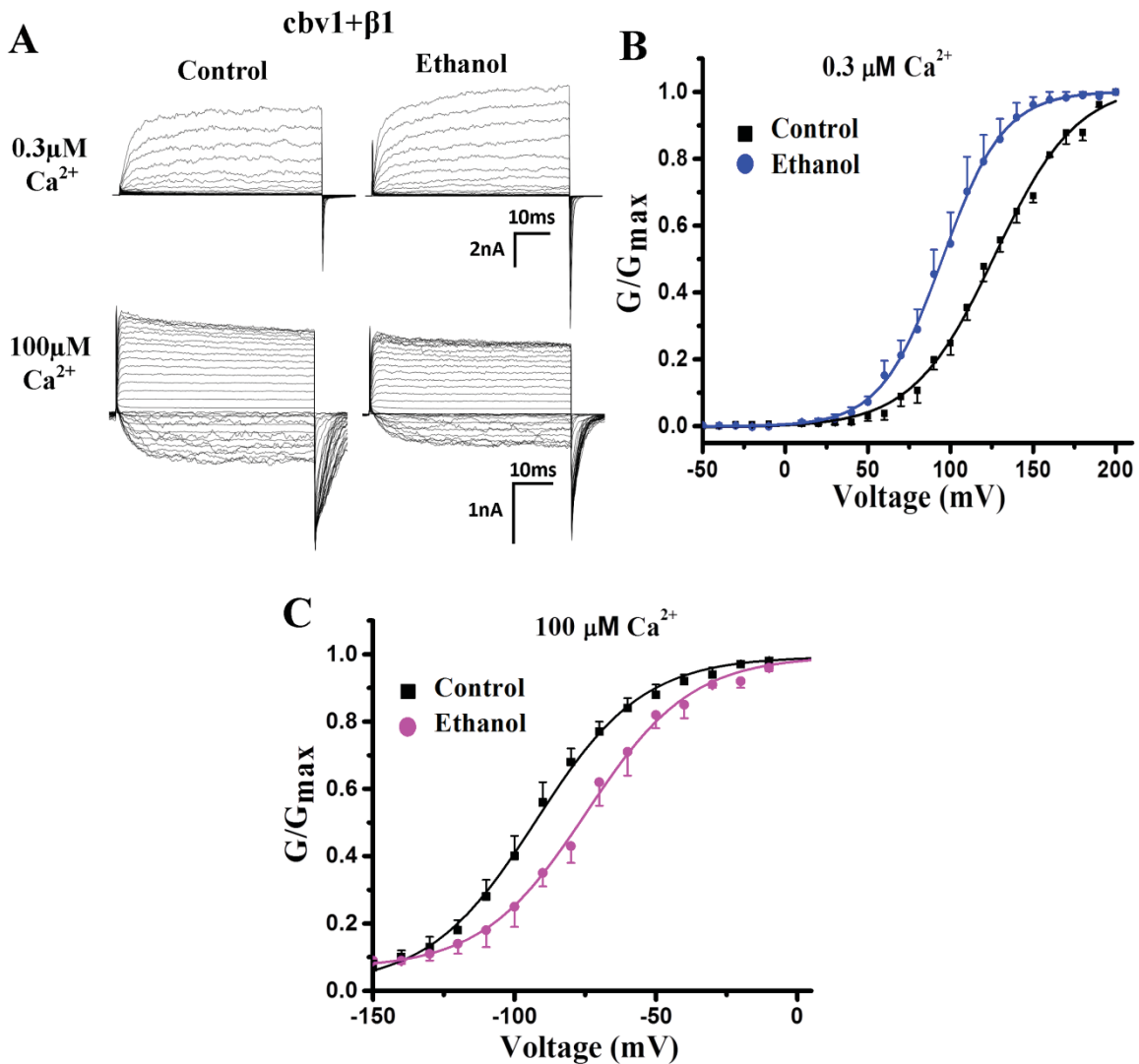
Figure 5-2. **Ethanol activates β1-containing BK channels at submicromolar (0.3 μM) Ca²⁺$_i$, while causing strong inhibition at higher (100 μM) Ca²⁺$_i$**

Notes: A) Macroscopic current recordings from I/O patches obtained at 0.3 and 100 μM Ca²⁺$_i$ in the absence or presence of 50 mM ethanol after cbv1+β1 expression in *Xenopus* oocytes. Ethanol shifts G/G_{max}-V plot to the left at 0.3 μM Ca²⁺$_i$ indicating BK current potentiation (B) while shifting the plot to the right at 100 μM Ca²⁺$_i$ indicating inhibition (C). Each data point represents the average of no less than 3 patches, each excised from a different cell.
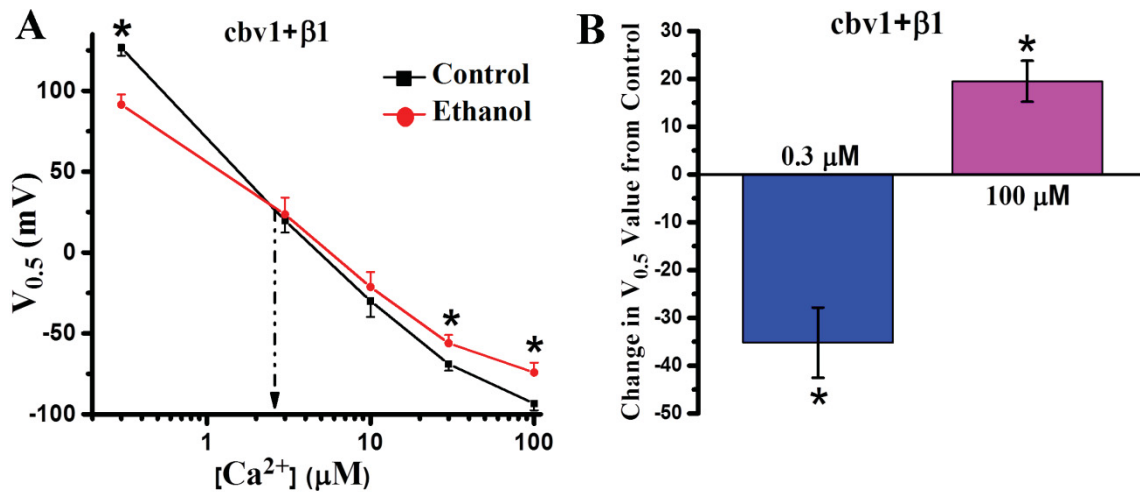
Figure 5-3. **BK β1 subunits determine ethanol-induced inhibition of BK channels at physiological Ca^{2+}$_i$ (3-45 µM) and voltages (-60 to -20 mV)**

Notes: A) β1 subunits set the activation-to-inhibition crossover of ethanol responses at ≈3 µM Ca^{2+}$_i$. B) Bar graph representing ethanol-induced change in $V_{0.5}$ values from pre-ethanol application obtained at 0.3 µM and 100 µM Ca^{2+}$_i$. Each data point represents the average of no less than 3 patches, each excised from a different cell. *Different from control (p<0.05).

Further, ethanol-induced activation-to-inhibition crossover shifted to ~3 µM (**Figure 5-3B**) when compared to that of cbv1 channels. It should be underscored that ethanol-mediated inhibition of β1-containnig BK channels occurs at physiological Ca^{2+}_i and voltage found near cerebral artery myocyte (Perez *et al.* 2001).

5.2.3. Ethanol Modulation of *wt* β2- and β2-IR-Containing BK Channel Activity Is Similar to the Alcohol Response of β1 Subunit-Containing BK Channels

Our next aim was to determine the role of *wt* β2 and β2-IR subunits in ethanol modulation of BK channel activity.

First we co-expressed *wt* β2 subunits with cbv1 channels. In these experiments, we obtained ionic currents at single channel resolution from inside-out patches in gap-free recording at V_m=-20 to -40 mV for 30 seconds under each experimental condition (control *vs.* 50 mM ethanol). Similar to previous studies, 50 mM ethanol was probed over a wide Ca^{2+}_i concentration range (nominal zero-100 µM). Results were analyzed using a built-in function of Clampfit 9.2. NP_o, an index of channel steady-state activity, represents product of number of channels in the membrane patch (N) and individual channel open probability (Po). Results demonstrated that ethanol activated cbv1+*wt* β2 channel at low $[Ca^{2+}]_i$, i.e., 0.3 µM, which was evident as a significant increase in NP_o (**Figure 5-4A** and **C**). As $[Ca^{2+}]$ increased, this activation turned into significant inhibition, which was evident as a significant reduction in NP_o (**Figure 5-4B** and **C**). Furthermore, as found with cbv1+β1 channels (**Figure 5-3A**), ethanol-induced activation-to-inhibition cross-over occurred at ~3 µM (**Figure 5-4C**).

Since *wt* β2 subunits contain an inactivation domain, we asked whether ethanol modulation of BK channels by *wt* β2 subunits was due to the presence of the inactivation peptide. Thus, we constructed a β2 subunit with its inactivation domain removed ("β2-IR). It should be underscored that the β2-IR-induced changes in the biophysical properties of BK channels, such as apparent increase in Ca^{2+}_i sensitivity, are very similar to those induced by β1 subunits (Behrens *et al.* 2000; Brenner *et al.* 2000; Orio *et al.* 2002). Once the functional expression of β2-IR subunit was confirmed, effect of ethanol was explored under experimental conditions similar to those used in cbv1+β1 studies. Results demonstrated that ethanol activated cbv1+β2-IR channels at low $[Ca^{2+}]_i$, i.e., 0.3 µM, which was evident as a marked decrease in $V_{0.5}$ values from the $V_{0.5}$-$[Ca^{2+}]$ plot (**Figure 5-5A** and **B**). As $[Ca^{2+}]_i$ increased, this activation turned to significant inhibition, which coud be noticed from a significant increase in $V_{0.5}$ values in the $V_{0.5}$-$[Ca^{2+}]_i$ plot (**Figure 5-5A** and **B**). Furthermore, ethanol-induced activation-to-inhibition cross-over shifted to ~3 µM (**Figure 5-5A**), a value similar to that found in cbv1+β1 channels exposed to ethanol (**Figure 5-3A**). These results seem to indicate that the β2 inactivation domain does not play a significant role in ethanol action on cbv1+*wt* β2 channels.
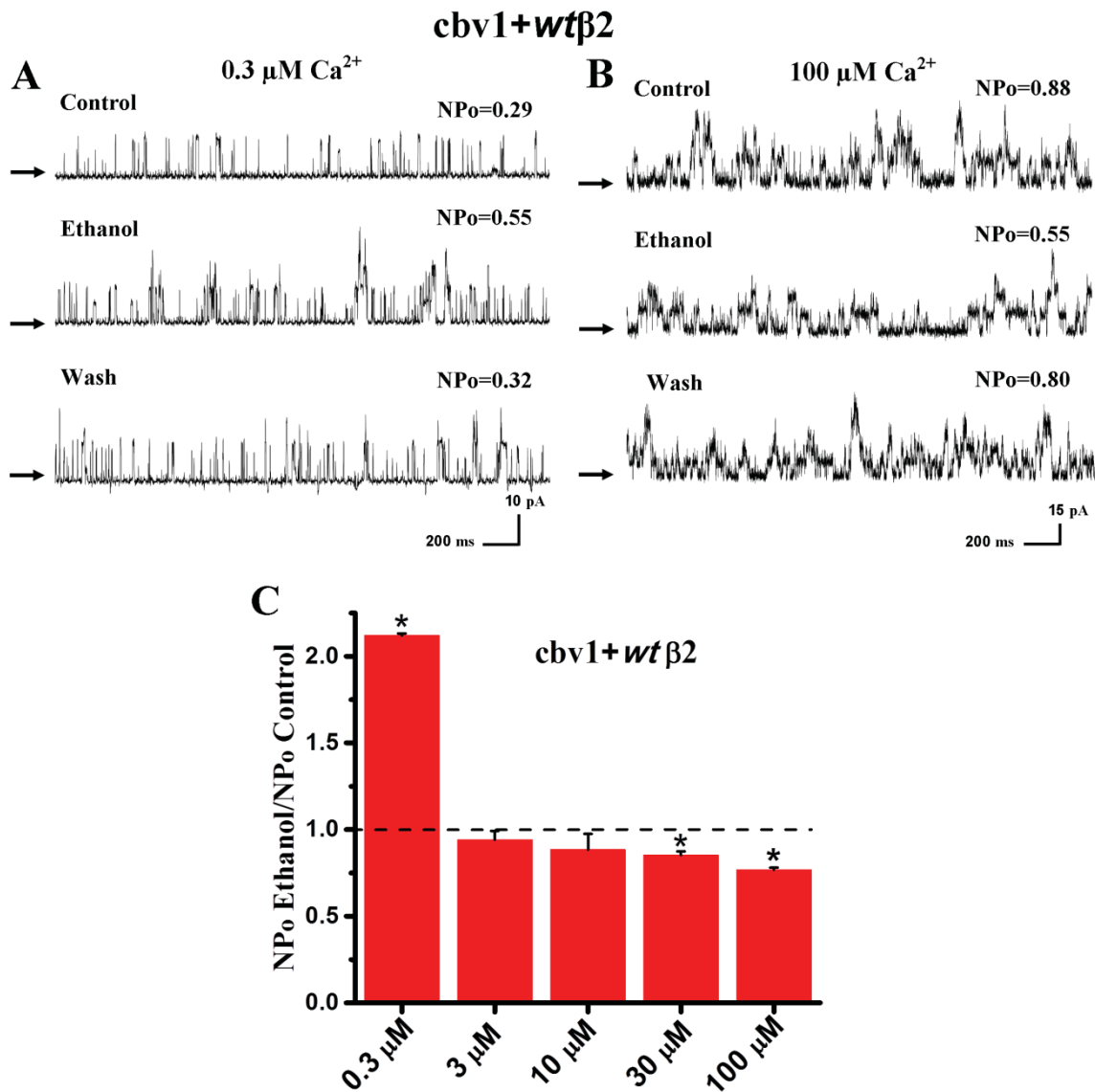
Figure 5-4. **Ethanol-mediated inhibition of *wt* β2-containing BK channels is similar to the ethanol response of cbv1+β1 channels**

Notes: A) Single-channel recordings of cbv1+*wt* β2 channels from I/O patches at 0.3 (left panel) and 100 µM Ca^{2+}_i (right panel); V_m=-40 mV. Records were obtained before (top trace on each panel), during (middle trace) and immediately after (bottom trace) patch exposure to 50 mM ethanol. Arrows indicate the baseline (all channels closed). B) Averaged NP_o ratios in presence and absence of ethanol from cbv1+*wt* β2 at 0.3, 3, 10, 30, and 100 µM Ca^{2+}_i (n=5). Data demonstrate that the activation-to-inhibition crossover for ethanol effect on cbv1+*w t*β2 channels occurs at ≈3 µM Ca^{2+}_i. Each data point represents the average of no less than 3 patches, each excised from a different cell. *Different from control (p<0.05).
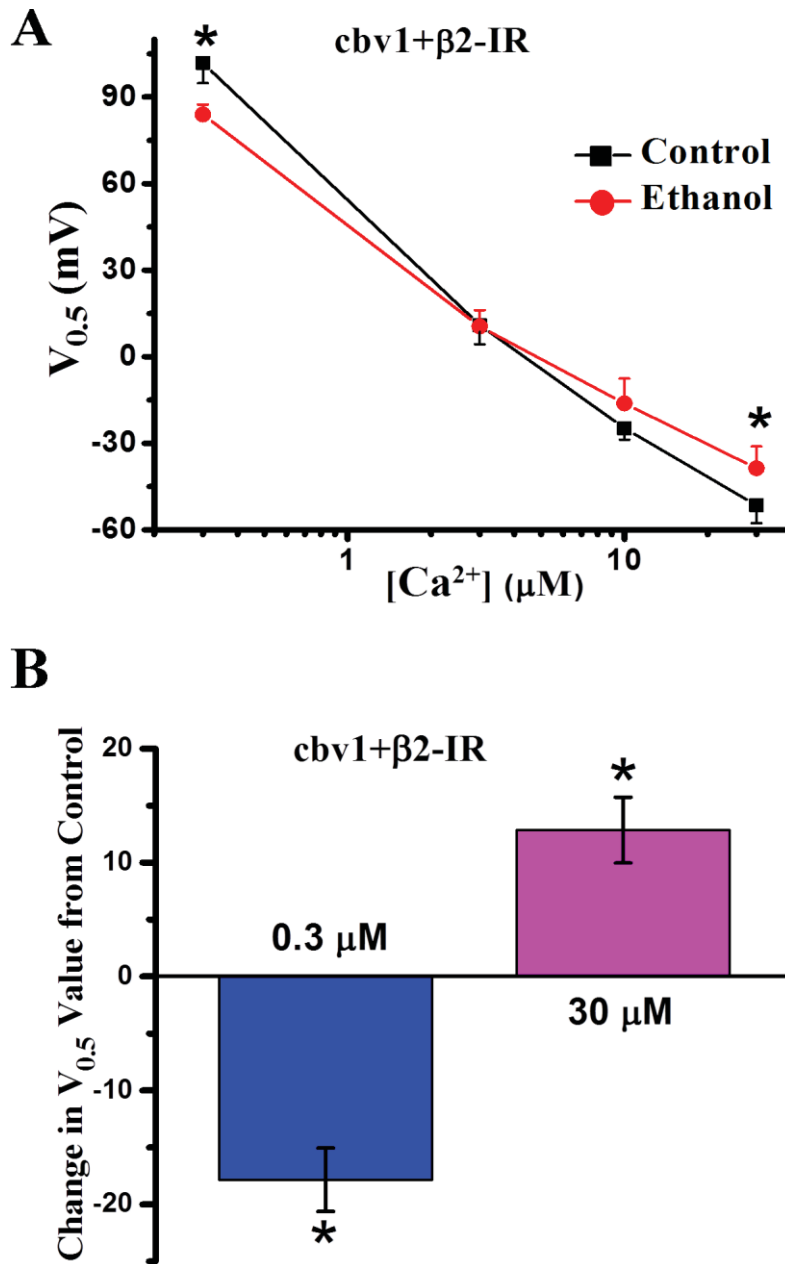
Figure 5-5. **Ethanol-mediated inhibition of β2-IR-containing BK channels is similar to the ethanol response of cbv1+β1 channels**

Notes: A) $V_{0.5}$ *vs.* $[Ca^{2+}_i]$ plot showing that the activation-to-inhibition crossover for ethanol effect on cbv1+β2-IR channels occurs at ≈2 μM Ca^{2+}_i, as found with cbv1+/-beta1 (**Figure 5-3A**) B) Bar graph showing ethanol-induced change in $V_{0.5}$ values from control obtained at 0.3 μM and 100 μM Ca^{2+}_i. Each data point represents the average of no less than 3 patches, each excised from a different cell. *Different from control (p<0.05).

5.2.4. Ethanol Modulation of β3- and β4-Containing BK Channel Activity Is Similar to the Alcohol Response of Homomeric Cbv1 Channels

Several groups, including our laboratory, documented that unlike β1 and β2 subunits, β3 and β4 subunits have a minor, if any, effect on the apparent Ca^{2+}_i sensitivity of slo1 channels (Behrens *et al.* 2000; Brenner *et al.* 2000; Bao and Cox 2005; Orio and Latorre 2005; Bukiya *et al.* 2009; Sun *et al.* 2013; Kuntamallappanavar *et al.* 2014) (**Figure 5-1B**). If β1- and β2-induced facilitation of ethanol inhibition of BK currents is somewhat linked to the channel apparent Ca^{2+}_i-sensitiivty, we expected that ethanol action on β3- or β4-containing BK channels should not differ from ethanol action on homomeric slo1.

Under experimental conditions similar to those of previous studies, cbv1+β3 and cbv1+β4 were co-expressed and probed with 50 mM ethanol. Results demonstrated that ethanol activated cbv1+β3 and cbv1+β4 channels at low $[Ca^{2+}]_i$ i.e., 0.3 μM, which was evident as a marked decrease in $V_{0.5}$ from the $V_{0.5}$-$[Ca^{2+}]$ plot (**Figure 5-6A, B, C** and **D**). As $[Ca^{2+}]$ increased, this activation turned into mild inhibition, which could be noticed by a mild increase in $V_{0.5}$ from the $V_{0.5}$-$[Ca^{2+}]$ plot (**Figure 5-6A, B, C** and **D**). In both heteromeric complexes, ethanol-induced activation-to-inhibition cross-over occurred at ~20 μM (**Figure 5-6A** and **C**). Thus, β3- and β4-containing BK channels response to Ethanol matched that of homomeric cbv1 channels, indicating that β3 and β4 subunits do not noticeably modulate ethanol action on homomeric BK channels.

5.2.5. Understanding BK Channel Function Requires a Complex Allosteric Model

The 70-state Horrigan-Aldrich (HA) model is widely considered the most advanced and complete model to understand BK channel function, in particular its allosteric gating (**Figure 5-7**). Other allosteric models include 10-state MWC (Monod-Wyman-Changeux) and the 50-state HA models. According to MWC model (Monod *et al.* 1965), ion channel exists in two conformations i.e., open and closed. Application of this concept to BK channels requires that the equilibrium between these two conformations is voltage-dependent, with depolarization favoring channel opening. The channel, however, is a homotetramer and contains four Ca^{2+} binding sites, one site in each subunit. Ca^{2+} can bind to both conformations of channel. Allosteric theory requires that the probability of Ca^{2+} binding to the open state is much higher than binding to the closed state, stabilizing the channel in the former. Further, the MWC model assumes binding of Ca^{2+} to each site is equivalent and independent of binding at other sites. This model is presented in the form of cartoon (**Scheme A** of **Figure 5-7**).

Although, the MWC model accounts for many aspects of BK channel gating, there are some aspects the model fails to incorporate: 1. movement of gating charges before the channel opens (Stefani *et al.* 1997; Horrigan and Aldrich 1999); 2. the complex relation between deactivation time constant and membrane voltage (Cox *et al.* 1997; Cox *et al.* 1997; Horrigan and Aldrich 1999).
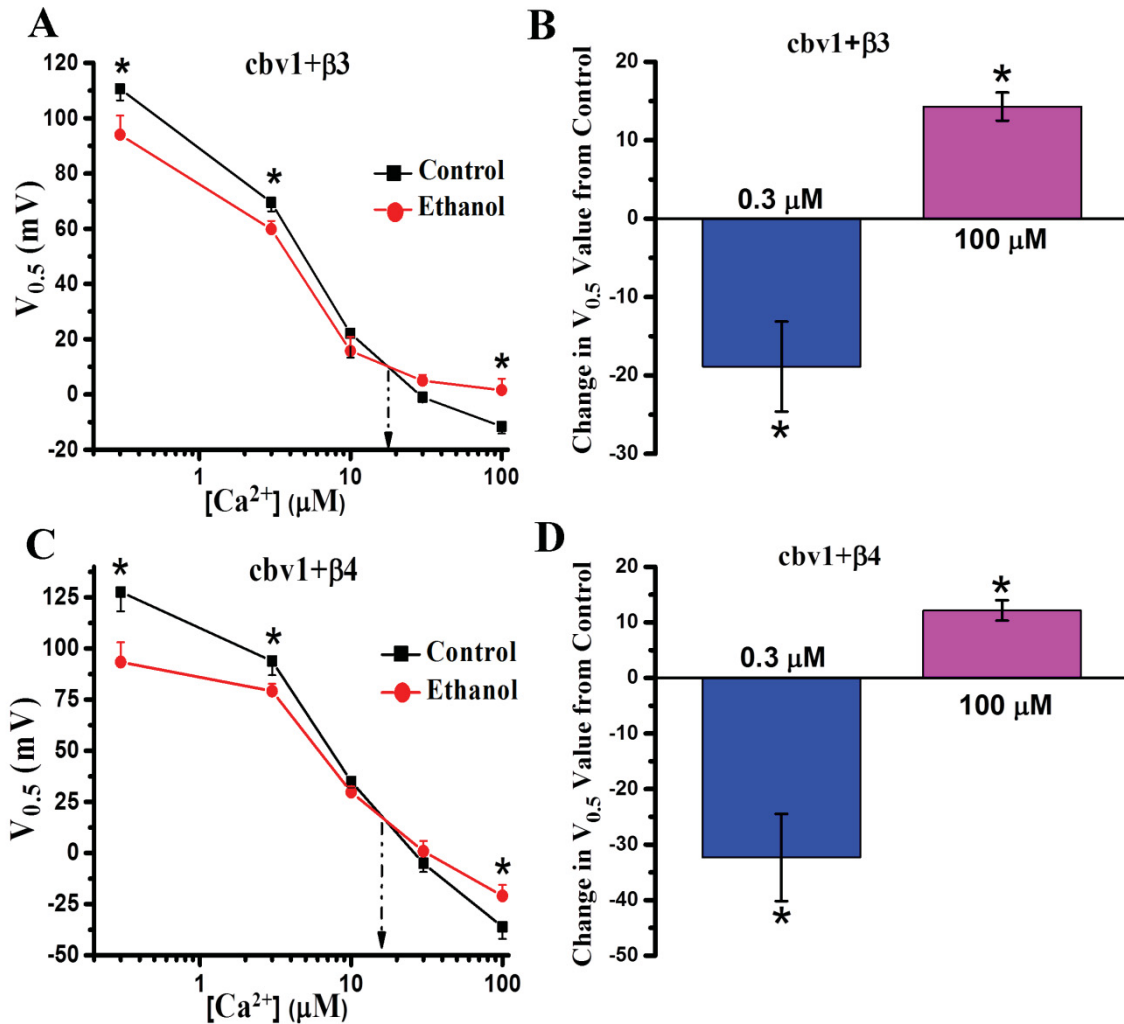
Figure 5-6. **Ethanol responses of β3- or β4-containing BK currents mimic those of homomeric BK (cbv1) channels**

Notes: $V_{0.5}$ *vs*. [Ca^{2+}_i] plot showing that the activation-to-inhibition crossover for ethanol effect on cbv1+β3 (A) and cbv1+β4 channel complexes (C) occurs at ≈20 µM Ca^{2+}_i, as found for homomeric cbv1 exposed to ethanol (see **Figure 4-2A**). Bar graphs representing ethanol-induced change in $V_{0.5}$ values from cbv1+β3 (B) and cbv1+β4 channel complexes (D) obtained at 0.3 µM and 100 µM Ca^{2+}_i. Each data point represents the average of no less than 3 patches, each excised from a different cell. *Different from control ($p<0.05$).
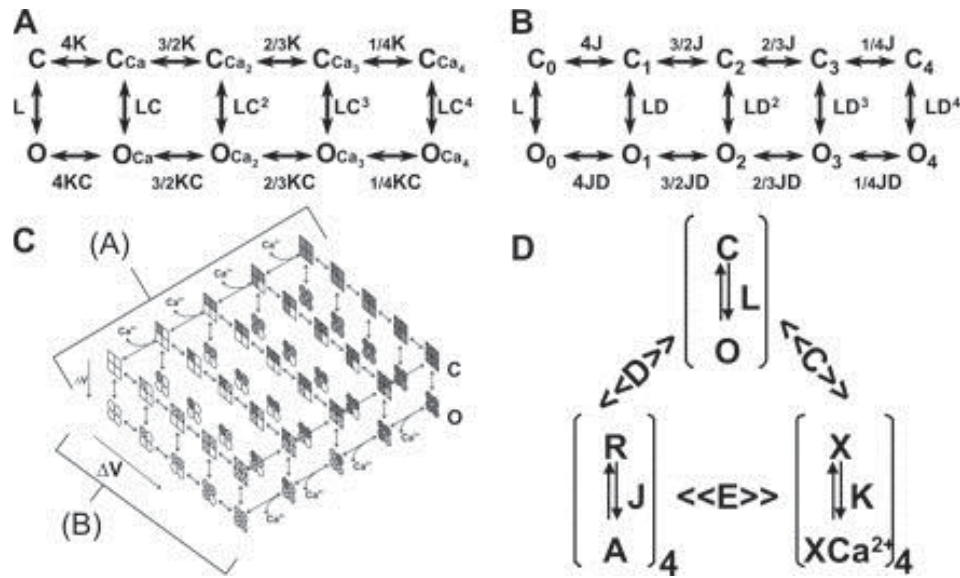
Figure 5-7.   Allosteric model for activation of BK channel

Notes: A) 10-state MWC model originated by allosteric activation by Ca^{2+}_i. It is a two-tier gating scheme. Top tier includes closed channel states and bottom tier includes open channel states. L represents the equilibrium constant between closed and open states. Once each Ca^{2+}_i binding site is occupied, L is multiplied by the allosteric factor C. When the channel is open, the Ca^{2+}_i binding equilibrium constant (K) is multiplied by the same allosteric factor C. B) 10-state MWC model representing activation by voltage. Top tier includes closed channel states and bottom tier includes open channel states. L represents the equilibrium constant between closed and open states. Upon each voltage sensor activation, L is multiplied by the allosteric factor D. When the channel is open, the equilibrium constant for voltage sensor activation (J) is multiplied by the same allosteric factor D. C) two-tired, 50-state model originated by combination of scheme A and scheme B. In this 50-state model, horizontal transitions represent movement of voltage sensors; an "X" within each box (homomer) of the tetrameric channel indicates that the voltage sensor is in its active conformation. Vertical transitions in the scheme represent channel opening. D) A 70-state allosteric model incorporates active interaction between Ca^{2+}_i binding and sensor activation (allosteric factor E). Voltage sensors can exist in resting (R) and activated (A) states. Ca^{2+}_i sensors can exist in Ca^{2+} free (X) or Ca^{2+} bound state. The function of each structural domain is defined by equilibrium constants for channel opening (L), voltage sensor activation (J), and Ca^{2+} binding (K). The energy transfer or coupling between different domains is indicated by allosteric factors (C, D, E), which define the ability of a transition in one domain to modulate the equilibrium constant in another domain.

Source: Reprinted with permission from Orio, P and Latorre, R. (2005). Diffrential effects of beta1 and beta2 subunits on BK channel Activity. *J Gen Physiol* 125(4): 395-411.

In order to address such limitations, 50-state HA model came into existence. In addition to the MWC model assumptions, the 50-state model requires the following: voltage sensors move rapidly in response to changes in membrane voltage regardless of whether the channel is open or closed. Such voltage sensor movement while favoring channel opening, in an allosteric manner, is not required itself for channel opening (Horrigan and Aldrich 1999; Horrigan *et al.* 1999; Cox and Aldrich 2000; Horrigan and Aldrich 2002) (**Scheme B** and **C** of **Figure 5-7**).

However, in the models shown above, any possible allosteric coupling among voltage sensor movement, Ca^{2+}_i binding and channel opening is ignored. The 70-state allosteric activation model, however, conceives these three processes (voltage sensor activation, Ca^{2+}_i binding and "intrinsic" channel opening) as independent equilibriums that interact on each other through allosteric coupling, this model being able to explain all characteristics of slo1 channel current phenotypes (Horrigan and Aldrich 1999; Horrigan *et al.* 1999; Horrigan and Aldrich 2002).

In addition to the parameters included in the 50-state model, the 70-state HA model further takes into account: 1) voltage dependence of voltage sensors; 2) voltage dependence of channel opening; 3) high-affinity Ca^{2+}_i binding and 4) allosteric interaction between Ca^{2+}_i binding and voltage sensor movement (**Scheme D** of **Figure 5-7**). For 70-state model, at any voltage and Ca^{2+}_i concentration, the open probability is given by the **Equation 5-1**.

$$P_o = \frac{L(1+JD+KC+JKCDE)^4}{L(1+JD+KC+JKCDE)^4+(1+JK+JKE)^4}$$ (**Eq. 5-1**)

Where,

$$J = \exp[\frac{z_J F(V-V_h(J))}{RT}]$$

$$.K = \frac{[Ca^{2+}]}{K_d}$$

$$L = L_0 \exp(\frac{z_L FV}{RT})$$

Where,

L_0, Closed to open conformation equilibrium constant, with no Ca^{2+}_i bound and V=0
z_L, the gating charge associate with the channel opening
$V_h(J)$, represents the voltage at which voltage sensors are half the time active when channel is closed
z_J, the gating charge associated with each voltage sensor's movement
K_d, is the dissociation constant for single Ca^{2+}_i binding site, when channel is closed and all voltage sensors are in the resting state
C, allosteric coupling factor between Ca^{2+}_i binding and channel opening

D, allosteric coupling factor between voltage sensor activation and channel opening
E, allosteric coupling factor between Ca^{2+}_i binding and voltage sensor activation
In the equations above, R, T, F have their usual meaning

Summary of various allosteric parameters and their likely corresponding structural domains of BK channel protein are given in **Table 5-1**.

5.2.6. Determining Ethanol's Effect on the Movement of Voltage Sensors for Homomeric BK Channels

Modulation of voltage sensor movement can be best estimated by determining the parameter $V_h(J)$, which corresponds to the half-activation voltage of the voltage sensors. As previously done by several other groups (Horrigan and Aldrich 1999; Horrigan *et al.* 1999; Horrigan and Aldrich 2002; Orio and Latorre 2005), this parameter can be obtained by measuring the voltage dependence of activation kinetics in the absence of Ca^{2+}_i. Thus, macroscopic current were evoked by 100 ms-long 10 mV depolarizing steps from a holding potential of -80 mV, stepping from -150 to +200 mV. Then, the time constant of activation kinetics (τ_{act}) was measured from a built-in function in Clampfit 9 and plotted as function of activation voltage. The voltage at which the τ_{act}-V plot reaches its maximum indicates the $V_h(J)$ parameter.

Our results demonstrated that half-activation voltage of the voltage sensors for cbv1 channels occurred at 150 mV (**Figure 5-8A** and **B**). This value is in agreement with previously published reports for slo1 channels other than cbv1 (Horrigan and Aldrich 1999; Horrigan *et al.* 1999; Bao and Cox 2005; Orio and Latorre 2005; Sun *et al.* 2013). Interestingly, ethanol failed to modulate cbv1 $V_h(J)$ (**Figure 5-8A** and **B**). This result indicates that ethanol at concentration obtained during binge drinking, while altering BK channel gating (Dopico *et al.* 1998; Liu *et al.* 2008) does not alter the movement of voltage sensors when the channel is closed.

5.2.7. Determining Ethanol Effect on the Closed-to-Open Conformational Change on Homomeric Cbv1 Channels

It has been previously demonstrated that by obtaining the P_{open} *vs.* V relation of BK channel at very negative potentials and nominal zero Ca^{2+}_i), it is possible to directly estimate two parameters associated with the closed-to-open conformational change i.e., z_L and L_0 (Horrigan and Aldrich 1999; Horrigan *et al.* 1999; Horrigan and Aldrich 2002). When no Ca^{2+}_i is bound to any Ca^{2+} binding site of the BK channel, at far negative voltages, voltage sensors are considered to be at their resting state.

Table 5-1.　**Summary of various allosteric model parameters and their likely corresponding structural BK channel domains**

Allosteric Model Parameters	Representative Domain/Interaction
L_0	Pore
z_L	Pore
$V_h(J)$	S4/S4-S5 linker
z_J	S4/S4-S5 linker
D	S4/S4-S5 linker-Pore
K_d	RCKs
C	RCKs-Pore
E	RCKs-S4/S4-S5 linker

Source: Modified with permission from Savalli, N., Pantazis, A., Yusifov, T., Sigg, D. and Olcese, R. (2012). The contribution of RCK domains to human BK channel allosteric activation. *J Biol Chem* 287(26): 21741-21750.
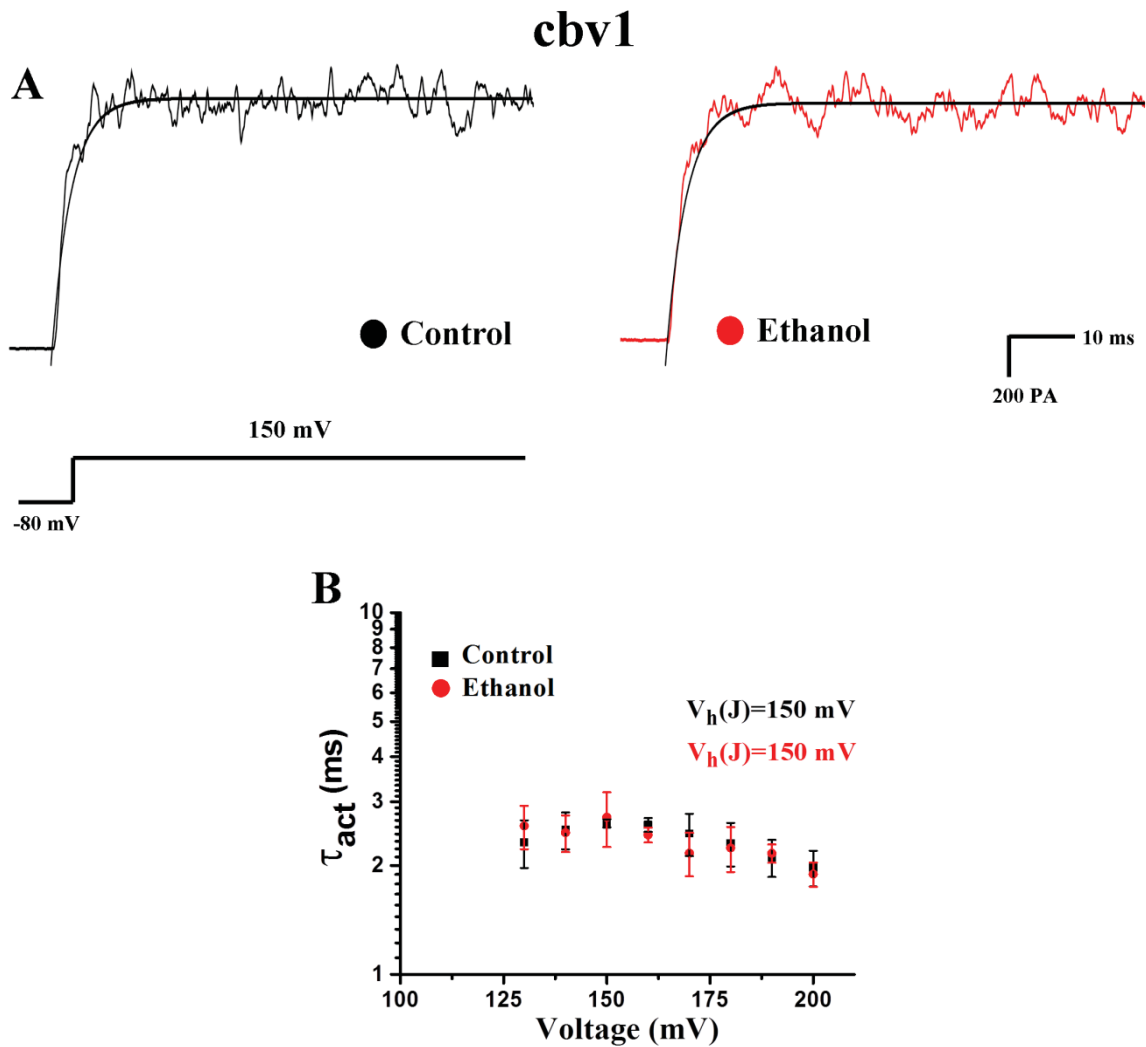
cbv1

Figure 5-8. **Ethanol modulation of voltage dependence of homomeric BK (cbv1) channel activation kinetics in absence of Ca^{2+}_i**

Notes: A) Macroscopic current traces evoked by a 150 mV pulse after a -80 mV pre-pulse in absence (dark trace) and presence (red trace) of 50 mM ethanol. B) Activation time constant (τ_{act}) plotted as a function of membrane step potential. Data demonstrate that the τ_{act}-V relationship reaches a maximum [which indicates $V_h(J)$] at 150 mV. Ethanol fails to modulate $V_h(J)$ in nominal zero Ca^{2+}_i. Each data point represents the average of no less than 3 patches, each excised from a different cell.

Thus the open probability becomes a direct function of voltage and, therefore, **Equation 5-1** is reduces to the following equation (i.e., **Equation 5-2**).

$$P_o = [1 + \frac{(1+J)^4}{L(1+JD)^4}]^{-1} \qquad \textbf{(Eq. 5-2)}$$

Where,

$$P_o = L_0 exp^{(z_L FV/RT)} \qquad \textbf{(Eq. 5-3)}$$

$$J = \exp(\frac{F[V - V_h(J)]}{RT})$$

According to **Equation 5-3**, when we hyperpolarize the membrane, a plot of $\log(P_{open})$-V will reach a limiting slope that is less than the maximum slope. This limiting slope reflects the voltage dependence of the closed-to-open conformational change (Horrigan and Aldrich 1999; Horrigan *et al.* 1999). Therefore, at this specific voltage range, the slope of $\log(P_{open})$-V relation will be solely determined by z_L while the position of the curve along the vertical axis will be determined only by L_0.

For cbv1 channels, the best fit values for parameters associated with closed-to-conformational change were: $L_0 = 2*10^{-6}$ and $z_L = 0.4$ (**Figure 5-9A and B**). These values are in accordance with previously published studies for lo1 channels other than cbv1 (Horrigan and Aldrich 1999; Horrigan and Aldrich 2002; Bao and Cox 2005; Orio and Latorre 2005; Sun *et al.* 2013). Ethanol, however, failed to alter these parameters ($L_0 = 2*10^{-6}$ and $z_L = 0.3$ in presence of 50 mM ethanol) (**Figure 5-9A, B** and **C**), indicating that ethanol does not modulate the conformational change associated with closed-to-open state.

5.2.8. Determining Ethanol's Effect on the Remaining Voltage-Dependent Parameters of Cbv1 Channel Gating

After establishing that ethanol failed to modify cbv1 $V_h(J)$, L_0 or z_L, we next determined ethanol action on cbv1 z_J and D. In order to perform this, we combined P_{open}-V data with G/G_{max}-V data to obtain P_{open}-V curves, as shown in the figure (**Figure 5-10A** and **B**). Then, these curves were fitted with **Equation 5-3**.

While fitting the data obtained from cbv1 channels, $V_h(J)$, L_0, z_L values were constrained to the following values for control *vs.* ethanol data: $V_h(J)=150$ mV *vs* 150 mV, $L_0 = 2*10^{-6}$ *vs*. $2*10^{-6}$, $Z_L = 0.4$ *vs*. 0.3. D and z_J were allowed to vary freely. Our fitting results show that for cbv1 channels in absence of ethanol, D=19.1 and $z_J = 0.6$ (**Figure 5-10A**). These results are approximately similar to the values obtained for slo1 channels other than cbv1 by different groups (Horrigan and Aldrich 1999; Cox and Aldrich 2000; Horrigan and Aldrich 2002; Bao and Cox 2005; Orio and Latorre 2005).

Ethanol, however, did not significantly change these values from control data.

54

cbv1

A

Control   Ethanol   Wash

-80mV

-100mV

0.5 s

5 pA

B

Control

$L_0 = 1*10^{-6}$

$z_L = 0.4$

C

Ethanol

$L_0 = 1*10^{-6}$

$z_L = 0.3$
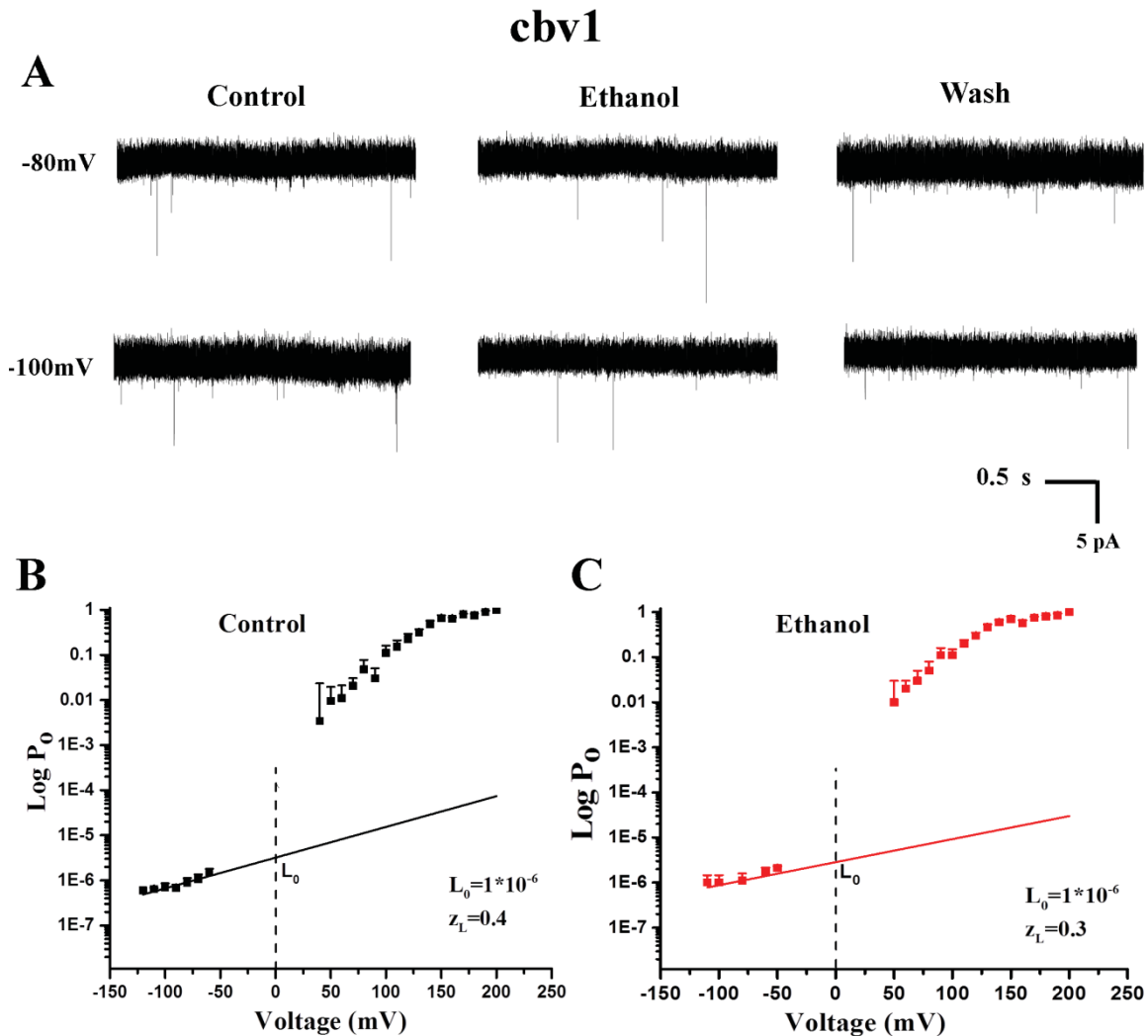
Figure 5-9. **Ethanol does not alter the parameters associated with closed-to-open conformational change and voltage dependence of cbv1 channels**

Notes: A) Representative unitary current recordings evoked from I/O patches in nominal zero Ca^{2+}_i; with membrane patches held at the indicated voltages. Recordings were obtained before (left trace), during (middle trace) and immediately after (right trace) patch exposure to 50 mM ethanol. Arrows indicate the baseline (all channels closed). B, C) Mean log P_o-V relations over a wide range of voltages in presence and absence of 50 mM ethanol. Below +60 mV, data points were obtained from unitary current recordings; above +60 mV, data points were obtained from macroscopic current recordings obtained at nominal zero Ca^{2+}_i. B) and C) P_o-V data at far negative voltages were fitted with the **Equation 5-3** to determine the values of L_0 and z_L. Best fit parameters are listed in the corresponding graphs. Each data point represents the average of no less than 3 patches, each excised from a different cell.

cbv1

A

Control

$L_0=1*10^{-6}$

$z_L=0.4$

$z_J=0.6$

$V_h(J)=150$

$D=19.1$

B

Ethanol

$L_0=1*10^{-6}$

$z_L=0.3$

$z_J=0.65$

$V_h(J)=150$

$D=19.5$
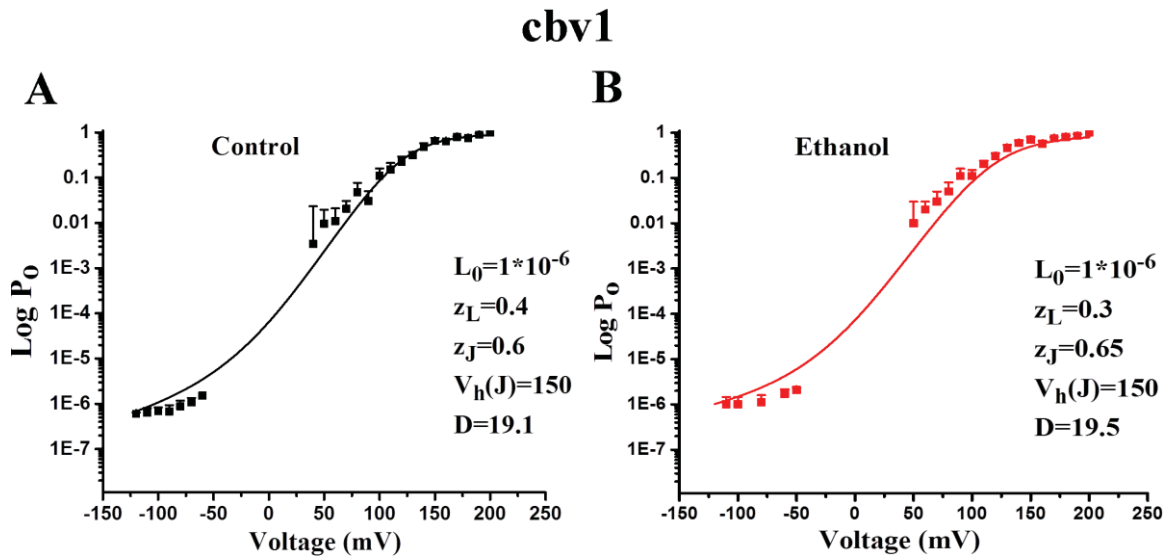
Figure 5-10.   Ethanol does not alter the voltage-dependent parameters of cbv1 channels

Notes: A) and B) Po-V data over a wide range of voltages were fitted with **Equation 5-2** after restricting $V_h(J)$, L0 and z_L, to determine the values of D and z_J. Best fit parameters are listed in the corresponding graphs. Each data point represents the average of no less than 3 patches, each excised from a different cell.

The values obtained were, D=19.5 and z_J=0.65 in presence of 50 mM ethanol (**Figure 5-10B**). These results from homomeric cbv1 channels indicate that ethanol does not alter either the voltage dependence of the voltage sensors or the coupling factor between voltage sensor activation and channel opening.

5.2.9. Determining Ethanol Effect on Homomeric BK Channel's Ca^{2+}_i Binding Affinity

Once we evaluated whether ethanol modulated the voltage sensitivity of the BK channel in the absence of Ca^{2+}_i, we next studied ethanol action on various 70-state HA model parameters as the Ca^{2+}_i concentration was increased. In order to do this, we used G/G_{max}-V relations obtained at various Ca^{2+}_i concentrations from nominal zero-100 μM levels from cbv1 channels in presence and absence of 50 mM ethanol. G/G_{max}-V relations were fitted with **Equation 5-1** by minimizing least-squares with a mixture of Marquardt-Levenverg and Simplex iterations using Origin Pro 8.5 software. Several fits were obtained with different sets of initial parameters and the fits with lower chi-square values were chosen.

Our best fit results obtained for cbv1 channels in absence of ethanol rendered K_d=6.93, C=19.3 and E=2.11 (**Figure 5-11A**). These values are in reasonable agreement with previously obtained best fit values for slo1 channels other than cbv1 (Horrigan and Aldrich 1999; Horrigan and Aldrich 2002; Orio and Latorre 2005). Interestingly, ethanol increased the Ca^{2+}_i binding affinity by ~60%, which is evident from decrease in K_d from 6.93 to 2.86 and (**Figure 5-11B**). Collectively, all our fitting results indicate that most of ethanol's effect on homomeric BK (cbv1) channels is due to drug-induced increase in Ca^{2+}_i binding affinity thus leading to increased channel activity.

5.2.10. Determining Ethanol Effect on BK Channel Voltage Sensor Movement in Presence of β1 Subunits

Our results showed that the half-activation voltage for voltage sensors V_h(J) for cbv1+β1 channels was 100 mV (**Figure 5-12A** and **B**). This value is in reasonable agreement with previously published reports for slo1 other than cbv1 when co-expressed with β1 subunits (Bao and Cox 2005; Orio and Latorre 2005; Sun *et al.* 2013). Ethanol failed to modulate this parameter for cbv1+β1 channels (**Figure 5-12A** and **B**), indicating that ethanol does not alter voltage sensor's movement of the Ca^{2+}_i-unliganded, closed channel.

cbv1

A Control

$L_0 = 2*10^{-6}$
$z_L = 0.4$
$V_h(J) = 150$
$z_J = 0.6$
$K_d = 6.93$
$C = 19.3$
$D = 19.1$
$E = 2.11$

B Ethanol

$L_0 = 2*10^{-6}$
$z_L = 0.3$
$V_h(J) = 150$
$z_J = 0.65$
$K_d = 2.86$
$C = 18.69$
$D = 19.5$
$E = 2.65$

■ 0.5 nM   ● 0.3 μM   ▲ 3 μM   ▼ 10 μM   ◆ 30 μM   ◣ 100 μM
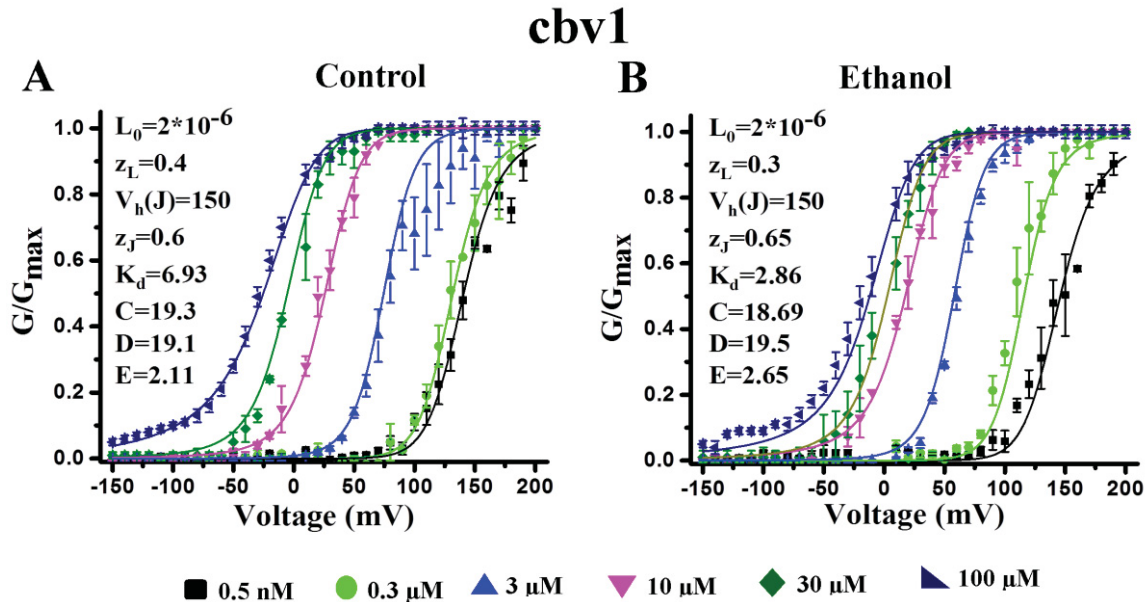
Figure 5-11.   Ethanol modulates the parameters associated with Ca^{2+}_i binding affinity of cbv1 channels

Notes: Averaged G/G_{max}-V curves obtained over a wide range of Ca^{2+}_i in absence (A) and presence (B) of 50 mM ethanol. G/G_{max}-V plots were fitted with **Equation 5-1**. For curves in panel A, L_0, z_L, $V_h(J)$, z_J, D were fixed to $2*10^{-6}$, 0.4, 150, 0.6, and 19.1, respectively while K_d, C, D and E were allowed to vary. For G-V curves in panel B, L_0, z_L, $V_h(J)$, z_J, D were fixed to $2*10^{-6}$, 0.3, 150, 0.65, and 19.5, respectively while K_d, C, D and E were allowed to vary. Best fit parameters are shown to the left of the corresponding plots. Each data point represents the average of no less than 3 patches, each excised from a different cell.
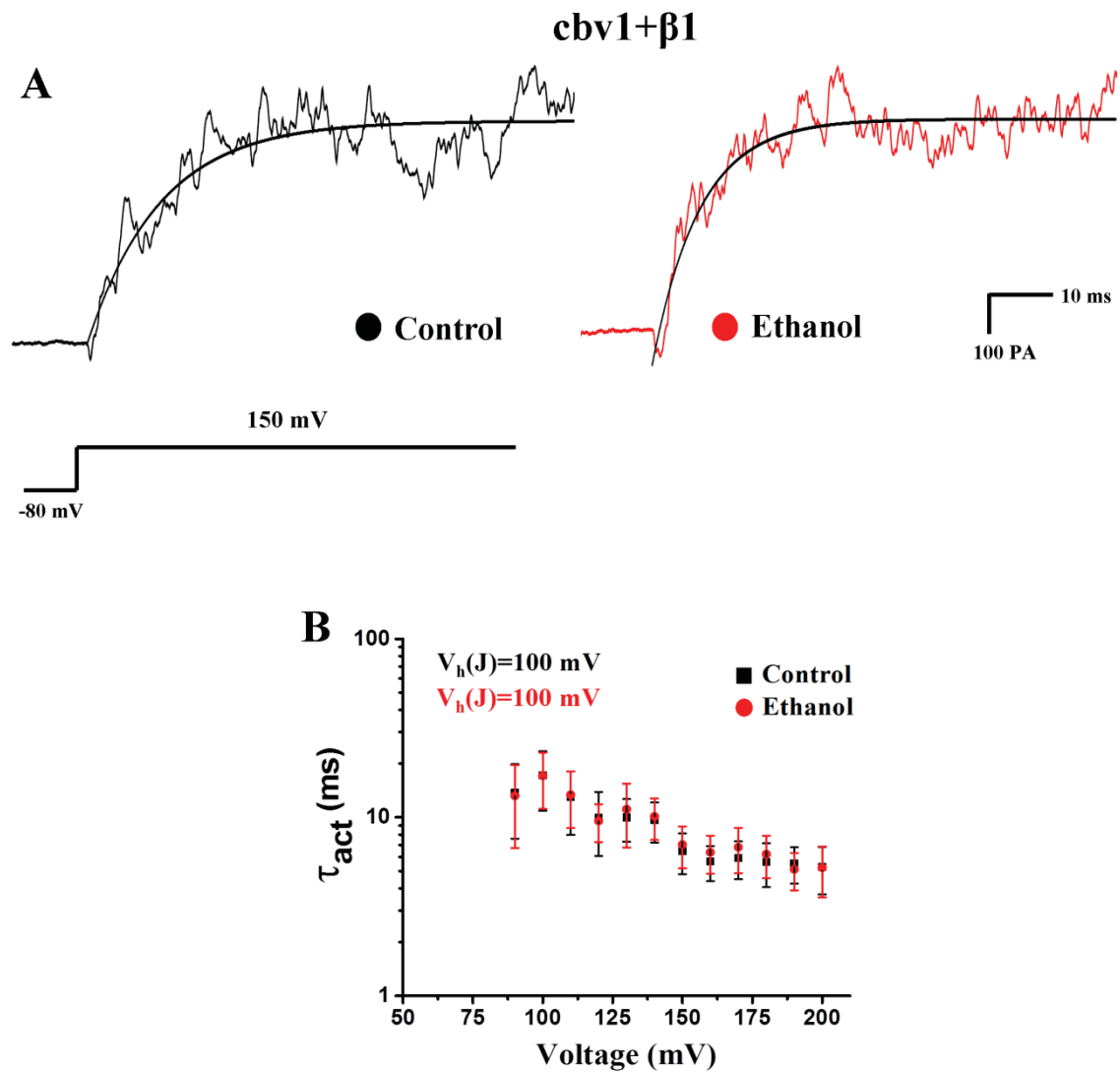
Figure 5-12.   Ethanol modulation of voltage-dependent activation kinetics from β1-containing BK channels in the absence of Ca$^{2+}_i$

Notes: A) Macroscopic current traces evoked by a 150 mV pulse after a -80 mV pre-pulse in absence (dark trace) or presence (red trace) of 50 mM ethanol. B) Activation time constant (τ_{act}) plotted as a function of membrane potential. Data demonstrate that the τ_{act}-V relationship reaches a maximum [which indicates V$_h$(J)] at 100 mV. Ethanol fails to modulate V$_h$(J) in nominal zero Ca$^{2+}_i$. Each data point represents the average of no less than 3 patches, each excised from a different cell.

5.2.11. Determining Ethanol Effect on the Closed-to-Open Conformational Change and Voltage-Dependent Parameters in β1-Containing BK Channels

As encountered by several groups (Bao and Cox 2005; Orio and Latorre 2005; Sun *et al.* 2013), we could not estimate the parameters associated with the closed-to-open equilibrium conformation, i.e., L_0 and z_L for slo1(cbv1 in our case)+β1 channels by fitting P_o-V data with **Equation 5-3**. This impossibility results from the fact that, in contrast from slo1 (cbv1) data, log(P_{open})-V plots from cbv1+β1 channels do not reach the limiting slope.

Therefore, we determined the effect of ethanol on parameters associated with closed-to-open conformation change (L_0, z_L) and the remaining voltage-dependent parameters (z_J, D) together for cbv1+β1 channels at once. In order to perform this, we combined P_{open}-V data with G/G_{max}-V data to obtain P_{open}-V curves (**Figure 5-13A, B** and **C**). Then, these P_{open}-V data were fitted with **Equation 5-2**. Thus, $V_h(J)$ was constrained to the following values for control *vs*. ethanol data: $V_h(J)$=100 *vs*. 100. L_0, z_L, D and z_J were allowed to vary freely. Our fitting results obtained for cbv1+β1 channels in absence of ethanol resulted in L_0=1*10^{-7}, z_L=0.4 D=37 and z_J=0.6 (**Figure 5-13B**). These values reasonably match the values obtained by different groups for slo1 other than cbv1 when co-expressed with β1 (Cox and Aldrich 2000; Bao and Cox 2005; Orio and Latorre 2005; Sun *et al.* 2013). Interestingly, ethanol failed to modify any of these parameters: L_0=1*10^{-7}, z_L=0.4 D=40 and z_J=0.56 in ethanol presence (**Figure 5-13C**). Our results indicate that ethanol does not alter 1) the equilibrium constant between closed-to-open conformation (L_0); 2) the voltage-dependence of such equilibrium constant (z_L); 3) the voltage dependence of the voltage sensors (z_J) or 4) the allosteric interaction (factor D) between voltage sensor activation and channel opening.

5.2.12. Determining Ethanol Effect on the Ca$^{2+}_i$ Binding Affinity of β1-Containing BK Channels

In order to measure the effect of ethanol on Ca$^{2+}_i$ binding affinity and related allosteric factors, we used G/G_{max}-V relations for cbv1+β1 channels in presence and absence of ethanol at various Ca$^{2+}_i$ concentrations from nominal zero to 100 μM. Then, G/G_{max}-V relations were fitted with **Equation 5-1**. Our best fit values obtained for cbv1+β1 channels in absence of ethanol were K_d=15.17, C=24.25 and E=6.16 (**Figure 5-14A**). These values are in good agreement with previously best fit values obtained for slo1 channels other than cbv1 when co-expressed with β1 subunits (Orio and Latorre 2005). Interestingly, ethanol 1) increased the Ca$^{2+}_i$ binding affinity by 50%, which was evident from a decrease in K_d from 15.17 to 7.55; 2) decreased the allosteric factor C by 25%, which represents the interaction between Ca$^{2+}_i$ binding and channel opening; and 3) decreased the allosteric interaction between Ca$^{2+}_i$ binding and voltage sensor activation by 65%, which was evident by a decrease in E from 6.16 to 2.09 (**Figure 5-14B**).

cbv1+β1

A

Control   Ethanol   Wash

-60mV
0 μM Ca^{2+}

-80mV
0 μM Ca^{2+}

1 s

5 pA

B

Control

Log P$_o$

$L_0=1*10^{-7}$
$z_L=0.4$
$z_J=0.62$
$V_h(J)=100$
$D=37$

Voltage (mV)

C

Ethanol

Log P$_o$

$L_0=1*10^{-7}$
$z_L=0.5$
$z_J=0.56$
$V_h(J)=100$
$D=40$
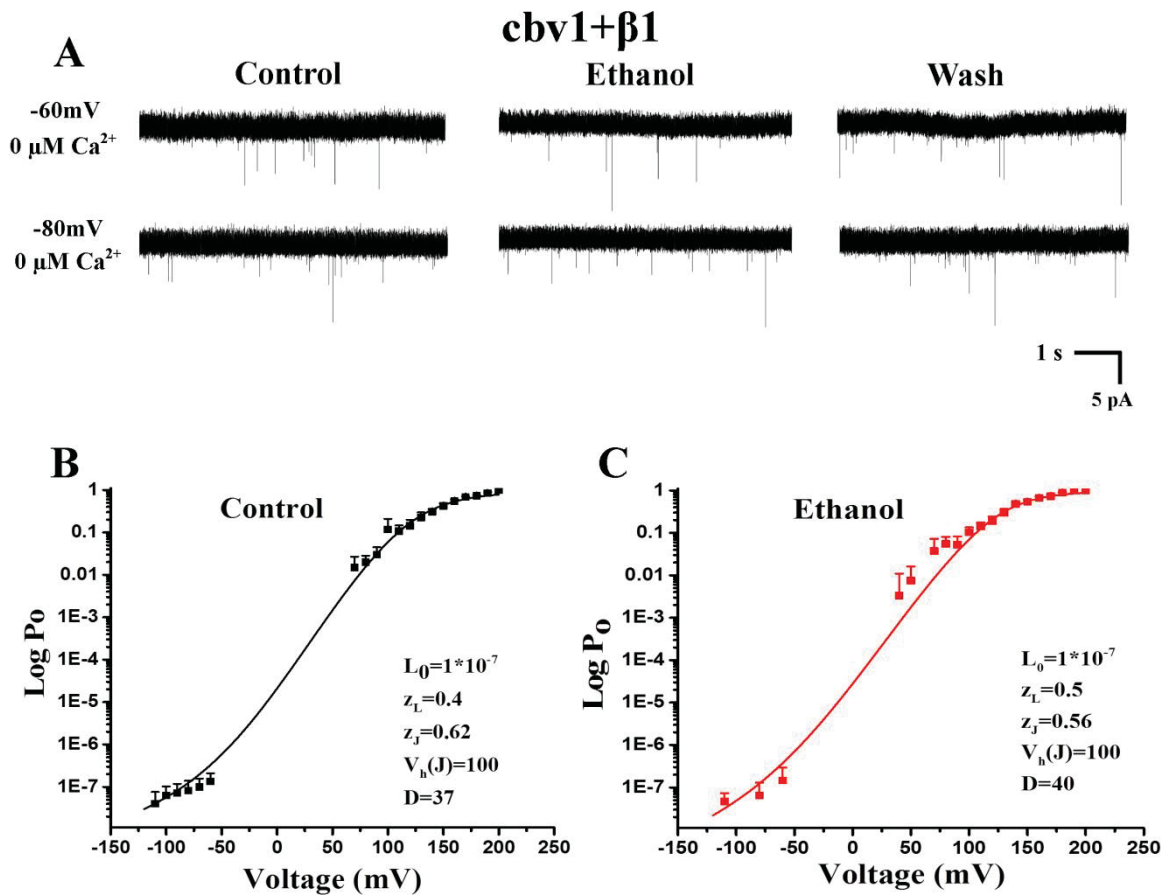
Voltage (mV)

Figure 5-13.   Ethanol does not alter the voltage-dependent parameters of cbv1+β1 channels

Notes: A) Representative unitary current recordings from I/O patches evoked in nominal zero Ca$^{2+}_i$ and within a wide range of membrane potentials. Recordings were obtained before (left trace), during (middle trace) and immediately after (right trace) patch exposure to 50 mM ethanol. Arrows indicate the baseline (all channels closed). B) and C) mean log P$_o$-V relations in presence and absence of 50 mM ethanol. At voltages less positive than +60 mV, data points were obtained from unitary current recordings; at voltages more positive than +60 mV, data points were obtained from macroscopic current recordings obtained at nominal zero Ca$^{2+}_i$. P$_o$-V data over a wide range of voltages were fitted with **Equation 5-2** after restricting $V_h(J)$ to determine the values of L_0, z_L, D and z_J. Best fit parameters are listed in the corresponding graphs. Each data point represents the average of no less than 3 patches, each excised from a different cell.
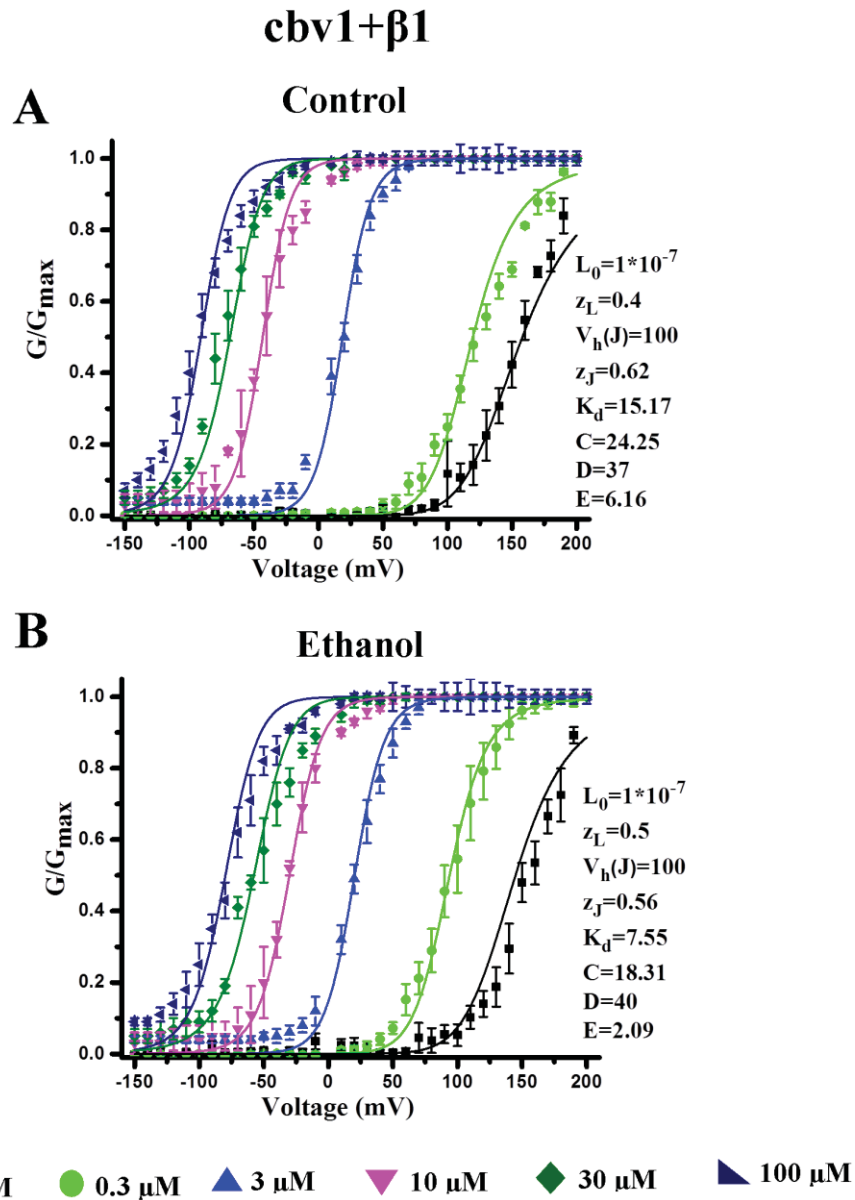
Figure 5-14.   Ethanol modulates the parameters associated with Ca^{2+}_i binding affinity of cbv1+β1 channels

Notes: Averaged G/G_{max}-V curves obtained over a wide range of Ca^{2+}_i, in absence (A) and presence (B) of 50 mM ethanol. These plots were fitted with **Equation 5-1**. For curves in panel A, L_0, z_L, $V_h(J)$, z_J, D were fixed to $1*10^{-7}$, 0.4, 100, 0.6 and 37 respectively, while K_d, C, D and E were allowed to vary. For in panel B, L_0, z_L, $V_h(J)$, z_J and D were fixed to $1*10^{-7}$, 0.5, 100, 0.56 and 40, respectively, while K_d, C, D and E were allowed to vary. Best fit parameters were shown in the corresponding plots. Data demonstrate that ethanol primarily modulates K_d, C and E. Each data point represents the average of no less than 3 patches, each excised from a different cell.

It is noteworthy that ethanol modulation of calcium binding affinity (K_d) of cbv1+β1 channel complex is similar (i.e., ~50% increase in Ca^{2+}_i biding affinity) to that of homomeric cbv1 channels (see **Table 5-2, Table 5-3** and **Figure 5-11A** and **B**). These results indicate that the presence of ethanol does not interfere with β1-induced change in Ca^{2+}_i binding affinity of BK channel-forming proteins. Collectively, our fitting results demonstrate that ethanol-induced inhibition of β1-containing BK channel activity is due to a combination of decreased allosteric coupling between 1) Ca^{2+}_i binding and voltage sensor activation and 2) Ca^{2+}_i binding and channel opening. Change in these two gating processes lead to overall decreased channel activity at low micro molar levels of Ca^{2+}_i.

5.3.   Discussion

In spite of recent advances in our understanding of how ethanol modulates BK channel behavior and thus cell physiology, the structural bases and molecular mechanisms underlying such modulation remain largely unresolved. In particular, while several groups documented that different auxiliary BK β subunits condition the channel's final response to ethanol, the use of different BK channel-forming alpha subunits and the largely descriptive electrophysiology approaches used make it impossible to derive any clear conclusion on targeted gating mechanisms and the proteins regions in the BK beta subunits that are responsible for regulating the channel's response to ethanol. In addition to systematically addressing the role of the different BK β subunits in ethanol action on BK channels, this study for the first time provides an in depth-analysis of the gating mechanisms that are perturbed by ethanol leading to modification of channel activity. Indeed, we aimed at addressing the following questions, 1) how ethanol distinctly modulates BK channels that *only* differ in beta subunit type composition and 2) what aspects of channel gating are modified for ethanol to reduce steady-state activity of β1-containing BK channels. To do so, we conducted pharmacological, electrophysiological and allosteric modeling approaches on BK macroscopic and single channel currents after expression of recombinant BK subunits in the same expression system, under similar patch-clamp recording conditions and across a wide range of voltage and Ca^{2+}_i concentrations. Importantly, and unlike all previous studies, we evaluated the ethanol responses of BK channel complexes formed by different beta subunit types (β1, β2, β2-IR, β3 or β4) and the same channel-forming slo1 protein (cbv1). Throughout the study we used an ethanol concentration (50 mM) reached in blood during moderate-to-heavy alcohol intoxication (Liu *et al.* 2008; Bukiya *et al.* 2009). Present data demonstrate that 1) ethanol differentially modulates BK currents that result from channel complexes containing different beta subunits; 2) ethanol similarly modulates β1-, β2- and β2-IR-containing BK channels; 3) the inactivation domain of *wt* β2 does not play a major role in ethanol action on cbv1+*wt* β2 channels; 4) ethanol modulation of β3-, β4- containing BK channels matches that of homomeric BK channels. 5) ethanol's major effect on homomeric cbv1 channel gating is to increase the apparent Ca^{2+}_i binding affinity, which leads to drug-induced potentiation of BK channel steady-state activity (**Table 5-2**); 6) On the other hand, ethanol-induced inhibition of β1-containing BK channels results from a combination of drug-induced gating modifications, as ethanol: 1) increases Ca^{2+}_i binding affinity of unliganded channel; 2) decreases the allosteric interaction between

Table 5-2. **Summary of best fit parameters obtained for homomeric BK channel in presence or absence of 50 mM ethanol**

Parameters	Control	50 mM Ethanol
L_0	$2X10^{-6}$	$2X10^{-6}$
z_L	0.4	0.3
$V_h(J)$	150	150
z_J	0.6	0.65
D	19.1	19.5
K_d	6.93	2.86
C	19.3	18.69
E	2.11	2.65

Table 5-3.   **Summary of best fit parameters obtained for β1-contianing BK channel in presence or absence of 50 mM ethanol**

Parameters	Control	50 mM Ethanol
L_0	1×10^{-7}	1×10^{-7}
z_L	0.4	0.5
$V_h(J)$	100	100
z_J	0.65	0.56
D	37	40
K_d	15.77	7.55
C	24.25	18.31
E	6.16	2.09

$Ca^{2+}{}_i$ binding and channel opening; and 3) decreases the allosteric interaction between $Ca^{2+}{}_i$ binding and voltage sensor activation (**Table 5-3**). Collectively, these three perturbations of normal gating process lead to decreased channel open probability.

The similar action of ethanol on β1- and β2-containing BK channels raises the hypothesis that ethanol action is related to a common mechanism(s) regulated by these two subunits, which is not extended to the other betas (β3-4). Previous data have shown that ethanol action on BK channel-forming proteins is absolutely dependent on $Ca^{2+}{}_i$ (Liu *et al.* 2008), with the drug final effect also being a function of this divalent concentration (Liu *et al.* 2008; Liu *et al.* 2013). Consistently, both β1 and β2 subunits drastically increase the apparent $Ca^{2+}{}_i$ sensitivity of the channel, an action not shared by β3 nor β4. Our ethanol data seem to indicate that auxiliary subunit regulation of ethanol action on slo1 channels is unique to β1 and β2 subunits, which modulate the channel by a common gating perturbation, that is, an increase in the apparent $Ca^{2+}{}_i$ sensitivity).

These findings raise speculation that the distinct ethanol sensitivity of β1- and β2-containing BK channels is due to amino acid residues that are highly conserved in these regulatory proteins. Previous studies have shown a higher conservation (43%) of residues between β1 and β2 subunits when compared to the other two regulatory subunit types (i.e., β1 *vs* β3 and β1 *vs* β4) (Behrens *et al.* 2000; Brenner *et al.* 2000). Thus, ethanol may directly interact with some of the residues conserved between β1 and β2 subunits, whether involved in modulating channel's $Ca^{2+}{}_i$ sensitivity or not, and thus enabling drug-induced inhibition of channel activity at low micro molar levels of $Ca^{2+}{}_i$.

Fitting our data to the 70-state model provide some mechanistic and structural insights on ethanol modulation of β1-containing BK channels. In order to interpret these data, we need to first discuss the allosteric interactions between $Ca^{2+}{}_i$ and ethanol on homomeric, BK channel-forming cbv1 proteins.

i) Ethanol action on slo1 channel gating and activating $Ca^{2+}{}_i$: Fitting the ethanol data obtained from homomeric BK channel reveals that most of the ethanol's effect on the channel activity is due to modulation of Ca^{2+}-driven gating i.e., increase in the $Ca^{2+}{}_i$ binding affinity (decrease in K_d) without significant modification of voltage-driven gating parameters or the channel intrinsic gating. From an structural point of view, the close spatial location of our newly identified ethanol sensing site in slo1 channels and the channel's high affinity (low μM) (Bukiya *et al.* 2014) $Ca^{2+}{}_i$ binding site (see below) suggests that channel conformational changes upon binding of these two ligands ($Ca^{2+}{}_i$ and ethanol) reciprocally interact to modulate overall channel activity. Indeed, previous data from our lab have demonstrated that if the two high affinity calcium-binding sites are disrupted by nonconserved mutations, the ethanol sensitivity is lost. The channel, however, remains ethanol-activatable as far as $Ca^{2+}{}_i$ is able to interact with either of the high affinity sites (Liu *et al.* 2008). Disruption of the RCK1 affinity site uniquely disrupts channel desensitization and eventual decrease in Po-driven by higher $Ca^{2+}{}_i$ levels, the latter process being favored by ethanol (Liu *et al.* 2008). Interestingly, recent studies (Bukiya *et al.* 2014) from our lab show

that, following mutated constructs: mslo1-K361N,R514N, mslo1-R514N, and mslo1-K361N lack sensitivity to ethanol. However, only the R514N-containing constructs demonstrate an altered Ca^{2+}_i sensitivity. Finally, R514 is shifted far away from the ethanol-interaction site when modeled in the "Ca^{2+}-free" state. Thus, R514 seems to be a key structural component in slo1 CTD that communicates ethanol- and Ca^{2+}_i-sensing machineries (Bukiya *et al.* 2014).

Ligand binding sites for ethanol and Ca^{2+}_i are nearby but do not overlap (Liu *et al.* 2008; Bukiya *et al.* 2014), which makes alcohol and Ca^{2+}_i heterotropic ligands of BK channel-forming proteins. The newly identified ethanol sensing site (which involves K361 for hydrogen bonding with the alcohol) in slo1 channels is located adjacent to the RCK1 high affinity Ca^{2+}_i binding site, which is determined by D362 and D367. Our recent computational modeling data demonstrate that ethanol cannot access the ethanol sensing pocket to hydrogen bond with K361 in the Ca^{2+}_i free closed channel (Bukiya *et al.* 2014), which explains the requirement of Ca^{2+}_i , but not Mg^{2+}_i, for ethanol to modulate channel activity (**Figure 4-2** and **Figure 4-3** in this thesis) (Liu *et al.* 2008; Liu *et al.* 2013). While the specific recognition sites for ethanol and Ca^{2+}_i do not overlap, they must converge on a common structure that couples gating to channel opening. It has been proposed that eight RCK domains form a "gating ring" (Jiang *et al.* 2002; Horrigan 2012) for BK channels. This overall design is shared with the two TM-expanding channel, MthK, which is, like slo1, Ca^{2+}_i-sensitive. Remarkably, our data show that Mthk and slo1 are also ethanol-sensitive (Liu *et al.* 2013). It is thought that the slo1/Mthk gating ring plays an important role in extracting the free energy from Ca^{2+}_i binding and thus coupling this ion binding to channel opening. In addition, it has been shown that the "linker" between the S6 transmembrane domain and the first RCK domain (which includes the ethanol binding site) acts as a spring, that couples gating ring expansion secondary to Ca^{2+} binding with channel opening itself (Jiang *et al.* 2002; Niu *et al.* 2004; Ye *et al.* 2006; Wu *et al.* 2009; Horrigan 2012; Yuan *et al.* 2012). Therefore, we advance the notion that upon Ca^{2+}-binding to the BK channel CTD high affinity sites, ethanol is able to modulate slo1 channel activity by interacting with a defined pocket nearby the RCK1 high affinity Ca^{2+}_i-binding site, leading to increased affinity of the Ca^{2+}_i and eventually resulting in channel activation.

ii) *Ethanol-induced gating modifications in β1-containing BK heteromers:* Like, homomeric BK channels, fitting the ethanol data obtained from β1-containing BK channels reveal that most of the ethanol's effect on the channel activity i.e., facilitation of inhibition, is mainly due to the Ca^{2+}-driven gating but not voltage-driven gating. In presence of β1, ethanol leads to perturbation of a two major gating processes, which ultimately leads to decreased channel open probability: 1) decrease in the allosteric interaction between Ca^{2+}_i binding and channel opening (i.e., significant decrease in allosteric factor C by 25%) and 2) decrease in the allosteric interaction between Ca^{2+}_i binding and voltage sensor activation (i.e., significant decrease in allosteric factor E by 65%). Collectively, final effect of ethanol leads to a reduced increase in the apparent Ca^{2+}_i sensitivity introduced

that is normally introduced by β1 subunits, a drug effect that we coined as alcohol's "anti-β1 action". At least three structural explanations can be provided for this ethanol's anti-β1 action: 1) β1 subunit does not contain ethanol sensing site. Rather, newly identified ethanol sensing site (slo1 "activation site") (Bukiya *et al.* 2014) in the cytosolic tail of the slo1 channel may serve as an "inhibition site", ethanol interaction with this site may disrupt the functional coupling between slo1 and β1 subunit 2) β1 subunit itself possesses an ethanol recognition/interaction site(s) and thereby causing in inhibition or perturbs the functional coupling between slo1 (cbv1 in our case) and β1 subunits upon ethanol binding to such site(s); 3) Ethanol may disrupt the lipid environment around the BK channel complex and thereby perturbs the functional coupling between slo1 and β1 subunits. In any case, the final effect of ethanol on β1-containing BK channels is to decrease the ability of this regulatory subunit to increase the channel's apparent Ca^{2+}_i-sensitivity.

From a structural point of view, present data may also provide insights on ethanol modulation of specific BK-β1 protein domains that participate in basal slo1-β1 coupling. Chimeric channel studies between mslo and dslo have demonstrated that slo1 N-end and S0 are both critical for the functional effects of β1 (Wallner *et al.* 1996; Morrow *et al.* 2006; Lee *et al.* 2010). Disulfide cross-linking studies shown that N-terminal EC end of S0 is in close proximity of S3 and S4 during resting state and move in concert during voltage sensor activation (Wu *et al.* 2009; Liu *et al.* 2010; Wu *et al.* 2013). Amino acid substitutions in S0 disrupt the voltage-dependent channel activation of BK channels, underscoring S0 interactions with other membrane-spanning domains of the channel VSD (Wallner *et al.* 1996). Similar disulfide cross-linking studies demonstrate that BK β TM1 and TM2 are both packed close to each other at the mouth of the cleft between the VSDs of two adjacent slo1 subunits (Wu *et al.* 2009; Liu *et al.* 2010; Wu *et al.* 2013). Within this cleft, TM1 is close to S1 of one VSD while TM2 is close to S0 of the adjacent VSD (Wu *et al.* 2009; Liu *et al.* 2010; Wu *et al.* 2013). I have recently demonstrated that both TMs of β1 subunit are essential to confer the β1-induced apparent increase in Ca^{2+}_i sensitivity (Kuntamallappanavar *et al.* 2014). Thus, the proposed location of both TM1 and TM2 (Wu *et al.* 2009; Liu *et al.* 2010; Wu *et al.* 2013) and our recent findings on functional coupling between slo1 and β1 (Kuntamallappanavar *et al.* 2014) suggest that both TMs of β1 subunit and slo1 VSD TMs are functionally coupled. It may be possible that ethanol targets transmembrane domains of β1 subunit to disrupt this functional coupling between slo1 and β1 subunit (see previous paragraph), thereby, antagonizing the functional effects of β1 subunits. It means in presence of β1 subunit, ethanol should allosterically modulate at least some interaction between structural domains that are coupled to gating and channel opening. Previous investigations demonstrated that RCK domains interact with VSD *via* voltage sensor paddle (i.e., S4 domain) as well as S4-S5 linker and RCKs also interact with PGD *via* "S6-RCK linker" (Horrigan and Aldrich 2002; Jiang *et al.* 2002; Hu *et al.* 2003; Orio and Latorre 2005). Our speculation seems to be consistent with the results obtained from HA model fitting that: in presence of β1 subunit,

ethanol seems to disrupt 1) the active allosteric interaction that involves RCKs and VSD *via* S4 and S4-S5 linker (i.e., decrease in allosteric factor E) and 2) destabilize the active interaction between RCKs and PGD *via* S6-RCK linker (i.e., decrease in allosteric factor C), eventually decreasing the channel open probability.

Current data presented and discussed in this section provides evidence of specific regions and gating mechanisms that are targeted by ethanol to modify beta1 subunit-containing BK channels. This information may lead to design of new agents that target such region and/or the specific ethanol-sensitive gating processes in order to oppose ethanol-induced modification of physiology *via* β1 subunit-containing BK channels. Future studies might lead to possible identification of specific amino acids in the β1 subunit TM2 domain, which can serve for pharmacophore design and drug discovery.

CHAPTER 6.   SPECIFIC BETA1 REGION(S) IS NECESSARY FOR ETHANOL-INDUCED INHIBITION OF BK CHANNELS AND EVENTUAL CEREBRAL ARTERY CONSTRICTION

6.1.   Overview

Ethanol at concentrations obtained in circulation during moderate to heavy episodic drinking, such as during binge drinking (30-60 mM) causes cerebral vasoconstriction in many species, including humans. Rodents serve as an excellent model to study ethanol-induced cerebral artery constriction. Using this model, our laboratory demonstrated that ethanol-induced cerebral artery constriction is due to a decrease in STOCs (Spontaneous Transient Outward Currents). In cerebral artery myocytes, STOCs result from the activity of BK channels. Ethanol (50 mM) decreases the NP_o of vascular myocyte BK channels leading to increase in cerebral artery tone. Functional BK channels are tetramers of pore-forming slo1 subunits. In most of the tissues, slo1 subunits are associated with small accessory subunits (β1-4) that modify the BK current phenotype and pharmacology. BK β1 subunit prevails in vascular smooth muscle while β4 subunits prevail in neurons. Previous studies and specific aim 2 of this dissertation demonstrated that smooth muscle cell-abundant BK β1 subunit enables ethanol-induced BK channel inhibition at physiological Ca^{2+}_i and voltages. In contrast, neuronally-predominant BK β4 subunit does not support this ethanol action (see results of chapter 5) (Liu *et al.* 2008; Bukiya *et al.* 2009). In this study, our goal was to understand the molecular basis of this pharmacological difference between these two β subunits and determine which region of BK β1 subunit is necessary for ethanol-induced inhibition of BK channels and eventual cerebral artery constriction. In order to address these questions, first we constructed a set of β1/β4 chimeras by swapping different domains of β1 and β4 in such a way that swapped region became progressively smaller. Secondly, we used patch-clamp studies to evaluate the ethanol responses of macroscopic currents mediated by recombinant BK channels that contained the different β1/β4 chimeras. Finally, we transfected cerebral arteries from *KCNMB1* K/O mouse with the different β1/β4 chimeric constructs and determined the impact of the BK β1 region(s) that mediates drug modification of channel function on ethanol-mediated vasoconstriction of pressurized cerebral arteries.

6.2.   Results

6.2.1.   β1/β4 Chimeric Constructs and Their Functional Characterization

As stated above, the overall strategy was to construct β1/β4 chimeras by swapping different domains of β1 and β4 subunits in such a way that the swapped region became progressively smaller. The resulting are: 1. β_1TMs_4, which contains hβ4 TMs on hβ1 "background" (i.e., hβ1 EC loop and IC ends); 2. β_4TMs_1, which contains hβ1 TMs on hβ4 "background" (i.e., hβ4 EC loop and IC ends); 3. β_4TM1_1, which contains hβ1 TM1

on hβ4 "background" (i.e., hβ4 TM2, EC loop and IC ends); 3. β_4TM2_1, which contains hβ1 TM2 on hβ4 "background" (i.e., hβ4 TM1, EC loop and IC ends); 4. β_4L_1, which contains EC loop from hβ1 on hβ4 "background" (i.e., hβ4 TMs and IC ends); 5. β_1L_4, which contains EC loop from hβ4 on hβ1 "background" (i.e., hβ1 TMs and IC ends) (**Figure 6-1**). These β1/β4 chimeric constructs have been routinely used in our laboratory, their surface expression and function when co-expressed with cbv1 being confirmed by pharmacological profiling as described elsewhere (Bukiya *et al.* 2008; Kuntamallappanavar *et al.* 2014).

6.2.2. Both Transmembrane Domains of BK-β1 Subunits Are Responsible for Ethanol-Induced Inhibition of BK Channels

We studied ethanol action using cbv1+β1 and cbv1+β4 as positive and negative control, respectively. All the experimental conditions, data acquisition and analysis were similar to those of the experiments described in SA1.

First, we co-expressed β_1TMs_4 subunits with cbv1 channels and explored ethanol action on the resulting channel complexes. Data demonstrate that ethanol increases the activity of these heterooligomeric channels at low $[Ca^{2+}]$ i.e., 0.3-10 µM, which is evident from the significant decrease in $V_{0.5}$ from the $V_{0.5}$-$[Ca^{2+}]$ plot. As $[Ca^{2+}]$ increased, activation turned to mild inhibition, which was evident from a mild increase in $V_{0.5}$. Furthermore, ethanol-induced activation-to-inhibition cross-over occurred at ~20 µM (**Figure 6-2A** and **B**). Thus, ethanol modulated cbv1+β_1TMs_4 channel activity in a pattern that matched that of homomeric BK channels. These results seem to indicate that regions that constitute the β1 background (IC ends and EC loops from β1) are not critical for ethanol-induced inhibition of β1-containing BK channels.

Next, we tested whether TMs could play a critical role in ethanol-induced action on β1-containing BK channels. Thus, we co-expressed β_4TMs_1 subunits with cbv1 channels and explored ethanol action on these channel complexes. Data demonstrate that ethanol increased channel activity at low $[Ca^{2+}]$ i.e., 0.3 µM, which is evident from the significant decrease in $V_{0.5}$ values in the $V_{0.5}$-$[Ca^{2+}]$ plot. As $[Ca^{2+}]$ increased, activation turned into significant inhibition, which is evident from the increased $V_{0.5}$. Remarkably, ethanol-induced activation-to-inhibition cross-over occurred at ~2 µM (**Figure 6-2C** and **D**), which exactly matched that of cbv1+β1 channels. These results seem to indicate that either or both transmembrane domains from β1 are critical for β1 subunit to facilitate ethanol inhibition of BK channels. This outcome encouraged me to identify whether an individual transmembrane domain (TM1 or TM2) of BK β1 could be responsible for this subunit-induced facilitation of ethanol inhibition of BK channel activity.

Figure 6-1.   Cartoons of β1/β4 chimeras constructed for this study

Notes: Cartoons depicting chimeric constructs that result from swapping different regions between β1and β4 subunits. 1. β_1TMs_4, which contains hβ4 TMs on hβ1 "background" (i.e., hβ1 EC loop and IC ends); 2. β_4TMs_1, which contains hβ1 TMs on hβ4 "background" (i.e., hβ4 EC loop and IC ends); 3. β_4TM1_1, which contains hβ1 TM1 on hβ4 "background" (i.e., hβ4 TM2, EC loop and IC ends); 3. β_4TM2_1, which contains hβ1 TM2 on hβ4 "background" (i.e., hβ4 TM1, EC loop and IC ends); 4. β_4L_1, which contains EC loop from hβ1 on hβ4 "background" (i.e., hβ4 TMs and IC ends); 5. β_1L_4, which contains EC loop from hβ4 on hβ1 "background" (i.e., hβ1 TMs and IC ends) Domains from β1 are given in black and those of β4 are given in grey.

Source: Modified with permission from Kuntamallappanavar G. Toro L. and Dopico A.M. (2014). Both transmembrane domains of BK beta1 subunits are essential to confer the normal phenotype of beta1-containing BK channels. *PLoS One* 9(10): e109306.

Figure 6-2. **BK β1 transmembrane domains determine ethanol-mediated inhibition of β1-containing BK channel**

Notes: A) TMs from β4 subunit on BK β1 background shift the activation-to-inhibition crossover of ethanol responses to ≈20 μM Ca^{2+}_i, mimicking cbv1+β4 and homomeric cbv1 channel responses. B) Bar graph representing ethanol-induced change in $V_{0.5}$ values from control and $β_1TMs_4$ obtained at 0.3 and 100 μM Ca^{2+}_i, respectively. C) TMs from β1 on a BK β4 background shift the activation-to-inhibition crossover of ethanol responses to 3 μM $[Ca^{2+}_i]$, mimicking cbv1+β1 responses. D) Bar graph representing ethanol-induced change in $V_{0.5}$ values from control and $β_4TMs_1$ obtained at 0.3 and 100 μM Ca^{2+}_i, respectively. *Different from control (P<0.05). Error bars show SEM; each point represents the average of ≥4 patches.

6.2.3. Second Transmembrane Domain of BK-β1 Subunit Determines the Ethanol-Induced Inhibition of BK Channels

To identify whether a particular BK β1 TM was sufficient to determine the ethanol action on β1-containing BK channels, we first co-expressed with cbv1 a β1/β4 chimera that contained TM1 from β1 on β4 background (β_4TM1_1). Data demonstrate that ethanol increased the activity of these heterooligomeric channel at low $[Ca^{2+}]$ i.e., 0.3-10 μM, which is evident as a significant decrease in $V_{0.5}$ from the $V_{0.5}$-$[Ca^{2+}]$ plot. As $[Ca^{2+}]$ increased, this activation turned into mild inhibition, evident from a small increase in $V_{0.5}$. Furthermore, ethanol-induced activation-to-inhibition cross-over occurred at ~20 μM (**Figure 6-3A** and **B**). Thus, the ethanol modulation cbv1+β_4TM1_1 channel activity follows a pattern that matches that of homomeric BK channels. These results seem to indicate that BK β1 TM1 is not critical for ethanol-induced inhibition of β1-containing BK channels. Collectively, this finding and the results obtained with β_4TMs_1 raise the hypothesis that β1 TM2 plays an important role in β1 subunit modulation of ethanol action.

Thus, we co-expressed with cbv1 a β1/β4 chimera that contained TM2 from β1 on β4 background (β_4TM2_1) and studied the ethanol response of the resulting channels. Data show that ethanol increases the activity of these channel complexes at low $[Ca^{2+}]$ i.e., 0.3 μM. As $[Ca^{2+}]$ increased, this activation turned to significant inhibition, resulting in an activation-to-inhibition cross over at ~3 μM (**Figure 6-3C** and **D**). This crossover matched that of cbv1+β1 channels, suggesting that β1 TM2 is critical for β1 subunits to facilitate ethanol-mediated inhibition of BK channels.

After identifying *via* patch-clamp electrophysiology studies the specific region of β1 subunit that was responsible for facilitating ethanol-induced inhibition of BK channels, we decided to determine any possible contribution e impact of such region to BK channel-mediated ethanol action on organ function, i.e., the cerebral artery. Thus, I next tested the hypothesis that "ethanol-induced constriction of cerebral arteries is critically dependent on specific region(s) of the arterial smooth muscle BK β1-subunit". This aim includes studies on organ function under physiological conditions with the combination of reversible permeabilization and myogenic tone experiments. To our knowledge, this experimental approach was the first to address the role of a specific domain of β1 subunit in ethanol action on organ function in alcohol research.

6.2.4. Reversible Permeabilization Leads to Overexpression of Desired Proteins and Resulting Functional Middle Cerebral Arteries

In order to achieve this goal, I took advantage of the reversible permeabilization technique (Lesh *et al.* 1995; Xi *et al.* 2008; Adebiyi *et al.* 2011; Bannister *et al.* 2011; Thomas-Gatewood *et al.* 2011). Using this technique, expressing vectors containing β1 or β1/β4 chimeras (**Figure 6-1**) were transfected into de-endothelized middle cerebral arteries of *KCNMB1* K/O mouse in order to express heteromeric BK β1 alone or β1/β4 chimeras following protocols described elsewhere (see **Chapter 3**) .
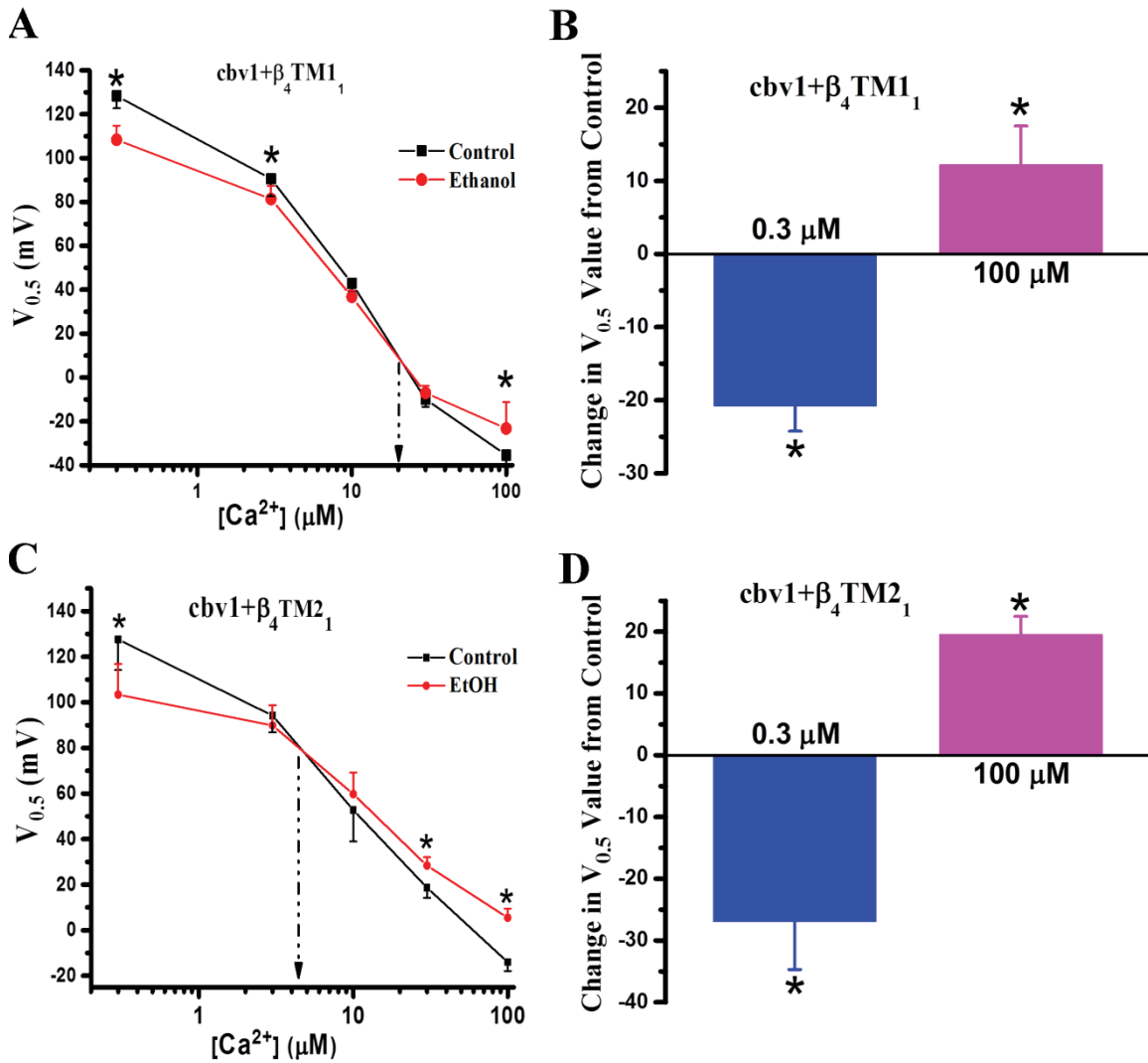
Figure 6-3. **Second transmembrane domain of BK β1 subunit determines the ethanol-induced inhibition of β1-containing BK channel**

Notes: A) TM1 domain from β1 on β4 background shifts the activation-to-inhibition crossover of ethanol responses to ≈20 μM $[Ca^{2+}_i]$, mimicking cbv1+β4 or homomeric BK channel responses. B) Bar graph representing ethanol-induced change in $V_{0.5}$ values from control and $β_4TM1_1$ obtained at 0.3 and 100 μM Ca^{2+}_i, respectively. C) TM2 from β1 on β4 background shifts the activation-to-inhibition crossover of ethanol responses to 3 μM $[Ca^{2+}_i]$, mimicking cbv1+β1 responses. D) Bar graph representing ethanol-induced change in $V_{0.5}$ values from control and $β_4TM2_1$ at 0.3 μM and 100 μM, respectively. *Different from control (P<0.05). Error bars show SEM; each point represents the average of ≥4 patches.

After 3-4 days of transfection, 1) successful overexpression of protein and 2) further resulting functional arteries were tested. First, successful reversible permeabilization resulting in protein overexpression was confirmed by western blotting. Arteries subjected to reverse permeabilization expressed significantly higher levels of BK β1 alone (**Figure 6-4A**) or β1/ β4 chimeras (**Figure 6-4B**) than those of control arteries transfected with empty vectors. These results underscore the effectiveness of reversible permeabilization to overexpress selective proteins, as previously demonstrated for other proteins and tissues (Lesh *et al.* 1995; Xi *et al.* 2008; Bannister *et al.* 2011; Thomas-Gatewood *et al.* 2011).

Next, we determined whether reversible permeabilization resulted in loss of arterial function. After 4 days of reversible permeabilization with either *wt* β1 or β1/β4 chimeras using the protocols proposed in SA4 (see **Chapter 3**), I evaluated the artery diameter response to 60 mM K^+ and vasodilation in response to Ca^{2+}-free bath solution to determine the vessel contractile response to depolarization and passive diameter, respectively. **Figure 6-4C** demonstrates one representative trace of cerebral artery diameter following organ transfection with *wt* β1. A summary of KCl-induced constrictive responses of middle cerebral arteries transfected with either β1 alone or β1/β4 chimeras is shown in **Figure 6-4D**. Collectively, these results suggest that reversible permeabilization technique in our hands results in overexpression of BK β1 or β1/β4 chimeras and renders functional *KCNMB1* K/O arteries that constrict and dilate as untransfected arteries from *wt* mouse do (Bukiya *et al.* 2009).

6.2.5. Ethanol-Induced Cerebral Artery Constriction Is Determined by β1 Subunit of BK Channels

Once we established that: 1) β1 subunit TM2 is largely responsible for facilitating ethanol-induced inhibition of BK channels, and 2) reversible permeabilization of *KCNMB1* K/O mouse middle cerebral arteries leads to overexpression of a β protein construct without perturbing vasomotion, we set to determine the contribution of BK β1 subunit TM2 to this subunit facilitation of ethanol-induced cerebral constriction.

We addressed this question using myogenic tone experiments identical to the protocols mentioned in **Chapter 3**. Briefly, after 4 days of permeabilization, a 2 mm long artery segment will be pressurized to 60 mmHg to develop myogenic tone and then vessel external diameter was continuously measured in response to application of following drugs: 1) depolarizing agent (60 mM KCl), 2) 50 mM ethanol, 3) 45 μM LCA, and 4) Ca^{2+}- free solution with sufficient wash in between each drug application (**Figure 6-5**).

First, we probed the arteries from wild type mice (C57BL/6 mice) with 50 mM ethanol, which caused vasoconstriction of 7.96±0.82% from pre-ethanol application level (**Figure 6-5A** and **C**). This response was used as positive control. These results are in agreement with previously published results (Bukiya *et al.* 2009; Bukiya *et al.* 2011).
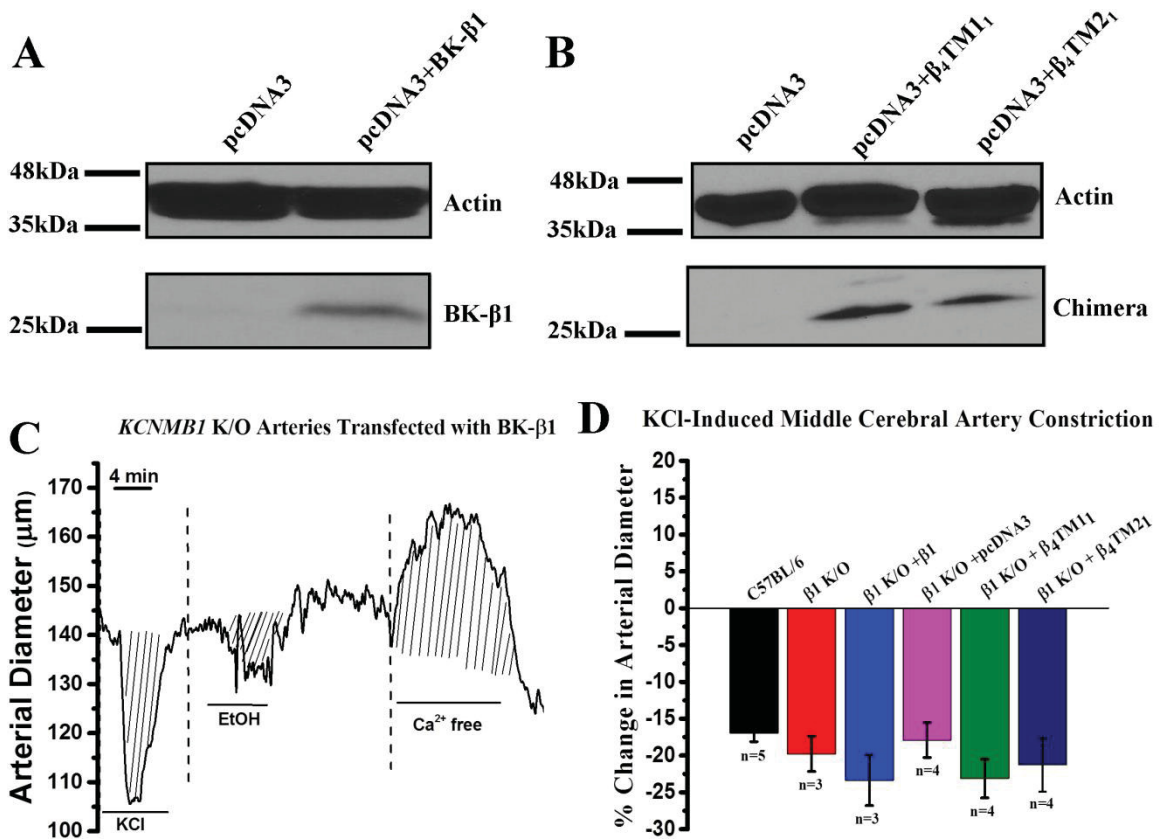
Figure 6-4. **Reversible permeabilization leads to overexpression BK β1 or β1/β4 chimeric protein and functioning mouse middle cerebral artery**

Notes: A) Representative western blots showing overexpression of BK-β1 proteins in arteries transfected with empty vector (left lane) or pcDNA3+BK β1 cDNA (right lane). B) Representative western blots showing overexpression of β1/β4 chimeric proteins in arteries transfected with empty vector (left lane) or pcDNA3+β_4TM1$_1$ (middle lane) or pcDNA3+β_4TM2$_1$ chimera cDNA.. C) Diameter trace from de-endothelized, pressurized middle cerebral artery after transfected with BK β1. After development of myogenic tone, application of 60 mM KCl causes reversible constriction; 50 mM ethanol produces constriction and Ca^{2+}-free solution causes dilation. All these responses are similar to those obtained in arteries from *wt* mouse (Bukiya *et al.* 2009); D) Bar graph showing averaged decrease in cerebral arterial diameter (in % change from pre-KCl diameter value) in response to 60 mM KCl after transfecting with various constructs as indicated; *wt* arteries from C57BL/6 mouse.
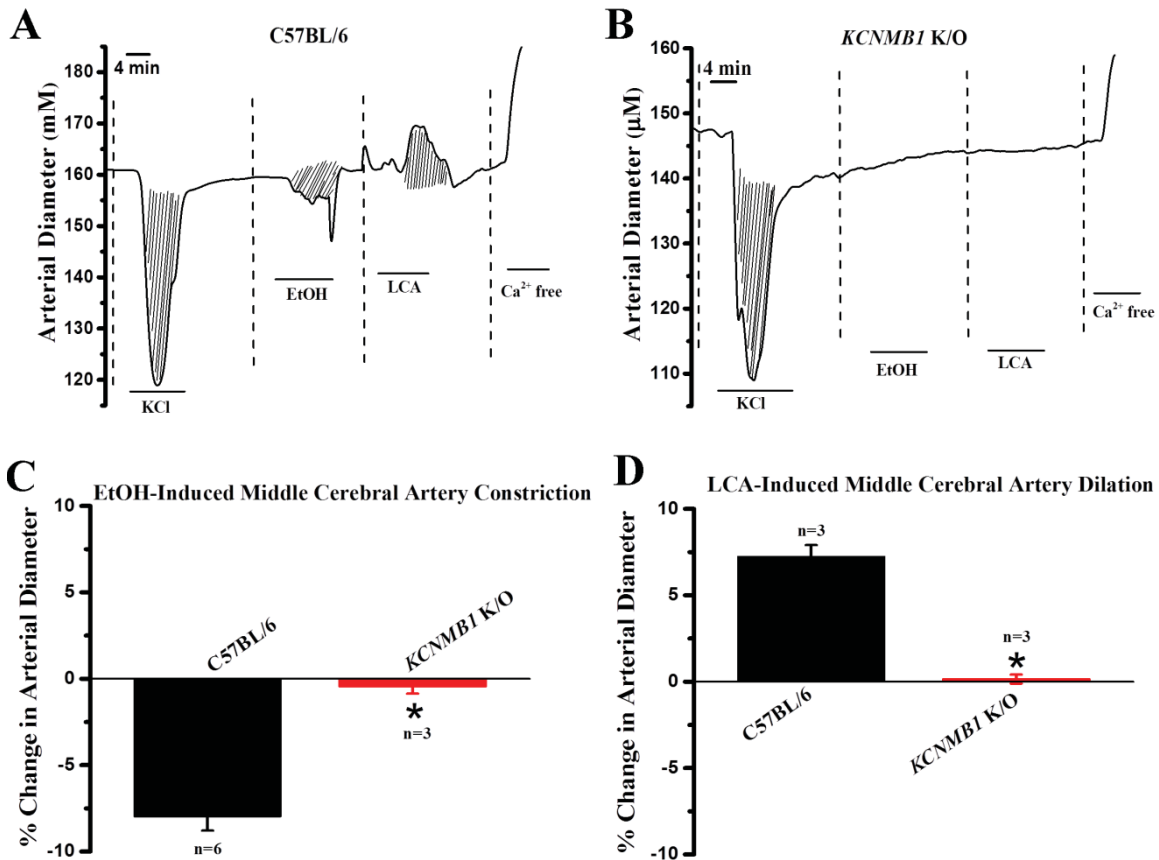
Figure 6-5.   BK β1 subunit determines ethanol-induced constriction of middle cerebral artery

Notes: A) Diameter trace from de-endothelized, pressurized middle cerebral artery from control (C57BL/6) mouse. After development of myogenic tone, application of 50 mM ethanol causes reversible constriction; 45 μM LCA produces dilation. B) However, arteries from *KCNMB1* K/O mouse failed to respond to acute application of 50 mM ethanol or 45 μM LCA. C, D) Bar graph showing percentage change in diameter in response to application of 50 mM ethanol (C) and 45 μM LCA (D) on arteries obtained control and *KCNMB1* K/O mice. *Different from control ($P<0.05$). Error bars show SEM; each point represents the average of 4-7 arteries.

Moreover, this ethanol action is similar to the constriction of middle cerebral artery in rats constriction (Liu *et al.* 2004), buttressing the fact that the primary mechanisms mediating ethanol action on cerebral arteries are conserved among the two species. After ethanol application, *wt* mouse arteries were probed with 45 µM LCA, which caused 7.23±0.68% dilation (**Figure 6-5A** and **D**). Again, these results are also consistent with previously reported studies (Bukiya *et al.* 2013).

Next, we tested the ethanol and LCA action on arteries obtained from *KCNMB1* K/O mice and *KCNMB1* K/O mice arteries transfected with empty vector, which were considered as our negative control. Indeed, and in contrast to *wt* mouse arteries, ethanol consistently failed to constrict cerebral arteries from *KCNMB1* K/O mouse and arteries transfected with empty vector (**Figure 6-5B** and **C, Figure 6-6A** and **Figure 6-7A**). These results indicate that BK β1 subunits are the primary determinants of alcohol-induced, cerebrovascular constriction. Furthermore, in contrary to arteries from *wt* mouse, LCA also failed to cause dilation of cerebral arteries obtained from *KCNMB1* K/O mouse (**Figure 6-5B** and **D, Figure 6-6A** and **Figure 6-7B**). Because LCA evokes BK channel activation *via* β1 but not other beta subunits (β2-4) (Bukiya *et al.* 2009). Further, it was already shown that amino acid residues in TM2 of BK β1 subunit is interacts with LCA to bring about cerebral artery dilation (Bukiya *et al.* 2011). Therefore, we used LCA as a tool to identify the presence of BK β1 subunit or TM2 region from β1-subunit. Our results indicate that BK β1 is responsible for LCA-induced cerebrovascular dilation *via* activation of smooth muscle cell BK channels. All These results are in agreement with previously published reports (Bukiya *et al.* 2008; Bukiya *et al.* 2009; Bukiya *et al.* 2013).

6.2.6. BK β1 Subunit Is Second Transmembrane Domain Is Necessary for Ethanol-Induced Cerebral Artery Constriction

First, we transfected arteries from *KCNMB1* K/O mouse with BK β1 subunit and measured changes in arterial diameter in response to 50 mM ethanol and 45 µM LCA to test whether BK β1subunit transfected arteries were able to recover sensitivity to ethanol and LCA. Indeed, data demonstrated that ethanol-induced arterial constriction in *KCNMB1* K/O mouse arteries transfected with BK β1 (**Figure 6-6B** and **Figure 6-7A)** reached 7.76+1.2%, which is similar to that evoked in control (C57BL/6) mouse. Likewise, LCA-induced artery dilation reached 8.41+2.6%
(**Figure 6-6B** and **Figure 6-7B**), which is similar to that observed in control (C57BL/6) mice arteries (**Figure 6-5A** and **C**). These results confirm the finding that BK β1 subunit is necessary for ethanol-induced constriction and LCA-induced dilation of cerebral artery.

After finding that TMs regions are important in controlling BK channel gating (Kuntamallappanavar et al., 2014) and that beta1 TM2 but not TM1 is largely responsible for β1-induced facilitation of ethanol inhibition of BK channels (see **section 6.2.3**), we addressed the roleTM1 and TM2 of BK β1 subunit in ethanol-induced constriction of cerebral arteries.
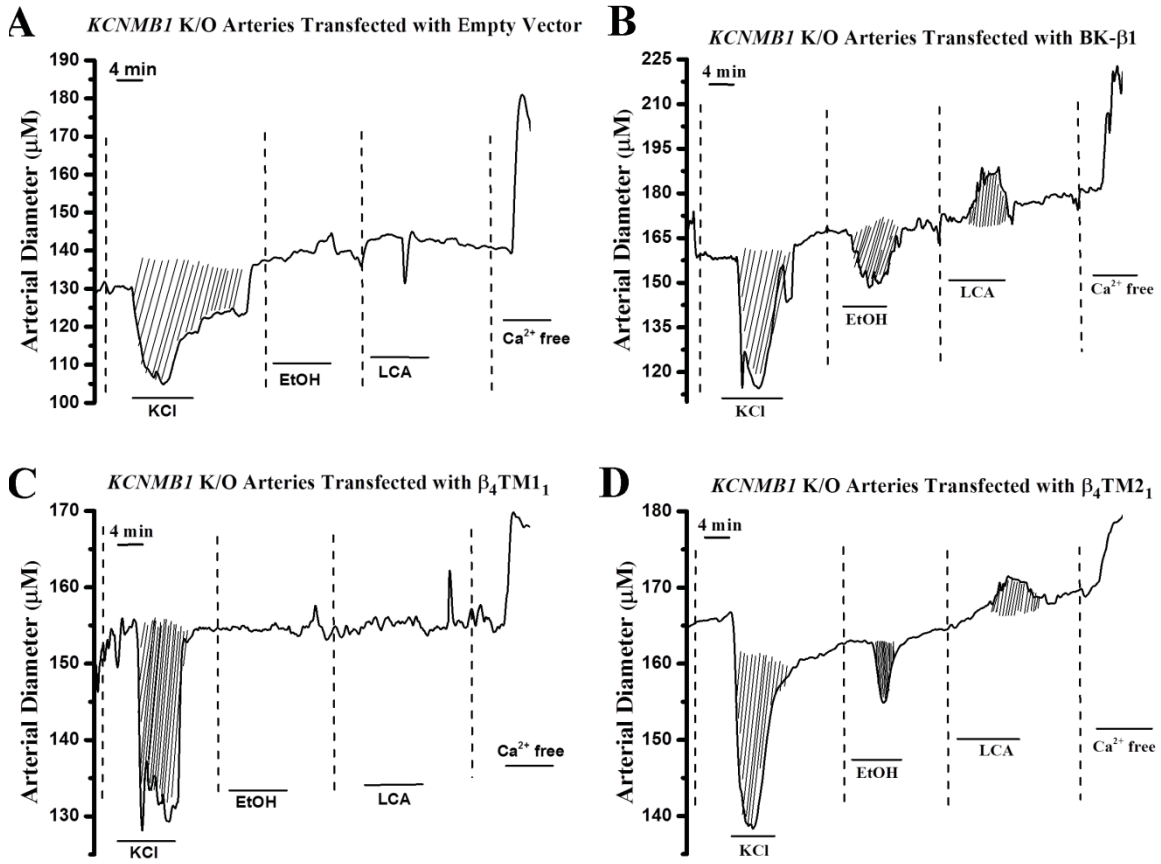
Figure 6-6. **Second transmembrane domain of BK β1 subunit determines ethanol-induced constriction of middle cerebral artery**

Notes: A) *KCNMB1* K/O arteries transfected with empty vector failed to respond to application of 50 mM ethanol and 45 μM LCA. B) Diameter trace from de-endothelized, pressurized *KCNMB1* K/O middle cerebral artery transfected with BK β1. Application of 50 mM ethanol caused reversible constriction; 45 μM LCA evokes artery dilation, which mimics the responses from control (C57BL/6) mice arteries. C) However, *KCNMB1* K/O arteries transfected with β_4TM1_1 failed to respond to application of 50 mM ethanol and 45 μM LCA. C) Interestingly, *KCNMB1* K/O arteries transfected with β_4TM2_1 responded with constriction and dilation to application of 50 mM ethanol and 45 μM LCA, respectively, these responses matching those from control (C57BL/6) mice arteries.

80
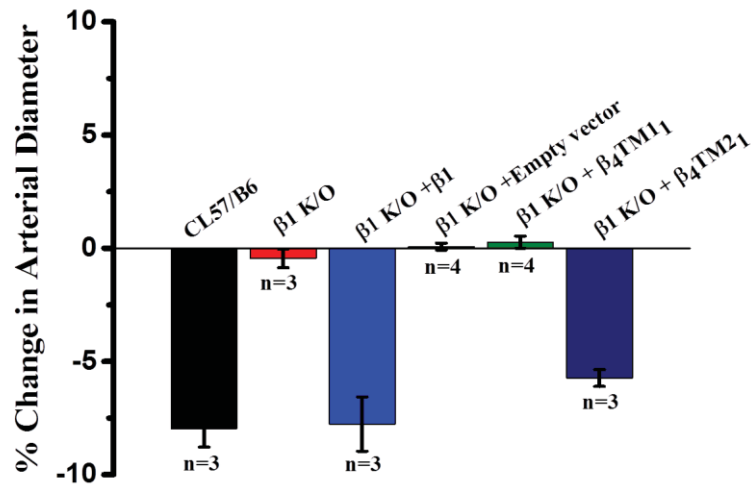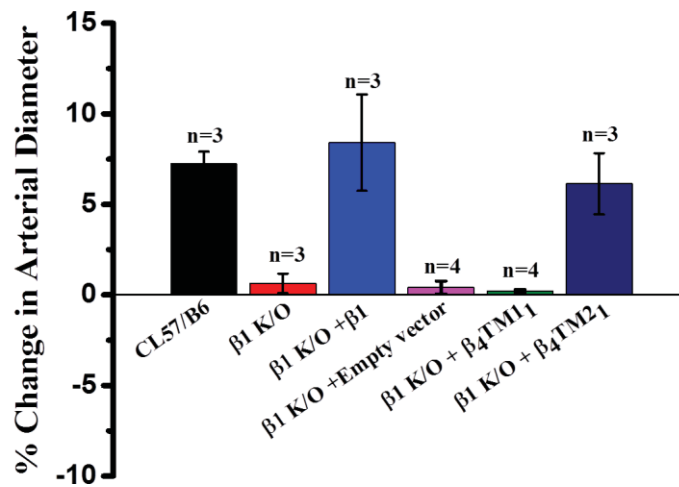
Figure 6-7. **Second transmembrane domain of BK β1 subunit is responsible for ethanol-induced constriction of middle cerebral artery**

Notes: A, B) Bar graph showing percentage change in diameter in response to application of 50 mM ethanol (A) and 45 μM LCA (B) from *KCNMB1* K/O mice arteries transfected with different constructs as indicated. *Different from control (CL57B/6) ($P<0.05$). Error bars show SEM; each point represents the average of 4-7 arteries.

Thus, we transfected KCNMB1 K/O mouse arteries with β4TM11 chimeric construct and then measured changes in arterial diameter in response to application of ethanol and LCA (**Figure 6-6C** and **D**).In contrast to the control (C57BL/6) mice arteries and arteries transfected with BK-β1, ethanol consistently failed to constrict *KCNMB1* K/O mouse arteries transfected with β_4TM1_1 (**Figure 6-6C,** and **Figure 6-7A**). These results indicate that EC loop, TM1 region and IC ends of BK β1 subunit do not mediate ethanol-induced cerebral artery constriction. Application of LCA also failed to evoke dilation of these arteries (**Figure 6-6C** and **Figure 6-7B**). This is an expected result, as LCA action on BK channels requires β1 TM2 (Bukiya *et al.* 2011), which is absent in the β_4TM1_1 chimera.

Finally, we determined the contribution of BK β1 subunit TM2 to ethanol-induced constriction of cerebral arteries. Thus, we transfected *KCNMB1* K/O mouse cerebral arteries with the β_4TM2_1 chimera and measured changes in arterial diameter in response to application of 50 mM ethanol and 45 μM LCA. In contrast to the arteries from *KCNMB1* knock-out mice, ethanol constricted cerebral arteries transfected with β_4TM2_1 by 5.73+0.37% (**Figure 6-6D** and **Figure 6-7A**). These results indicate that BK β1 subunit TM2 is critical for the ethanol-induced cerebral artery constriction. Further, functional expression of β_4TM2_1 and its coupling to the BK channel-forming subunit chimera was confirmed by the artery diameter response to LCA application. The latter caused dilated these arteries by 6.14+1.69% (**Figure 6-6D** and **Figure 6-7B**). This response is almost identical to the response to LC from control (C57BL/6) and *KCNMB1* K/O mouse arteries transfected with β1. These results seem to indicate that of BK β1 subunit TM2 region is necessary for ethanol-induced cerebral artery constriction.

6.3.   Discussion

Using a combination of patch-clamp electrophysiology on BK channels made of cbv1 and *wt* β1 or chimeric β1/β4 subunits, reversible permeabilizaton and in vitro pressurization of rat cerebral arteries, we identified for the first time the specific domain of the BK channel regulatory β1 subunit that is critical for ethanol-induced inhibition of channel activity and artery constriction mediated by this channel type. Indeed, our results clearly demonstrate that β1 TM2 is critical for ethanol-mediated action on BK channels and cerebral artery constriction. To our knowledge, this is the first time that a specific domain of an accessory subunit of any member of the voltage-activated TM6 ion channel super family is shown critical for ethanol action on ion channel function and vascular physiology.

Two studies have mapped alcohol-sensing sites to intracellular domains of the channel-forming subunit, as reported for GIRK (Aryal *et al.* 2009) and recently for BK themselves by us (Bukiya *et al.* 2014). These findings are rather unique, as multiple groups have previously documented that it is up to *transmembrane regions* to provide alcohol-sensing sequences in ion channels, as proposed for GABA-A, glycine, nACh and prokaryotic *Gleobacter violaceus* (GLIC) ionotropic receptor. We are hereby documenting for the first time that ethanol functionally targets a TM region of an

auxiliary subunit of BK channel to modulate channel activity and eventually rendering cerebral artery constriction.

As we proposed in previous chapter, at least three structural interpretations on this crucial role of a β1 subunit domain (TM2) on ethanol action ("anti-β1") are possible: 1) β1 subunit TM2 itself possess an ethanol recognition/interaction site(s) and thereby perturbs the functional coupling between slo1 (cbv1 in our case) and β1 subunits upon ethanol binding to this site; 2) newly identified ethanol sensing site K361 (slo1 "activation site") (Bukiya *et al.* 2014) in the cytosolic tail of the slo1 channel may serve as an "inhibition site", ethanol interaction with this site may disrupt the functional coupling between slo1 and β1 subunit; 3) Ethanol disrupts the lipid around the channel complex, TM2 in particular, and thereby perturbs the functional coupling between slo1 and β1 subunits, which involves TM2 (Kuntamallappanavar *et al.* 2014). Disregarding the structural specifics, it is clear from out data that β1 subunit TM2 plays a critical role in ethanol action on β1-containing BK channels and eventual cerebral artery constriction.

From a structural point of view, present data may provide further insights on ethanol modulation of specific BK-β1 protein domains that participate in basal slo1-β1 coupling. Chimeric channel studies between mslo and dslo have demonstrated that slo1 N-end and S0 are both critical for the functional effects of β1 (Wallner *et al.* 1996; Morrow *et al.* 2006; Lee *et al.* 2010). Disulfide cross-linking studies shown that N-terminal EC end of S0 is in close proximity of S3 and S4 during resting state and move in concert during voltage sensor activation (Wu *et al.* 2009; Liu *et al.* 2010; Wu *et al.* 2013). Amino acid substitutions in S0 disrupt the voltage-dependent channel activation of BK channels, underscoring S0 interactions with other membrane-spanning domains of the channel VSD (Wallner *et al.* 1996). Similar disulfide cross-linking studies demonstrated that BK β TM1and TM2 are both packed close to each other at the mouth of the cleft between the VSDs of two adjacent slo1 subunits (Wu *et al.* 2009; Lee *et al.* 2010; Wu *et al.* 2013). Within this cleft, TM1 is close to S1 of one VSD and TM2 close to S0 of the adjacent VSD (Wu *et al.* 2009; Lee *et al.* 2010; Wu *et al.* 2013). The proposed location of both TM1 and TM2 and my own findings (Kuntamallappanavar *et al.*, 2014) suggest that both TMs of β1 subunit and slo1 VSD TMs are functionally coupled. Results of present study show that ethanol targets TM2 of β1 subunit to disrupt the functional coupling between slo1 and β1 subunit, thereby, antagonizing the functional effects of β1 subunit. This speculation seems to be consistent with the results of HA model fitting that in presence of β1 subunit, ethanol perturbs the allosteric interaction that involves RCKs and VSD (decrease in allosteric factor E). Thus decreasing channel open probability.

Current information will lead to consider TM2-targeting agents, whether endogenous steroids such as lithocholate (Bukiya *et al.* 2007; Bukiya *et al.* 2008; Bukiya *et al.* 2009; Bukiya *et al.* 2011) or synthetic agents such as hydroxyl-alkynoic acids and HENA (Bukiya *et al.* 2013) that target β1 TM2 and thus, oppose alcohol-induced cerebral artery constriction. Future studies using point mutagenesis and pharmacophore design will help to a better rationale design of novel agents that would counteract such ethanol action without altering organ physiology that is not dependent on BK β1 subunits.

6.4. Overall Summary of Results

1. Slo1sensitivity to ethanol channel is dependent on Ca^{2+} but not Mg^{2+}, even when the latter is present at levels that do activate slo1channels.
2. Activating ion is required for and modulates ethanol final on slo1 channel activity while being unable to embold slo2 or slo3 channels with ethanol sensitivity.
3. Ethanol inhibition of BK channels is facilitated by $\beta1$, $\beta2$ and $\beta2$-IR subunits.
4. The inactivation domain of $\beta2$ does not play a major role in ethanol action.
5. BK $\beta3$ and $\beta4$ subunits fail to alter ethanol overall effect on - homomeric slo1 (cbv1) channels.
6. Ethanol-induced inhibition of $\beta1$-containing BK channels is allosterically coupled to Ca^{2+}_i-driven gating.
7. Ethanol-induced modification of activity of slo1 (cbv1) is due to modification of Ca^{2+}_i binding affinity wherease, ethanol-induced modification of heteromeric cbv1+$\beta1$ BK channels is primarily due to alteration in allosteric interaction between 1) RCK and voltage sensing domains and 2) RCKs and pore gate domains.
8. $\beta1$ TM2 is critical for ethanol to inhibit vascular smooth muscle cell BK channels and drug-induced cerebral artery constriction.

6.5. Final Conclusion

BK $\beta1$ TM2 enables ethanol-induced inhibition of $\beta1$-conaining BK channels and cerebral artery constriction, with drug action on channel activity being dependent on modification of calcium-gating parameters.

6.6. Future Directions

Our study shows that a specific region of BK-$\beta1$ subunit critically controls ethanol-induced inhibition of BK channels and its involvement in cerebral artery constriction. The following future studies are considered:

1. Identify the specific gating processes that are targeted by ethanol leading to differential modification of BK currents contains different β subunit composition ($\beta2$-$\beta4$).
2. Pinpoint mutagenesis strategies to identify possible amino acid residues in TM2 region of $\beta1$ subunit that could be involved in sensing or interacting with ethanol molecules.
3. Design a pharmacophore based on amino acid interaction and then discover or design pharmacological agents that antagonize the effect of ethanol on cerebral artery constriction *via* BK $\beta1$ subunits.

LIST OF REFERENCES

Adebiyi, A., Narayanan, D. and Jaggar, J. H. (2011). "Caveolin-1 assembles type 1 inositol 1,4,5-trisphosphate receptors and canonical transient receptor potential 3 channels into a functional signaling complex in arterial smooth muscle cells." *J Biol Chem* **286**(6): 4341-4348.

Altura, B. M. and Altura, B. T. (1982). "Microvascular and vascular smooth muscle actions of ethanol, acetaldehyde, and acetate." *Fed Proc* **41**(8): 2447-2451.

Altura, B. M. and Altura, B. T. (1984). "Alcohol, the cerebral circulation and strokes." *Alcohol* **1**(4): 325-331.

Altura, B. M., Altura, B. T. and Gebrewold, A. (1983). "Alcohol-induced spasms of cerebral blood vessels: relation to cerebrovascular accidents and sudden death." *Science* **220**(4594): 331-333.

Amberg, G. C. and Santana, L. F. (2003). "Downregulation of the BK channel beta1 subunit in genetic hypertension." *Circ Res* **93**(10): 965-971.

Arkwright, P. D., Beilin, L. J., Vandongen, R., Rouse, I. A. and Lalor, C. (1982). "The pressor effect of moderate alcohol consumption in man: a search for mechanisms." *Circulation* **66**(3): 515-519.

Aryal, P., Dvir, H., Choe, S. and Slesinger, P. A. (2009). "A discrete alcohol pocket involved in GIRK channel activation." *Nat Neurosci* **12**(8): 988-995.

Asano, M., Masuzawa-Ito, K. and Matsuda, T. (1993). "Charybdotoxin-sensitive K+ channels regulate the myogenic tone in the resting state of arteries from spontaneously hypertensive rats." *Br J Pharmacol* **108**(1): 214-222.

Bannister, J. P., Thomas-Gatewood, C. M., Neeb, Z. P., Adebiyi, A., Cheng, X. and Jaggar, J. H. (2011). "Ca(V)1.2 channel N-terminal splice variants modulate functional surface expression in resistance size artery smooth muscle cells." *J Biol Chem* **286**(17): 15058-15066.

Bao, L. and Cox, D. H. (2005). "Gating and ionic currents reveal how the BKCa channel's Ca2+ sensitivity is enhanced by its beta1 subunit." *J Gen Physiol* **126**(4): 393-412.

Barnett, N. P., Monti, P. M., Spirito, A., Colby, S. M., Rohsenow, D. J., Ruffolo, L. and Woolard, R. (2003). "Alcohol use and related harm among older adolescents treated in an emergency department: the importance of alcohol status and college status." *J Stud Alcohol* **64**(3): 342-349.

Beaglehole, R. (1990). "International trends in coronary heart disease mortality, morbidity, and risk factors." *Epidemiol Rev* **12**: 1-15.

Behrens, R., Nolting, A., Reimann, F., Schwarz, M., Waldschutz, R. and Pongs, O. (2000). "hKCNMB3 and hKCNMB4, cloning and characterization of two members of the large-conductance calcium-activated potassium channel beta subunit family." *FEBS Lett* **474**(1): 99-106.

Bhattacharjee, A. and Kaczmarek, L. K. (2005). "For K+ channels, Na+ is the new Ca2+." *Trends Neurosci* **28**(8): 422-428.

Brayden, J. E. and Nelson, M. T. (1992). "Regulation of arterial tone by activation of calcium-dependent potassium channels." *Science* **256**(5056): 532-535.

Brenner, R., Jegla, T. J., Wickenden, A., Liu, Y. and Aldrich, R. W. (2000). "Cloning and functional characterization of novel large conductance calcium-activated potassium channel beta subunits, hKCNMB3 and hKCNMB4." *J Biol Chem* **275**(9): 6453-6461.

Brenner, R., Perez, G. J., Bonev, A. D., Eckman, D. M., Kosek, J. C., Wiler, S. W., Patterson, A. J., Nelson, M. T. and Aldrich, R. W. (2000). "Vasoregulation by the beta1 subunit of the calcium-activated potassium channel." *Nature* **407**(6806): 870-876.

Brodie, M. S., Scholz, A., Weiger, T. M. and Dopico, A. M. (2007). "Ethanol interactions with calcium-dependent potassium channels." *Alcohol Clin Exp Res* **31**(10): 1625-1632.

Bukiya, A. N., Kuntamallappanavar, G., Edwards, J., Singh, A. K., Shivakumar, B. and Dopico, A. M. (2014). "An alcohol-sensing site in the calcium- and voltage-gated, large conductance potassium (BK) channel." *Proc Natl Acad Sci U S A* **111**(25): 9313-9318.

Bukiya, A. N., Liu, J. and Dopico, A. M. (2009). "The BK channel accessory beta1 subunit determines alcohol-induced cerebrovascular constriction." *FEBS Lett* **583**(17): 2779-2784.

Bukiya, A. N., Liu, J., Toro, L. and Dopico, A. M. (2007). "Beta1 (KCNMB1) subunits mediate lithocholate activation of large-conductance Ca2+-activated K+ channels and dilation in small, resistance-size arteries." *Mol Pharmacol* **72**(2): 359-369.

Bukiya, A. N., McMillan, J. E., Fedinec, A. L., Patil, S. A., Miller, D. D., Leffler, C. W., Parrill, A. L. and Dopico, A. M. (2013). "Cerebrovascular dilation via selective targeting of the cholane steroid-recognition site in the BK channel beta1-subunit by a novel nonsteroidal agent." *Mol Pharmacol* **83**(5): 1030-1044.

Bukiya, A. N., Singh, A. K., Parrill, A. L. and Dopico, A. M. (2011). "The steroid interaction site in transmembrane domain 2 of the large conductance, voltage- and calcium-gated potassium (BK) channel accessory beta1 subunit." *Proc Natl Acad Sci U S A* **108**(50): 20207-20212.

Bukiya, A. N., Vaithianathan, T., Kuntamallappanavar, G., Asuncion-Chin, M. and Dopico, A. M. (2011). "Smooth muscle cholesterol enables BK beta1 subunit-mediated channel inhibition and subsequent vasoconstriction evoked by alcohol." *Arterioscler Thromb Vasc Biol* **31**(11): 2410-2423.

Bukiya, A. N., Vaithianathan, T., Toro, L. and Dopico, A. M. (2008). "The second transmembrane domain of the large conductance, voltage- and calcium-gated potassium channel beta(1) subunit is a lithocholate sensor." *FEBS Lett* **582**(5): 673-678.

Bukiya, A. N., Vaithianathan, T., Toro, L. and Dopico, A. M. (2009). "Channel beta2-4 subunits fail to substitute for beta1 in sensitizing BK channels to lithocholate." *Biochem Biophys Res Commun* **390**(3): 995-1000.

Callahan, A. (2001). "Cerebrovascular disease and statins: a potential addition to the therapeutic armamentarium for stroke prevention." *Am J Cardiol* **88**(7b): 33j-37j.

Chen, H., Kronengold, J., Yan, Y., Gazula, V. R., Brown, M. R., Ma, L., Ferreira, G., Yang, Y., Bhattacharjee, A., Sigworth, F. J., Salkoff, L. and Kaczmarek, L. K. (2009). "The N-terminal domain of Slack determines the formation and trafficking of Slick/Slack heteromeric sodium-activated potassium channels." *J Neurosci* **29**(17): 5654-5665.

Cheng, H. and Lederer, W. J. (2008). "Calcium sparks." *Physiol Rev* **88**(4): 1491-1545.

Contreras, G. F., Neely, A., Alvarez, O., Gonzalez, C. and Latorre, R. (2012). "Modulation of BK channel voltage gating by different auxiliary beta subunits." *Proc Natl Acad Sci U S A* **109**(46): 18991-18996.

Cox, D. H. and Aldrich, R. W. (2000). "Role of the beta1 subunit in large-conductance Ca(2+)-activated K(+) channel gating energetics. Mechanisms of enhanced Ca(2+) sensitivity." *J Gen Physiol* **116**(3): 411-432.

Cox, D. H., Cui, J. and Aldrich, R. W. (1997). "Allosteric gating of a large conductance Ca-activated K+ channel." *J Gen Physiol* **110**(3): 257-281.

Cox, D. H., Cui, J. and Aldrich, R. W. (1997). "Separation of gating properties from permeation and block in mslo large conductance Ca-activated K+ channels." *J Gen Physiol* **109**(5): 633-646.

Crowley, J. J., Treistman, S. N. and Dopico, A. M. (2003). "Cholesterol antagonizes ethanol potentiation of human brain BKCa channels reconstituted into phospholipid bilayers." *Mol Pharmacol* **64**(2): 365-372.

Crowley, J. J., Treistman, S. N. and Dopico, A. M. (2005). "Distinct structural features of phospholipids differentially determine ethanol sensitivity and basal function of BK channels." *Mol Pharmacol* **68**(1): 4-10.

Dopico, A. M. (2003). "Ethanol sensitivity of BK(Ca) channels from arterial smooth muscle does not require the presence of the beta 1-subunit." *Am J Physiol Cell Physiol* **284**(6): C1468-1480.

Dopico, A. M., Anantharam, V. and Treistman, S. N. (1998). "Ethanol increases the activity of Ca(++)-dependent K+ (mslo) channels: functional interaction with cytosolic Ca++." *J Pharmacol Exp Ther* **284**(1): 258-268.

Dopico, A. M., Bukiya, A. N. and Singh, A. K. (2012). "Large conductance, calcium- and voltage-gated potassium (BK) channels: regulation by cholesterol." *Pharmacol Ther* **135**(2): 133-150.

Dopico, A. M., Chu, B., Lemos, J. R. and Treistman, S. N. (1999). "Alcohol modulation of calcium-activated potassium channels." *Neurochem Int* **35**(2): 103-106.

Dopico, A. M., Lemos, J. R. and Treistman, S. N. (1996). "Ethanol increases the activity of large conductance, Ca(2+)-activated K+ channels in isolated neurohypophysial terminals." *Mol Pharmacol* **49**(1): 40-48.

Dryer, S. E. (1994). "Na(+)-activated K+ channels: a new family of large-conductance ion channels." *Trends Neurosci* **17**(4): 155-160.

Erdos, B., Miller, A. W. and Busija, D. W. (2002). "Alterations in KATP and KCa channel function in cerebral arteries of insulin-resistant rats." *Am J Physiol Heart Circ Physiol* **283**(6): H2472-2477.

Feinberg-Zadek, P. L., Martin, G. and Treistman, S. N. (2008). "BK channel subunit composition modulates molecular tolerance to ethanol." *Alcohol Clin Exp Res* **32**(7): 1207-1216.

Gil-Nunez, A. C. and Villanueva, J. A. (2001). "Advantages of lipid-lowering therapy in cerebral ischemia: role of HMG-CoA reductase inhibitors." *Cerebrovasc Dis* **11 Suppl 1**: 85-95.

Gonzalez-Perez, V., Xia, X. M. and Lingle, C. J. (2014). "Functional regulation of BK potassium channels by gamma1 auxiliary subunits." *Proc Natl Acad Sci U S A* **111**(13): 4868-4873.

Gordon, E. L., Nguyen, T. S., Ngai, A. C. and Winn, H. R. (1995). "Differential effects of alcohols on intracerebral arterioles. Ethanol alone causes vasoconstriction." *J Cereb Blood Flow Metab* **15**(3): 532-538.

Haapaniemi, H., Hillbom, M. and Juvela, S. (1997). "Lifestyle-associated risk factors for acute brain infarction among persons of working age." *Stroke* **28**(1): 26-30.

Horrigan, F. T. (2012). "Perspectives on: conformational coupling in ion channels: conformational coupling in BK potassium channels." *J Gen Physiol* **140**(6): 625-634.

Horrigan, F. T. and Aldrich, R. W. (1999). "Allosteric voltage gating of potassium channels II. Mslo channel gating charge movement in the absence of Ca(2+)." *J Gen Physiol* **114**(2): 305-336.

Horrigan, F. T. and Aldrich, R. W. (2002). "Coupling between voltage sensor activation, Ca2+ binding and channel opening in large conductance (BK) potassium channels." *J Gen Physiol* **120**(3): 267-305.

Horrigan, F. T., Cui, J. and Aldrich, R. W. (1999). "Allosteric voltage gating of potassium channels I. Mslo ionic currents in the absence of Ca(2+)." *J Gen Physiol* **114**(2): 277-304.

Hu, L., Shi, J., Ma, Z., Krishnamoorthy, G., Sieling, F., Zhang, G., Horrigan, F. T. and Cui, J. (2003). "Participation of the S4 voltage sensor in the Mg2+-dependent activation of large conductance (BK) K+ channels." *Proc Natl Acad Sci U S A* **100**(18): 10488-10493.

Iwase, S., Matsukawa, T., Ishihara, S., Tanaka, A., Tanabe, K., Danbara, A., Matsuo, M., Sugiyama, Y. and Mano, T. (1995). "Effect of oral ethanol intake on muscle sympathetic nerve activity and cardiovascular functions in humans." *J Auton Nerv Syst* **54**(3): 206-214.

Jackson, R., Stewart, A., Beaglehole, R. and Scragg, R. (1985). "Alcohol consumption and blood pressure." *Am J Epidemiol* **122**(6): 1037-1044.

Jaggar, J. H., Li, A., Parfenova, H., Liu, J., Umstot, E. S., Dopico, A. M. and Leffler, C. W. (2005). "Heme is a carbon monoxide receptor for large-conductance Ca2+-activated K+ channels." *Circ Res* **97**(8): 805-812.

Jaggar, J. H. and Nelson, M. T. (2000). "Differential regulation of Ca(2+) sparks and Ca(2+) waves by UTP in rat cerebral artery smooth muscle cells." *Am J Physiol Cell Physiol* **279**(5): C1528-1539.

Jaggar, J. H., Porter, V. A., Lederer, W. J. and Nelson, M. T. (2000). "Calcium sparks in smooth muscle." *Am J Physiol Cell Physiol* **278**(2): C235-256.

Jakab, M., Weiger, T. M. and Hermann, A. (1997). "Ethanol activates maxi Ca2+-activated K+ channels of clonal pituitary (GH3) cells." *J Membr Biol* **157**(3): 237-245.

Jiang, Y., Lee, A., Chen, J., Cadene, M., Chait, B. T. and MacKinnon, R. (2002). "The open pore conformation of potassium channels." *Nature* **417**(6888): 523-526.

Klatsky, A. L., Friedman, G. D. and Armstrong, M. A. (1986). "The relationships between alcoholic beverage use and other traits to blood pressure: a new Kaiser Permanente study." *Circulation* **73**(4): 628-636.

Kuntamallappanavar, G., Toro, L. and Dopico, A. M. (2014). "Both transmembrane domains of BK beta1 subunits are essential to confer the normal phenotype of beta1-containing BK channels." *PLoS One* **9**(10): e109306.

Latorre, R., Oberhauser, A., Labarca, P. and Alvarez, O. (1989). "Varieties of calcium-activated potassium channels." *Annu Rev Physiol* **51**: 385-399.

Lee, U. S. and Cui, J. (2010). "BK channel activation: structural and functional insights." *Trends Neurosci* **33**(9): 415-423.

Lee, U. S., Shi, J. and Cui, J. (2010). "Modulation of BK channel gating by the ss2 subunit involves both membrane-spanning and cytoplasmic domains of Slo1." *J Neurosci* **30**(48): 16170-16179.

Lesh, R. E., Somlyo, A. P., Owens, G. K. and Somlyo, A. V. (1995). "Reversible permeabilization. A novel technique for the intracellular introduction of antisense oligodeoxynucleotides into intact smooth muscle." *Circ Res* **77**(2): 220-230.

Liu, G., Niu, X., Wu, R. S., Chudasama, N., Yao, Y., Jin, X., Weinberg, R., Zakharov, S. I., Motoike, H., Marx, S. O. and Karlin, A. (2010). "Location of modulatory beta subunits in BK potassium channels." *J Gen Physiol* **135**(5): 449-459.

Liu, J., Asuncion-Chin, M., Liu, P. and Dopico, A. M. (2006). "CaM kinase II phosphorylation of slo Thr107 regulates activity and ethanol responses of BK channels." *Nat Neurosci* **9**(1): 41-49.

Liu, J., Bukiya, A. N., Kuntamallappanavar, G., Singh, A. K. and Dopico, A. M. (2013). "Distinct sensitivity of slo1 channel proteins to ethanol." *Mol Pharmacol* **83**(1): 235-244.

Liu, J., Vaithianathan, T., Manivannan, K., Parrill, A. and Dopico, A. M. (2008). "Ethanol modulates BKCa channels by acting as an adjuvant of calcium." *Mol Pharmacol* **74**(3): 628-640.

Liu, P., Liu, J., Huang, W., Li, M. D. and Dopico, A. M. (2003). "Distinct regions of the slo subunit determine differential BKCa channel responses to ethanol." *Alcohol Clin Exp Res* **27**(10): 1640-1644.

Liu, P., Xi, Q., Ahmed, A., Jaggar, J. H. and Dopico, A. M. (2004). "Essential role for smooth muscle BK channels in alcohol-induced cerebrovascular constriction." *Proc Natl Acad Sci U S A* **101**(52): 18217-18222.

Lohn, M., Lauterbach, B., Haller, H., Pongs, O., Luft, F. C. and Gollasch, M. (2001). "beta(1)-Subunit of BK channels regulates arterial wall[Ca(2+)] and diameter in mouse cerebral arteries." *J Appl Physiol (1985)* **91**(3): 1350-1354.

Marmot, M. and Brunner, E. (1991). "Alcohol and cardiovascular disease: the status of the U shaped curve." *BMJ* **303**(6802): 565-568.

Martin, G., Puig, S., Pietrzykowski, A., Zadek, P., Emery, P. and Treistman, S. (2004). "Somatic localization of a specific large-conductance calcium-activated potassium channel subtype controls compartmentalized ethanol sensitivity in the nucleus accumbens." *J Neurosci* **24**(29): 6563-6572.

Meera, P., Wallner, M., Jiang, Z. and Toro, L. (1996). "A calcium switch for the functional coupling between alpha (hslo) and beta subunits (KV,Ca beta) of maxi K channels." *FEBS Lett* **382**(1-2): 84-88.

Meissner, G., Rousseau, E. and Lai, F. A. (1989). "Structural and functional correlation of the trypsin-digested Ca2+ release channel of skeletal muscle sarcoplasmic reticulum." *J Biol Chem* **264**(3): 1715-1722.

Miledi, R. and Parker, I. (1984). "Chloride current induced by injection of calcium into Xenopus oocytes." *J Physiol* **357**: 173-183.

Mohler, E. R., 3rd, Delanty, N., Rader, D. J. and Raps, E. C. (1999). "Statins and cerebrovascular disease: plaque attack to prevent brain attack." *Vasc Med* **4**(4): 269-272.

Monod, J., Wyman, J. and Changeux, J. P. (1965). "On the Nature of Allosteric Transitions: A Plausible Model." *J Mol Biol* **12**: 88-118.

Moore, R. D. and Pearson, T. A. (1986). "Moderate alcohol consumption and coronary artery disease. A review." *Medicine (Baltimore)* **65**(4): 242-267.

Morrow, J. P., Zakharov, S. I., Liu, G., Yang, L., Sok, A. J. and Marx, S. O. (2006). "Defining the BK channel domains required for beta1-subunit modulation." *Proc Natl Acad Sci U S A* **103**(13): 5096-5101.

Nimigean, C. M. and Magleby, K. L. (2000). "Functional coupling of the beta(1) subunit to the large conductance Ca(2+)-activated K(+) channel in the absence of Ca(2+). Increased Ca(2+) sensitivity from a Ca(2+)-independent mechanism." *J Gen Physiol* **115**(6): 719-736.

Niu, X., Qian, X. and Magleby, K. L. (2004). "Linker-gating ring complex as passive spring and Ca(2+)-dependent machine for a voltage- and Ca(2+)-activated potassium channel." *Neuron* **42**(5): 745-756.

Orio, P. and Latorre, R. (2005). "Differential effects of beta 1 and beta 2 subunits on BK channel activity." *J Gen Physiol* **125**(4): 395-411.

Orio, P., Rojas, P., Ferreira, G. and Latorre, R. (2002). "New disguises for an old channel: MaxiK channel beta-subunits." *News Physiol Sci* **17**: 156-161.

Patterson, A. J., Henrie-Olson, J. and Brenner, R. (2002). "Vasoregulation at the molecular level: a role for the beta1 subunit of the calcium-activated potassium (BK) channel." *Trends Cardiovasc Med* **12**(2): 78-82.

Perez, G. J., Bonev, A. D. and Nelson, M. T. (2001). "Micromolar Ca(2+) from sparks activates Ca(2+)-sensitive K(+) channels in rat cerebral artery smooth muscle." *Am J Physiol Cell Physiol* **281**(6): C1769-1775.

Pluger, S., Faulhaber, J., Furstenau, M., Lohn, M., Waldschutz, R., Gollasch, M., Haller, H., Luft, F. C., Ehmke, H. and Pongs, O. (2000). "Mice with disrupted BK channel beta1 subunit gene feature abnormal Ca(2+) spark/STOC coupling and elevated blood pressure." *Circ Res* **87**(11): E53-60.

Potter, J. F. and Beevers, D. G. (1984). "Pressor effect of alcohol in hypertension." *Lancet* **1**(8369): 119-122.

Puddey, I. B., Beilin, L. J. and Vandongen, R. (1987). "Regular alcohol use raises blood pressure in treated hypertensive subjects. A randomised controlled trial." *Lancet* **1**(8534): 647-651.

Puddey, I. B., Beilin, L. J., Vandongen, R., Rouse, I. L. and Rogers, P. (1985). "Evidence for a direct effect of alcohol consumption on blood pressure in normotensive men. A randomized controlled trial." *Hypertension* **7**(5): 707-713.

Puddey, I. B., Rakic, V., Dimmitt, S. B. and Beilin, L. J. (1999). "Influence of pattern of drinking on cardiovascular disease and cardiovascular risk factors--a review." *Addiction* **94**(5): 649-663.

Qian, X., Nimigean, C. M., Niu, X., Moss, B. L. and Magleby, K. L. (2002). "Slo1 tail domains, but not the Ca2+ bowl, are required for the beta 1 subunit to increase the apparent Ca2+ sensitivity of BK channels." *J Gen Physiol* **120**(6): 829-843.

Reynolds, K., Lewis, B., Nolen, J. D., Kinney, G. L., Sathya, B. and He, J. (2003). "Alcohol consumption and risk of stroke: a meta-analysis." *JAMA* **289**(5): 579-588.

Rimm, E. B., Klatsky, A., Grobbee, D. and Stampfer, M. J. (1996). "Review of moderate alcohol consumption and reduced risk of coronary heart disease: is the effect due to beer, wine, or spirits." *Bmj* **312**(7033): 731-736.

Salkoff, L., Butler, A., Ferreira, G., Santi, C. and Wei, A. (2006). "High-conductance potassium channels of the SLO family." *Nat Rev Neurosci* **7**(12): 921-931.

Santi, C. M., Ferreira, G., Yang, B., Gazula, V. R., Butler, A., Wei, A., Kaczmarek, L. K. and Salkoff, L. (2006). "Opposite regulation of Slick and Slack K+ channels by neuromodulators." *J Neurosci* **26**(19): 5059-5068.

Schreiber, M., Wei, A., Yuan, A., Gaut, J., Saito, M. and Salkoff, L. (1998). "Slo3, a novel pH-sensitive K+ channel from mammalian spermatocytes." *J Biol Chem* **273**(6): 3509-3516.

Seppa, K., Laippala, P. and Sillanaukee, P. (1996). "High diastolic blood pressure: common among women who are heavy drinkers." *Alcohol Clin Exp Res* **20**(1): 47-51.

Shi, J., Krishnamoorthy, G., Yang, Y., Hu, L., Chaturvedi, N., Harilal, D., Qin, J. and Cui, J. (2002). "Mechanism of magnesium activation of calcium-activated potassium channels." *Nature* **418**(6900): 876-880.

Stefani, E., Ottolia, M., Noceti, F., Olcese, R., Wallner, M., Latorre, R. and Toro, L. (1997). "Voltage-controlled gating in a large conductance Ca2+-sensitive K+channel (hslo)." *Proc Natl Acad Sci U S A* **94**(10): 5427-5431.

Subramani, J., Kathirvel, K., Leo, M. D., Kuntamallappanavar, G., Uttam Singh, T. and Mishra, S. K. (2009). "Atorvastatin restores the impaired vascular endothelium-dependent relaxations mediated by nitric oxide and endothelium-derived hyperpolarizing factors but not hypotension in sepsis." *J Cardiovasc Pharmacol* **54**(6): 526-534.

Sun, X., Shi, J., Delaloye, K., Yang, X., Yang, H., Zhang, G. and Cui, J. (2013). "The interface between membrane-spanning and cytosolic domains in Ca(2)+-dependent K+ channels is involved in beta subunit modulation of gating." *J Neurosci* **33**(27): 11253-11261.

Suter, P. M. and Vetter, W. (1999). "Alcohol and ischemic stroke." *Nutr Rev* **57**(10): 310-314.

Tanaka, Y., Meera, P., Song, M., Knaus, H. G. and Toro, L. (1997). "Molecular constituents of maxi KCa channels in human coronary smooth muscle: predominant alpha + beta subunit complexes." *J Physiol* **502 (Pt 3)**: 545-557.

Thomas-Gatewood, C., Neeb, Z. P., Bulley, S., Adebiyi, A., Bannister, J. P., Leo, M. D. and Jaggar, J. H. (2011). "TMEM16A channels generate Ca(2)(+)-activated Cl(-) currents in cerebral artery smooth muscle cells." *Am J Physiol Heart Circ Physiol* **301**(5): H1819-1827.

Treistman, S. N. and Martin, G. E. (2009). "BK Channels: mediators and models for alcohol tolerance." *Trends Neurosci* **32**(12): 629-637.

Uebele, V. N., Lagrutta, A., Wade, T., Figueroa, D. J., Liu, Y., McKenna, E., Austin, C. P., Bennett, P. B. and Swanson, R. (2000). "Cloning and functional expression of two families of beta-subunits of the large conductance calcium-activated K+ channel." *J Biol Chem* **275**(30): 23211-23218.

Wallner, M., Meera, P., Ottolia, M., Kaczorowski, G. J., Latorre, R., Garcia, M. L., Stefani, E. and Toro, L. (1995). "Characterization of and modulation by a beta-subunit of a human maxi KCa channel cloned from myometrium." *Receptors Channels* **3**(3): 185-199.

Wallner, M., Meera, P. and Toro, L. (1996). "Determinant for beta-subunit regulation in high-conductance voltage-activated and Ca(2+)-sensitive K+ channels: an additional transmembrane region at the N terminus." *Proc Natl Acad Sci U S A* **93**(25): 14922-14927.

Wallner, M., Meera, P. and Toro, L. (1999). "Molecular basis of fast inactivation in voltage and Ca2+-activated K+ channels: a transmembrane beta-subunit homolog." *Proc Natl Acad Sci U S A* **96**(7): 4137-4142.

Walters, F. S., Covarrubias, M. and Ellingson, J. S. (2000). "Potent inhibition of the aortic smooth muscle maxi-K channel by clinical doses of ethanol." *Am J Physiol Cell Physiol* **279**(4): C1107-1115.

Wannamethee, S. G. and Shaper, A. G. (1996). "Patterns of alcohol intake and risk of stroke in middle-aged British men." *Stroke* **27**(6): 1033-1039.

Wechsler, H., Lee, J. E., Kuo, M., Seibring, M., Nelson, T. F. and Lee, H. (2002). "Trends in college binge drinking during a period of increased prevention efforts. Findings from 4 Harvard School of Public Health College Alcohol Study surveys: 1993-2001." *J Am Coll Health* **50**(5): 203-217.

Wellman, G. C., Nathan, D. J., Saundry, C. M., Perez, G., Bonev, A. D., Penar, P. L., Tranmer, B. I. and Nelson, M. T. (2002). "Ca2+ sparks and their function in human cerebral arteries." *Stroke* **33**(3): 802-808.

Wellman, G. C. and Nelson, M. T. (2003). "Signaling between SR and plasmalemma in smooth muscle: sparks and the activation of Ca2+-sensitive ion channels." *Cell Calcium* **34**(3): 211-229.

Welsh, D. G., Morielli, A. D., Nelson, M. T. and Brayden, J. E. (2002). "Transient receptor potential channels regulate myogenic tone of resistance arteries." *Circ Res* **90**(3): 248-250.

Wu, R. S., Chudasama, N., Zakharov, S. I., Doshi, D., Motoike, H., Liu, G., Yao, Y., Niu, X., Deng, S. X., Landry, D. W., Karlin, A. and Marx, S. O. (2009). "Location of the beta 4 transmembrane helices in the BK potassium channel." *J Neurosci* **29**(26): 8321-8328.

Wu, R. S., Liu, G., Zakharov, S. I., Chudasama, N., Motoike, H., Karlin, A. and Marx, S. O. (2013). "Positions of beta2 and beta3 subunits in the large-conductance calcium- and voltage-activated BK potassium channel." *J Gen Physiol* **141**(1): 105-117.

Wynne, P. M., Puig, S. I., Martin, G. E. and Treistman, S. N. (2009). "Compartmentalized beta subunit distribution determines characteristics and ethanol sensitivity of somatic, dendritic, and terminal large-conductance calcium-activated potassium channels in the rat central nervous system." *J Pharmacol Exp Ther* **329**(3): 978-986.

Xi, Q., Adebiyi, A., Zhao, G., Chapman, K. E., Waters, C. M., Hassid, A. and Jaggar, J. H. (2008). "IP3 constricts cerebral arteries via IP3 receptor-mediated TRPC3 channel activation and independently of sarcoplasmic reticulum Ca2+ release." *Circ Res* **102**(9): 1118-1126.

Xia, X. M., Ding, J. P. and Lingle, C. J. (1999). "Molecular basis for the inactivation of Ca2+- and voltage-dependent BK channels in adrenal chromaffin cells and rat insulinoma tumor cells." *J Neurosci* **19**(13): 5255-5264.

Xia, X. M., Ding, J. P. and Lingle, C. J. (2003). "Inactivation of BK channels by the NH2 terminus of the beta2 auxiliary subunit: an essential role of a terminal peptide segment of three hydrophobic residues." *J Gen Physiol* **121**(2): 125-148.

Xia, X. M., Zeng, X. and Lingle, C. J. (2002). "Multiple regulatory sites in large-conductance calcium-activated potassium channels." *Nature* **418**(6900): 880-884.

Xia, X. M., Zhang, X. and Lingle, C. J. (2004). "Ligand-dependent activation of Slo family channels is defined by interchangeable cytosolic domains." *J Neurosci* **24**(24): 5585-5591.

Xu, L., Jones, R. and Meissner, G. (1993). "Effects of local anesthetics on single channel behavior of skeletal muscle calcium release channel." *J Gen Physiol* **101**(2): 207-233.

Yang, Z., Wang, J., Zheng, T., Altura, B. T. and Altura, B. M. (2001). "Importance of extracellular Ca2+ and intracellular Ca2+ release in ethanol-induced contraction of cerebral arterial smooth muscle." *Alcohol* **24**(3): 145-153.

Ye, S., Li, Y., Chen, L. and Jiang, Y. (2006). "Crystal structures of a ligand-free MthK gating ring: insights into the ligand gating mechanism of K+ channels." *Cell* **126**(6): 1161-1173.

Yuan, C., Chen, M., Covey, D. F., Johnston, L. J. and Treistman, S. N. (2011). "Cholesterol tuning of BK ethanol response is enantioselective, and is a function of accompanying lipids." *PLoS One* **6**(11): e27572.

Yuan, P., Leonetti, M. D., Hsiung, Y. and MacKinnon, R. (2012). "Open structure of the Ca2+ gating ring in the high-conductance Ca2+-activated K+ channel." *Nature* **481**(7379): 94-97.

Yusifov, T., Savalli, N., Gandhi, C. S., Ottolia, M. and Olcese, R. (2008). "The RCK2 domain of the human BKCa channel is a calcium sensor." *Proc Natl Acad Sci U S A* **105**(1): 376-381.

Zakhari, S. (1997). "Alcohol and the cardiovascular system: molecular mechanisms for beneficial and harmful action." *Alcohol Health Res World* **21**(1): 21-29.

Zhang, A., Altura, B. T. and Altura, B. M. (1993). "Ethanol-induced contraction of cerebral arteries in diverse mammals and its mechanism of action." *Eur J Pharmacol* **248**(3): 229-236.

Zhang, Z., Rosenhouse-Dantsker, A., Tang, Q. Y., Noskov, S. and Logothetis, D. E. (2010). "The RCK2 domain uses a coordination site present in Kir channels to confer sodium sensitivity to Slo2.2 channels." *J Neurosci* **30**(22): 7554-7562.

VITA

Guruprasad Kuntamallappanavar was born on March 22, 1984 in Karnataka, India. He graduated from high school in 2000. He pursued his Bachelor of Veterinary Science (B.V.Sc) degree from Veterinary College, Karnataka Veterinary Animal Fisheries Sciences University, Bidar, India in August, 2007. Later, he obtained his Masters of Veterinary Sciences (M.V.Sc.) degree from Indian Veterinary Research Institute, Uttar Pradesh, India in August, 2009. In August 2009, he joined the Integrated Program in Biomedical Sciences (IPBS) at the University of Tennessee Health Science Center (UTHSC), Memphis, Tennessee. Currently, he is a member of the Biophysical Society and the Research Society on Alcoholism. He is a recipient of the most prestigious predoctoral fellowship award (January 2013 – December 2014) from the American Heart Association, Greater Southeast Affiliate. He was also a recipient of four travel awards during his graduate studies: a Biophysical Society Education Travel award (2013) a Research Society on Alcoholism Student Merit Award (2014), and two educational travel awards from the College of Graduate Health Sciences, UTHSC in 2013 and 2014. These awards helped him to present his scientific work at national and international scientific meetings, such as the Biophysical Society, Research Society on Alcoholism and International Society for Biomedical Research on Alcoholism meetings. He was awarded his Ph.D. from the University of Tennessee Health Science Center, Memphis, Tennessee, in May, 2015.